# NUMERICAL MODELING OF A POLYMER ELECTROLYTE FUEL CELL IN DIFFERENT COMMERCIAL FLOW FIELD GEOMETRIC CONFIGURATIONS USING ANSYS FLUENT

Patcharawat Charoen-amornkitt

A Thesis Submitted in Partial Fulfillment of Requirements
for The Degree of Master of Engineering Program in Engineering Technology
Graduate School
Thai-Nichi Institute of Technology
Academic Year 2014

| | |
|---|---|
| Thesis Topic | Numerical modeling of a polymer electrolyte fuel cell in different commercial flow field geometric configurations using ANSYS FLUENT |
| By | Patcharawat Charoen-amornkitt |
| Field of Study | Engineering Technology |
| Thesis Advisor | Asst. Prof. Dr. Nuttapol Limjeerajarus |

---

The Graduate School of Thai-Nichi Institute of Technology has been approved and accepted as partial fulfillment of the requirement for the Master's Degree.

…… Dean of the Graduate School
(Assoc. Prof. Dr. Pichit Sukcharoenpong)
Month……Date……Year……

Thesis Committees

…… Chairman
(Asst. Prof. Dr. Somchai Sripattanapipat)

…… Member
(Asst. Prof. Dr. Wipawadee Wongsuwan)

…… Member
(Dr. Ek-U Thammakornbunjut)

…… Thesis Advisor
(Asst. Prof. Dr. Nuttapol Limjeerajarus)

PATCHARAWAT CHAROEN-AMORNKITT: NUMERICAL MODELING OF A POLYMER ELECTROLYTE FUEL CELL IN DIFFERENT COMMERCIAL FLOW FIELD GEOMETRIC CONFIGURATIONS USING ANSYS FLUENT. ADVISOR: ASSISTANCE PROFESSOR DR. NUTTAPOL LIMJEERAJARUS, 100 PP.

An improper designed flow field of a polymer electrolyte fuel cell (PEFC) stack can cause the maldistributions of current density, temperature, and water concentration, which lead to localized mechanical stress, flooding or drying of the membrane, and flooding in flow channel. These problems, consequently, reduce performance and shorten the membrane electrode assembly (MEA) lifetime. In this work, a numerical investigation on the distributions in six different flow field designs, namely single, three, and five channel serpentine; three and five channel parallel in series; and z-type parallel over 5 $cm^2$ PEFC has been systematically carried out using CFD techniques via ANSYS FLUENT software. The model was validated with experimental data obtained from our previous work. The results revealed that, for a small size PEFC, the flow fields with a longer channel (less number of channels) provided both a better uniformity and cell performance. With the same number of channels, the parallel in series flow fields clearly performed better than the multi-channel serpentine flow fields in both uniformity and water management. However, the effect of flow field design on the PEFC performance was found lower than the length of channel. In summary, for making a small stack, the single channel serpentine is suggested to be used as a flow field with its outstanding performance.

Graduate School Student's Signature……

Field of Engineering Technology Advisor's Signature……

Academic Year 2014

# Acknowledgement

I wish to convey my deepest gratitude and respect to my thesis and research advisor, Asst. Prof. Dr. Nuttapol Limjeerajarus, whom I am totally indebted for patiently correcting my writing and providing me a motivation and inspiration. Without his guidance and persistent help this thesis would not have been possible.

I would like to thank my committee chair, Asst. Prof. Dr. Somchai Sripattanapipat, the director of graduate study, Mahanakorn University of Technology, for his valuable advices in the techniques for achieving the simulation results and his kindness for devoting his valuable time to be a chairman of the examination committee.

I am also sincerely thankful to my thesis committee, Asst. Prof. Dr. Wipawadee Wongsuwan, the associate dean for academic affairs, Thai-Nichi Institute of Technology, for her encouragement, supports, comments and questions which highly benefited to this research.

I would like to express my gratitude to Dr. Ek-u Thammakornbunjut, my thesis committee, who helped me to develop my background in numerical modeling and kindly introduced me to Prof. Dr. Pramote Dechaumphai and also Prof. Dr. Pramote for providing me a valuable opportunity to sit in the computational fluid dynamics class at Chulalongkorn University.

Finally, I would like to thank my family who encouraged me and prayed for me throughout the tough time of my research. This thesis is heartily dedicated to my father.

Patcharawat Charoen-amornkitt

# Table of Contents

# Table of Contents (Continued)

# List of Tables

# List of Figures

# List of Figures (Continued)

# List of Figures (Continued)

# Nomenclature

| Symbols | Definitions |
|---|---|
| $a$ | water activity |
| $D$ | mass diffusivity, $m^2\ s^{-1}$ |
| $F$ | Faraday constant, $C\ mol^{-1}$ |
| $h$ | rate of enthalpy change, $J\ s^{-1}$ |
| $i_0^{ref}$ | volumetric reference exchange current density, $A\ m^{-3}$ |
| $J$ | diffusion flux |
| $K$ | permeability, $m^2$ |
| $M_w$ | molecular mass, $kg\ kmol^{-1}$ |
| $n_d$ | osmotic drag coefficient |
| $p_c$ | capillary pressure, Pa |
| $R$ | universal gas constant, $J\ K^{-1}\ mol^{-1}$ |
| $R_i$ | volumetric transfer current, $A\ m^{-3}$ |
| $r_w$ | condensation rate, $kg\ m^{-3}s^{-1}$ |
| $S_\phi$ | source of variable $\phi$ |
| $s$ | water saturation |
| $T$ | temperature, K |
| t | time, s |
| $V_{OCV}$ | open circuit voltage, V |
| $\vec{V}$ | velocity, $m\ s^{-1}$ |
| $X$ | mole fraction |
| $Y$ | mass fraction |
| [ ] | species concentration, $mol\ m^{-3}$ |
| *Greek letters* | |
| $\alpha$ | charge transfer coefficient |
| $\varepsilon$ | porosity |
| $\gamma$ | concentration exponent |

# Nomenclature (Continued)

| Symbols | Definitions |
|---|---|
| *Greek letters (Continued)* | |
| $\Gamma_\phi$ | diffusivity of variable $\phi$ |
| $\eta$ | overpotential, V |
| $\lambda$ | water content |
| $\mu$ | kinematic viscosity, Pa s |
| $\xi$ | surface to volume ratio, $m^2$-Pt $m^{-3}$-electrode |
| $\rho$ | density, kg $m^{-3}$ |
| $\sigma$ | conductivity, 1 $\Omega^{-1}m^{-1}$ |
| $\phi$ | transported quantity |
| $\varphi$ | potential, V |
| *Subscripts/superscripts* | |
| *An* | anode |
| *bd* | back diffusion |
| *cat* | cathode |
| *e* | electric |
| *h* | heat |
| *i* | solid- or membrane-phase |
| *j, k* | species ($H_2$, $O_2$, $H_2O$, $N_2$) |
| *l* | liquid |
| *m* | membrane |
| *N* | number of the chemical species |
| *ohm* | ohmic |
| *p* | protonic |
| *react* | reaction |
| *s, sat* | saturated |
| *T* | thermal |
| *wv* | water vapor |
| *0* | reference |

# Chapter 1
# Introduction

## 1.1 Background & Rationale

At present, the carbon dioxide concentration in the earth's atmosphere has increased remarkably due to the use of the fossil fuel based energy converter, resulting in the critical greenhouse effect. Therefore, finding new power sources and energy converters is becoming a very important issue. Among various candidates, fuel cells, the devices that transform chemical energy to electrical energy via electrochemical reaction, has been considered as one of the most promising energy conversion devices since they are not restricted by the thermodynamics limitation such as Carnot cycle which is the restriction of fossil fuel based energy converter. Among the different types of fuel cells, polymer electrolyte fuel cell (PEFC) has received a high attention as a strong contender of an alternative power source for automotive and stationary applications because of their high energy conversion efficiency, zero greenhouse gas emission, low operating temperature and pressure, high power densities, low noise and fast start ups. PEFC consists of 9 important components as shown in figure 1.1.

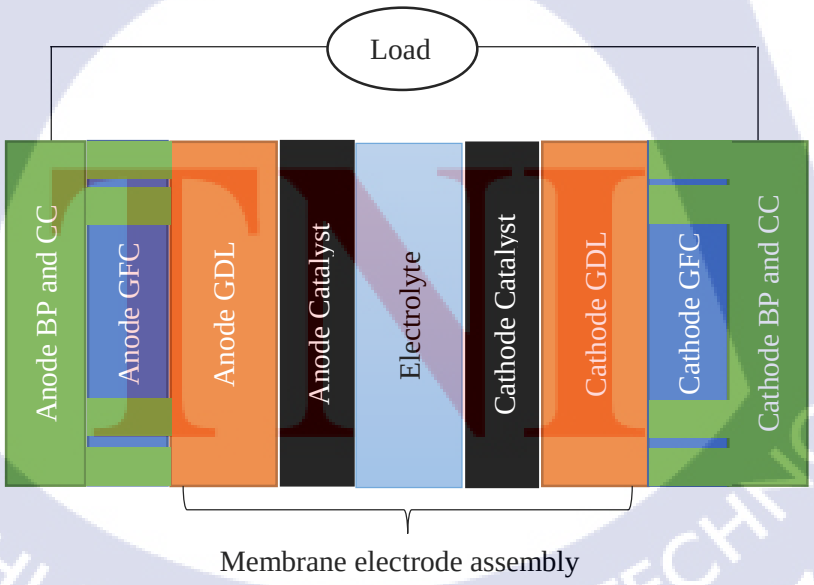


Figure 1.1 Schematic of PEFC components

To operate PEFC, Hydrogen is supplied into an anode gas flow channel (GFC), while Oxygen is supplied into a cathode GFC, to diffuse through a gas diffusion layer (GDL) and thus chemical energy is converted to electrical energy via electrochemical reactions inside a catalyst layer. The electrochemical reactions take place on both sides as describe in Eq. 2.1 and Eq. 2.2,

$$H_2 \rightarrow 2H^+ + 2e^- \qquad \text{(Anode)} \qquad (1.1)$$

And,

$$O_2 + 4e^- + 4H^+ \rightarrow 2H_2O \qquad \text{(Cathode)} \qquad (1.2)$$

The electrons, which produce at anode, travel through the bipolar plate (BP) and the current collector (CC), while the protons, which also produce at anode, travel through specific membrane, mostly Nafion of Dupont, to cathode and form up the water.

Although PEFC is one of the most promising candidates in transportation and stationary power generation, it still needs to be developed to overcome a number of challenges such as high cost, cell durability and degradation, before competing in the global energy market. In order to overcome those barriers, both experimentation and modeling play an important role in fuel cell research. They allow researchers to gain understanding in non-linear physical aspects of fuel cell and perform a design optimization. However, experimental approaches are time-consuming, expensive and highly uncertain. As a result, modeling approaches, which are less time-consuming and inexpensive, have attracted a lot of interests. Among various available modeling, computational fluid dynamics (CFD) is a very special tool since they are very powerful in fuel cell performance evaluation and parametric design optimization. Furthermore, CFD can also give a better understanding in transport phenomena inside a PEFC stack because experimentation has a limitation in measuring technology.

However, the major concerns of working with PEFC CFD modeling are the quality and accuracy of the obtained solution due to a complexity of the governing equation, an accuracy and reliability of model parameters, mesh quality, mesh dependency results and the others. Iranzo et al. [1] performed a model validation of 50 $cm^2$ commercial fuel cell stack with parallel and serpentine flow field by using model

parameters which obtained from technical data sheets, literature review and experimental measurement. The investigation of convergence criteria of 50 $cm^2$ fuel cell by using published model parameters was explored by Arvay et al. [2]. Kamarajugadda and Mazumder [3] compared the accuracy of various membrane models by using predicted results against experimental data and also performed a grid independence analysis to suggest the optimum value of computational cells within each layer of the model. These works are a good example of an attempt to create best practice guidelines for computational fuel cell dynamics (CFCD). However, such guidelines are not yet available for all PEFC CFD models and still need to be developed. Thus, all those basic analysis has to be performed in case by case to ensure the quality of PEFC CFD modeling. Once the model is validated, the parametric design evaluation and optimization, the estimation of PEFC performance, and the understanding of the complex non-linear physical and electrochemical processes occurring inside a PEFC can be done by using the model.

Many researchers used CFD to study the problem of water, current density, temperature and pressure distribution inside a PEFC, which effort to develop more efficient PEFC. Shimpalee et al. [4] studied the distribution of current density, water, temperature and pressure in a 480 $cm^2$ PEFC flow-field selected from the US patent literature. He et al. [5] investigated the effect of the anisotropic gas diffusion layer thermal conductivity on temperature and water distribution of the PEFC. Water flooding in the gas diffusion layer was investigated using a numerical CFD model by Shimpalee et al. [6]

One of the major factors which affects the efficiency of PEFC is geometric parameters of the flow fields since the bipolar plates performs keeping the reactants separates from each other, distributing them to the catalyst layer and also helping of water management. There are several works which attempt to propose a flow field that distributing the reactants more uniformly [7 - 9] since uniform distribution of reactants leads to a uniform distribution of current density, temperature and liquid water production, and reduction in localized hot spots, which reduce both performances, and material degradation. On the other hand, maldistribution of reactants leads to non-uniform current density, and mechanical stress in membrane electrode assembly, which causes performance and material degradation. Thus, the cell performance is

significantly affected by the flow field design and can be increased up to 50% by using an optimal design of the flow field only. Manso et al. [10] performed a comprehensive review of PEFC on an influence of geometric parameters of the flow fields and classified the parameters into eight types. After a study, many researchers have studied an impact of flow field designs by comparing them [11-13]. It was found that the two most popular designs are parallel and serpentine flow field as displayed in figure 1.2.

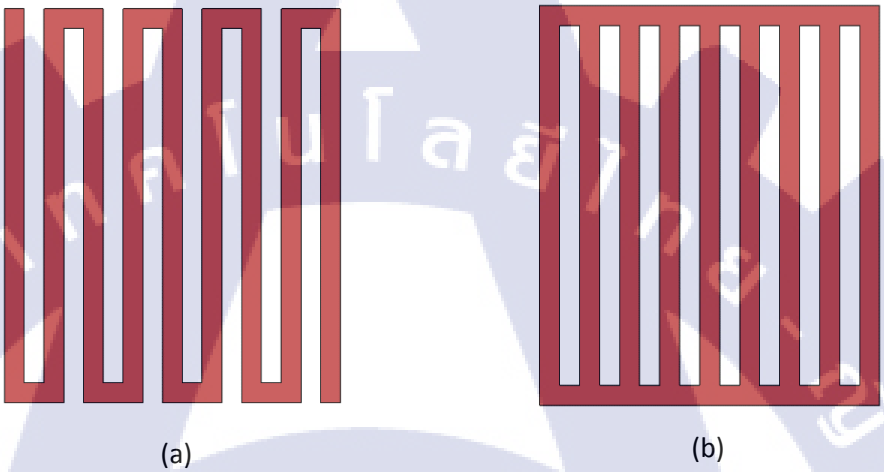


Figure 1.2 The popular flow field designs a) Serpentine and b) Parallel flow field

Serpentine channel configurations, the most famous of studying as shown in figure 1.3, are widely used in commercial fuel cell stacks, such as the one for Electrochem, due to their simplicity and excellent performance. Figure 1.3 also indicates that numerical study (NS) has received higher attention than experimental analysis (EA) resulting in the amount of papers. Note that the detail of different flow field configurations in thoroughly presented in chapter 2.

Although a 5 $cm^2$ fuel cell stack, three channels parallel in series (or three channels parallel discontinuous) as displayed in figure 1.4, has also sold by Electrochem, the effect of those channel configuration has received less attention in such researches (see figure 1.3). Therefore, the broad objectives of the present work are to investigate transport behaviors of the parallel in series flow field configuration as compared with those popular flow fields, such as serpentine and parallel configurations. In this work, the fuel cell stack and membrane electrode assembly will

be modelled using ANSYS FLUENT software and validated with experimental data. Finally, the best flow field among the different flow fields for a small-scaled MEA applications in overall aspects can be suggested.

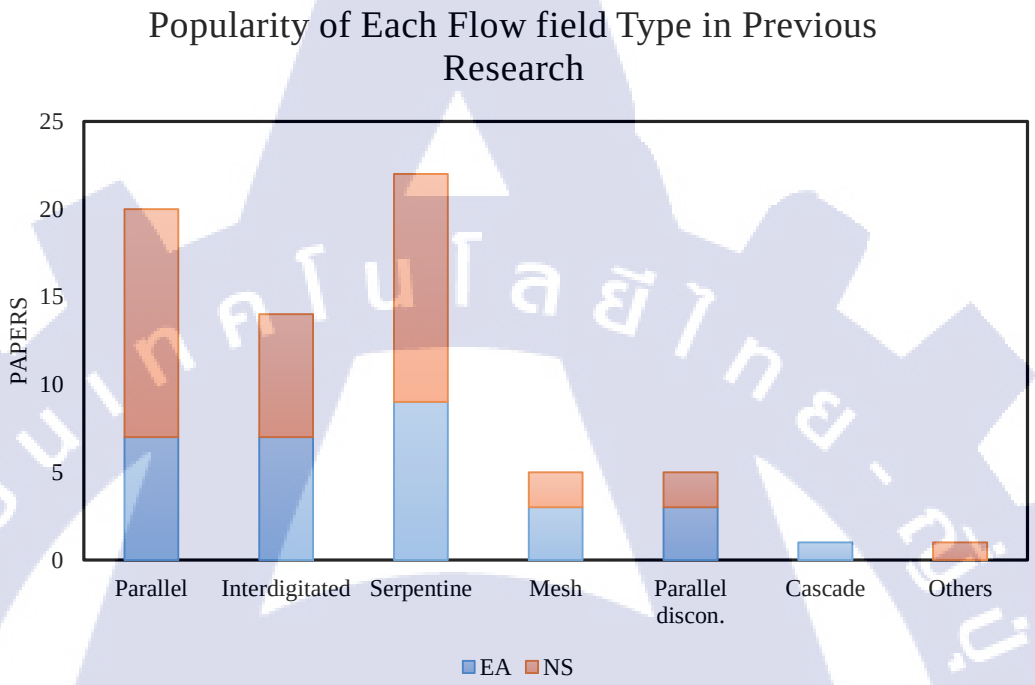


Figure 1.3 Popularity of each flow field type in previous research

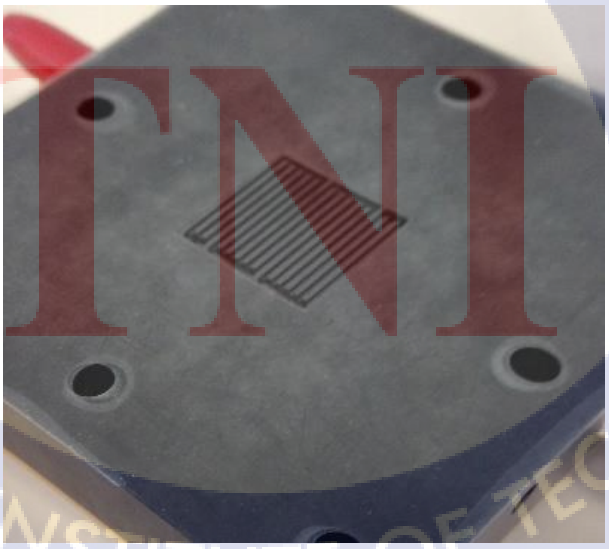

Figure 1.4 Three channels parallel in series flow field of commercial fuel cell stack

## 1.2 Objectives

1.2.1 Predict the performance of PEFC in different flow field designs

1.2.2 Study transport behaviors such as water, temperature and reactant distribution in different flow field designs

## 1.3 Scopes

- The numerical modeling is conducted by using ANSYS FLUENT.
- The model is validated with an experimental data of our previous work.
- The model is a 5 $cm^2$ PEFC with 6 different flow field designs which are one, three, five channel serpentine configuration, parallel configuration and three, five channel parallel in series configuration.

## 1.4 Expected Outcomes

1.4.1 The performance of 5 $cm^2$ PEFC in the 6 different flow field designs can be predicted.

1.4.2 The transport behaviors such as water, temperature and reactant distribution of 5 $cm^2$ PEFC in the 6 different flow field designs can be well understood.

1.4.3 The best flow field among the 6 different flow fields for a small-scaled MEA applications in overall aspects can be suggested.

## 1.5 Research Plan

Table 1.1 Research Plan

| Research Methodology | 2014 | | | | | | | | 2015 | | |
|---|---|---|---|---|---|---|---|---|---|---|---|
| | 5 | 6 | 7 | 8 | 9 | 10 | 11 | 12 | 1 | 2 | 3 |
| 1. Literature study | ■ | ■ | | | | | | | | | |
| 2. Model development | | ■ | ■ | ■ | | | | | | | |
| 3. Validation of the simulation results with experimental data | | | | ■ | ■ | | | | | | |
| 4. Other flow field designs models simulation | | | | | ■ | ■ | ■ | ■ | | | |
| 5. Result analysis | | | | | | | | ■ | ■ | ■ | |
| 6. Conclusion | | | | | | | | | | ■ | ■ |
| 7. Research publication | | | | | | | | | | | ■ |

# Chapter 2
# Literature Study

In this present work, a reference theory of the PEFC CFD model of ANSYS FLUENT [14] and several academic literatures, which have been studied, will be discussed as follows;

2.1 Theory

2.1.1 PEFC model theory

2.2 Previous study

2.2.1 CFCD role in PEFC research

2.2.2 Geometric parameters of flow fields

2.3 Related Research

In section 2.1.1, the governing equation of ANSYS FLUENT PEFC modeling will be discussed. The discussion of CFCD role in PEFC research will be presented in section 2.2.1. Section 2.2.2 will discuss about the geometric parameters of flow fields and its effect. Finally, in section 2.3, related research, which investigates the transport behaviors of parallel in series flow fields configuration, will be discussed

## 2.1 Theory

### 2.1.1 PEFC Model Theory

A comprehensive review of fuel cell and PEFC modeling was performed by Wang [15], Weber and Newman [16], and Siegel [17]. In this research, the three-dimensional model will be conducted by ANSYS FLUENT. The Navier-Stokes equations (conservation equations), which include mass, momentum and energy conservation, is used to solve those transport phenomena, fluid and heat flows, numerically based on CFD techniques using finite volume method, the governing equation which can be expressed as

$$\frac{\partial}{\partial t}(\rho\phi) + \nabla \cdot \left(\rho\phi\vec{V}\right) = \nabla \cdot (\Gamma_\phi \nabla\phi) + S_\phi \qquad (2.1)$$

Where,

| | | |
|---|---|---|
| $\phi$ | = | the transported quantity (mass, energy, and momentum) |
| t | = | the time |
| $\rho$ | = | the density |
| $\vec{V}$ | = | the velocity vector |
| $\Gamma_\phi$ | = | the transported quantity diffusivity |
| $S_\phi$ | = | the source of $\phi$ |

This conservation equation states that the rate of change of the transport quantity $\phi$ plus the transport by convection mechanism is equal to the diffusive transport of transport quantity $\phi$ plus the source $S_\phi$. The equations of each transport quantity such as electron, proton, species and liquid water are presented below.

2.1.1.2 Electrochemistry modeling

The electrochemical reactions are modelled by computing Hydrogen oxidation reaction (HOR) and Oxygen reduction reaction (ORR) which takes place within the catalyst layers. The equations of the potential used in this model, which are the electronic potential and protonic potential, are solved for solid phase (j = solid) and the membrane phase (j = membrane), respectively.

$$\nabla \cdot \sigma_j \nabla \varphi_j + R_j = 0 \tag{2.2}$$

Where,

| | | | |
|---|---|---|---|
| $\sigma$ | = | the electrical conductivity | unit: 1/(Ω·m-elec) |
| $\varphi$ | = | the electric potential | unit: V |
| $R$ | = | the volumetric transfer current | unit: A/m$^3$-elec |

For the solid phase, the equation describes the electron transport through the solid conductive materials; the gas diffusion layer and current collector, while membrane phase describes the proton transport through the membrane.

The volumetric transfer current of equation 2.2 is calculated by the Butler-Volmer equation [14].

$$R_{an} = \left(\zeta_{an} j_{an}^{ref}\right)\left(\frac{[H_2]}{[H_2]_{ref}}\right)^{\gamma_{an}} \left(e^{\frac{\alpha_{an} F \eta_{an}}{RT}} - e^{-\frac{\alpha_{cat} F \eta_{an}}{RT}}\right) \quad (2.3)$$

$$R_{cat} = \left(\zeta_{cat} j_{cat}^{ref}\right)\left(\frac{[O_2]}{[O_2]_{ref}}\right)^{\gamma_{cat}} \left(-e^{\frac{\alpha_{an} F \eta_{cat}}{RT}} + e^{-\frac{\alpha_{cat} F \eta_{cat}}{RT}}\right) \quad (2.4)$$

Where,

| | | | |
|---|---|---|---|
| $j^{ref}$ | = | the exchange current density | unit: A/m$^2$-Pt |
| $\zeta$ | = | the surface to volume | unit: m$^2$-Pt/m$^3$-elec |
| [] | = | the local species concentration | unit: kmol/m$^3$ |
| $[]_{ref}$ | = | the reference concentration | unit: kmol/m$^3$ |
| $\gamma$ | = | the concentration exponent | |
| $\alpha$ | = | the charge transfer coefficient | |
| $F$ | = | the Faraday constant | |
| $\eta$ | = | the activation loss | unit: V |
| R | = | the universal gas constant | |
| T | = | the temperature | |

The activation loss $\eta$ also called the local surface over-potential, which is the driving force for the kinetics, is computed by this following equations.

$$\eta_{an} = \varphi_{sol} - \varphi_{mem} \quad (2.5)$$

$$\eta_{cat} = \varphi_{sol} - \varphi_{mem} - V_{OC} \quad (2.6)$$

Where,

| | | | |
|---|---|---|---|
| $\varphi$ | = | the electric potential | unit: V |
| $V_{OC}$ | = | the open circuit voltage | unit: V |

2.1.1.2 Species transport modeling

The general form of the conservation of chemical species, which predicts the local mass fraction of each species, is expressed as

$$\frac{\partial}{\partial t}(\rho Y_i) + \nabla \cdot (\rho \vec{v} Y_i) = -\nabla \cdot \vec{J}_i + R_i + S_i \quad (2.7)$$

Where,

| | | | |
|---|---|---|---|
| $Y_i$ | = | the local mass fraction of each species | |

$\vec{J}_i$ = the diffusion flux of each species

$R_i$ = the source of chemical species due to the reaction

$S_i$ = the species source term

Volumetric source terms of the species in the catalyst layers are as follows.

$$S_{H_2} = -\frac{M_{W,H_2}}{2F} R_{an} < 0 \quad (2.8)$$

$$S_{O_2} = -\frac{M_{W,O_2}}{4F} R_{cat} < 0 \quad (2.9)$$

$$S_{H_2O} = \frac{M_{W,H_2O}}{2F} R_{cat} > 0 \quad (2.10)$$

Where,

$M_W$ = the molecular mass of the species unit: kg/kmol

The sign of the equations indicates that hydrogen and oxygen species are consumed while $H_2O$ is generated.

The total electric current which produces in the catalyst layers on both sides is the same. Therefore, the current is conserved by this following equation.

$$\int_{an} R_{an} dV = \int_{cat} R_{cat} dV \quad (2.11)$$

2.1.1.3 Heat source modeling

Since all chemical energy cannot be completely converted to electrical energy due to the second law of thermodynamics, therefore volumetric heat sources are presented.

$$S_h = h_{react} - R_{an,cat}\eta_{an,cat} + I^2 R_{ohm} + h_l \quad (2.12)$$

Where,

$h_{react}$ = the net rate of enthalpy change due to electrochemical reactions unit: J/s

$R_x\eta_x$ = the product of the transfer current and the over-potential in the anode or cathode side unit: J/s

$R_{ohm}$ = the ohmic resistivity of the conducting media unit: Ω

$h_l$ = the rate of enthalpy change due to Phase changes of the water unit: J/s

2.1.1.4 Liquid water formation and transport modeling

In saturation model, when PEFC operates under low temperature, especially at low voltage, the water may condense and form a liquid water blocking the gas diffusion passage. Therefore, the cell performance will be reduced since the diffusion rate and the effective reacting surface area are decreased. The saturation model using in ANSYS FLUENT, is based on the model of Nam and Karviany [18], and Nguyen [19], which is governed by the following conservation equation for the water saturation.

$$\frac{\partial(\varepsilon\rho_l s)}{\partial t} + \nabla\cdot\left(\rho_l\vec{V}_l S\right) = r_w \quad (2.13)$$

Where,

$\rho_l$ = the liquid water density unit: kg/m$^3$

$r_w$ = the condensation rate

$\varepsilon$ = the porosity

$\vec{V}_l$ = the liquid water velocity unit: m/s

The liquid water velocity is assumed to be equal to gas velocity inside the gas flow channel, and the condensation rate is modelled as follows.

$$r_w = C_r\max\left(\left[(1-s)\frac{P_{wv}-P_{sat}}{RT}M_{W,H_2O}\right],[-s\rho_l]\right) \quad (2.14)$$

Where,

$C_r$ = the condensation rate constant

$P_{wv}$ = the pressure of the water vapor unit: N/m$^2$

$P_{sat}$ = the saturation pressure unit: N/m$^2$

Since the porous zone is highly-resistant, the convective term is replaced by the capillary diffusion term and hence becomes

$$\frac{\partial(\varepsilon\rho_l s)}{\partial t} + \nabla \cdot \left(\rho_l \frac{Ks^3}{\mu_l}\frac{dp_c}{ds}\nabla S\right) = r_w \quad (2.15)$$

Where,

K = the permeability unit: 1/m$^2$

$\mu_l$ = the kinematic viscosity of liquid water unit: Pa·s

$p_c$ = the capillary pressure unit: N/m$^2$

The capillary pressure $p_c$ is calculated by using the Leverett function.

$$p_c = \begin{cases} \frac{\sigma_t cos\theta_c}{\left(\frac{K}{\varepsilon}\right)^{0.5}}(1.417(1-s) - 2.12(1-s)^2 + 1.263(1-s)^3) & \theta_c < 90^o \\ \frac{\sigma_t cos\theta_c}{\left(\frac{K}{\varepsilon}\right)^{0.5}}(1.417s - 2.12s^2 + 1.263s^3) & \theta_c > 90^o \end{cases} \quad (2.16)$$

Where,

$\sigma_t$ = the surface tension unit: N/m$^2$

$\theta_c$ = the wetting angle of the porous media

2.1.1.5 Species transport modeling in porous media

Although the Stefan-Maxwell equation is governing the multi-species diffusion in the porous media, the dilute approximation method can also provide a good result when pure oxygen is used as oxidant. Therefore, the model for validating the numerical result is using the dilute approximation method which can be described as follows.

$$\vec{J}_k = -\rho D_j \nabla Y_k \quad (2.17)$$

Where,

$D_j$ = the diffusion coefficient

$$D_j = \varepsilon^{1.5}(1-s)^{r_s} D_j^0 \left(\frac{P_0}{P}\right)^{\gamma_p} \left(\frac{T}{T_0}\right)^{\gamma_t} \quad (2.18)$$

Where,

$D_j^0$ = the mass diffusivity of species i at reference pressure and temperature unit: $m^2/s$

$P_0$ = the reference pressure unit: $N/m^2$

$T_0$ = the reference temperature unit: K

$\varepsilon$ = the porosity

$r_s$ = the exponent of pore blockage

s = the saturation term

However, when air is used as oxidant, the dilute approximation method cannot give the result accurately. Thus, Stefan-Maxwell equation, which can be described as follows, is used.

$$\vec{J}_j = -\sum_{k=1}^{N-1} \rho D_{jk} \nabla Y_k - D_{T,j} \frac{\nabla T}{T} \quad (2.19)$$

Where,

$N$ = the number of the chemical species

$D_{ij}$ = the binary mass diffusion coefficient

$D_T$ = the thermal diffusion coefficient

$$D_{ij} = [D] = [A]^{-1}[B] \quad (2.20)$$

$$A_{ii} = -\left(\frac{X_i}{D_{i,N}} \frac{M_w}{M_{w,N}} + \sum_{\substack{j=1 \\ j \neq i}}^{N} \frac{X_j}{D_{ij}} \frac{M_w}{M_{w,i}}\right) \quad (2.21)$$

$$A_{ij} = X_i \left(\frac{1}{D_{ij}} \frac{M_w}{M_{w,j}} - \frac{1}{D_{i,N}} \frac{M_w}{M_{w,N}}\right) \quad (2.22)$$

$$B_{ii} = -\left(X_i \frac{M_w}{M_{w,N}} + (1 - X_i) \frac{M_w}{M_{w,i}}\right) \quad (2.23)$$

$$B_{ij} = X_i \left( \frac{M_w}{M_{w,l}} - \frac{M_w}{M_{w,N}} \right) \quad (2.24)$$

Where,

$X_i$ = the mole fraction

2.1.1.6 Membrane modeling

The electrolyte phase conductivity can be computed by the correlation from Springer et al. [20].

$$\sigma_{mem} = \beta(0.00514\lambda - 0.00326)^{\omega} e^{1268(\frac{1}{303} - \frac{1}{T})} \quad (2.25)$$

Where,

$\lambda$ = the water content

The water content is also obtained by using Springer et al.'s correlation.

$$\lambda = \begin{cases} 0.043 + 17.18a - 39.85a^2 + 36a^3 & (a < 1) \\ 14 + 1.4(a - 1) & (a > 1) \end{cases} \quad (2.26)$$

Where,

$a$ = the water activity

The water activity is defined as,

$$a = \frac{P_{wv}}{P_{sat}} + 2s \quad (2.27)$$

The osmotic drag coefficient can be calculated by this following equation.

$$n_d = 2.5 \frac{\lambda}{22} \quad (2.28)$$

The back diffusion flux is computed as follows.

$$J_{bd} = -\frac{\rho_m}{M_m} M_{W,H_2O} D_l \nabla\lambda \quad (2.29)$$

Where,

$\rho_m$ = the density of dry membrane unit: kg/m$^3$

$M_m$ = the equivalent weight of dry membrane unit: kg/kmol

Membrane water diffusivity can be modelled using this following relation.

$$D_l = f(\lambda) e^{2416(\frac{1}{303}-\frac{1}{T})} \quad (2.30)$$

The developed CFCD models are consisted of 9 components as described in chapter 1 which indicate that the models can give a better understanding than the others since they are modelled in 3-D true dimension. Hence, CFCD is a very powerful tool which has been used so far. In next section, the discussion of CFCD role in PEFC study and its geometric parameters will be presented.

## 2.2 Previous Study

### 2.2.1 CFCD Role in PEFC Research

Since the powerfulness of CFCD has been accepted so far, they have been used in performance evaluation and parametric design optimization. However, solving the PEFC model numerically is a very complex task due to the complicated governing equation. Therefore, the quality and accuracy of the model are needed to be checked before doing a design optimization. Although several CFD best practice guidelines have been published in order to ensure the results quality [21-23], the CFCD best practice guidelines has not available yet since fuel cells are very complicated. All these following research groups attempt to create best practice guidelines of CFCD. Iranzo et al. [1] attempted to validate their model of 50 cm$^2$ commercial fuel cell stack with parallel and parallel in series flow field in several boundary conditions, such as feeding Oxygen with 100%, 60% relative humidity, and feeding Air with 60%, 0% relative humidity on the cathode side, by using model parameters which obtained from technical

data sheets, literature review and experimental measurement. However, two important parameters, platinum utilization and exchange current density, were unknown. Platinum utilization is a variable which controls the surface to volume ratio as described in equation 2.25

$$a_c = \frac{ESA}{t_{cl}} = \frac{u_{pt} \times A_s \times S}{t_{cl}} \tag{2.31}$$

Where,

| | | | |
|---|---|---|---|
| $ESA$ | = | the electrochemical surface area | unit:$m^2$-pt/$m^2$-elec |
| $t_{cl}$ | = | the thickness of catalyst layer | unit: m-elec |
| $u_{pt}$ | = | the platinum utilization | |
| $A_s$ | = | the specific surface area of platinum | unit: $m^2$-pt/g-pt |
| $S$ | = | the catalyst loading | unit: g-pt/$m^2$-elec |

Since cyclic voltammetry were not available, platinum utilization was assumed to be 0.5, which is in an acceptable range. The exchange current density, which can be determined from the Tafel plot, was adjusted to fit the polarization curve. However, their adjusted exchange current density is out of the general range. Furthermore, mesh independence analysis have been performed; 0.5, 1.0, 1.8 million mesh elements were used. It was found that the obtained solution still differed more than 5% between those two finest meshes and the finer resolution meshes cannot be accomplished according to their computing power. Note that their minimum cell angle is 19$^o$, which means there is skewed elements and thus, the mesh quality could be improved.

Arvay et al. [2] investigated convergence criteria of 50 $cm^2$ commercial single channel serpentine fuel cell by using model parameters from the published paper [1]. Polarization curve and species mass fluxes were used to prove that the solutions are converged. It was found that minimum 15,000 iterations are required to achieve an error within 5% of current density. The accuracy and efficiency of various strategies of implementing membrane models; Springer model, Nguyen and White model, and Fuller and Newman model, were compared using predicted results to validate against

experimental data by Kamarajugadda and Mazumder [3]. Moreover, this work also performed a grid independence analysis to suggest the optimum value of computational cells across each layer of the model, concluding that 10, 5, 40 computational cells across the layers is needed for gas diffusion layer, catalyst layer, and membrane, respectively. Note that their models are two-dimensional and one-dimensional through-plane CFD membrane model, which concentrate on an investigation of the transport behavior of the membrane layer. By now, all those basic analysis has to be performed in case by case to ensure the quality of PEFC CFD modeling. Once the model is validated, the parametric design evaluation and optimization, the estimation of PEFC performance, and the understanding of the complex non-linear physical and electrochemical processes occurring inside a PEFC can be done by using the model.

Shimpalee et al. have used CFD to investigate the transport behaviors of fuel cell in several works. A parallelized 3-D model of a 480 $cm^2$ PEFC flow-field selected from the US patent literature to study the distribution of current density, water, temperature and pressure has been performed using STAR-HPC software [4]. The patented flow-field gives no significant difference in power output between humidified cathode and dry cathode cases, concluding that this flow field can give a high performance with a good water management. Furthermore, it was found that by using parallel computing techniques, the computational time is significantly reduced while maintaining less than 1% error in mass balance. A simplified approach, a homogenous and stationary liquid water phase inside gas diffusion layer, was proposed to investigate the effect of water flooding in a gas diffusion layer on cell performance in a 25 $cm^2$ PEFC with triple serpentine flow channels [6]. The validation of the model was performed showing the good agreement with the experimental data.

The effect of the anisotropic gas diffusion layer thermal conductivity on the heat transfer and liquid water removal of a single channel serpentine flow field PEFC was investigated by He et al. [5]. It was found that in a comparison to isotropic case, the anisotropic gas diffusion layer produces higher temperature difference specifically on the in-plane direction. To be concluded, the isotropic gas diffusion layer is better than the anisotropic for several reasons; such as higher cell performance, uniform current density, lower material degradation, higher cell durability and others. Since it has been known that cell assembly force significantly affect the cell performance,

Zhou et al. [24] have studied the effect of single channel PEFC using ANSYS FLUENT. The results showed that the thick gas diffusion layer can sustain a larger assembly force without the risk of water flooding in gas diffusion layer and yield a less sensitivity cell performance to the variations of the assembly force while thin gas diffusion layer had a better water content, resulting in a better cell performance, however the cell performance are more sensitive to the variation of the assembly force.

In next section, the discussion of the geometric parameters of flow fields will be presented since the cell performance is significantly affected by the flow field design and can be increased up to 50% only an optimal design of the flow field is used. This discussion is based on a review of Manso et al. [10]

### 2.2.2 Geometric parameters of flow fields

The maldistribution of reactant gases is considered as a major impact on the cell performance and its efficiency since uniform distribution of reactants lead to a uniform distribution of current density, a uniform distribution of temperature and liquid water production, and reduce localized hot spots which reduce both performance degradation, and material degradation. On the contrary, maldistribution of reactants leads to non-uniform current density, and mechanical stress in membrane electrode assembly which causes performance degradation and material degradation. For this reason, the flow field designs are a very important factor because its functions are distributing the reactants to the catalyst surfaces and also helping to remove a surplus water, which causes the water flooding, from the cell. Manso et al. [10] classified the geometric parameters of flow fields into eight types; 1. Flow field designs 2. Flow direction 3. Channel length and number of channels 4. Use of baffles in the flow direction 5. Cross section shape 6. Channel and rib width 7. Channel depth (or height) 8. Height to width ratio of channel cross section. All these parameters are going to be discussed in this section.

#### 2.2.2.1 Flow field designs

Recently, the flow field geometric configurations have received a high attention as shown in an increasing of a new design in the literature (will talk about this in a later section). Depending on the operating conditions, each of these designs show

advantages and disadvantages. The most studied flow field designs; which are parallel, serpentine, interdigitated, and pin or mesh flow field, are shown in figure 2.1.

The parallel flow field is the simplest design from the point of view that flow field function is, distributing the reactant gases to the TPB which usually spread in all over catalyst layer. For this flow field, if the pressure drop on each channel is not in the same level, which may occur by the water droplet in flow channels, the reactant gases, however, may not uniformly distribute and thus, the cell performance will decrease. The serpentine flow field was proposed to solve such problem since the reactant gases are forced to flow through one single path, which may consist of one or multiple channels. The reactants flow speed and the pressure drop along the channels are both increased in this flow field configuration resulting in an enhancement of water management by removing the surplus water out of the flow channels. The interdigitated flow field is the flow field with a dead end design which forces the reactants to flow under-rib path which enhancing the use of catalysts by removing the liquid water in the porous region. The flow field that consists the pin, which generally cubical or circular, arranged in a pattern are called pin (or mesh) type flow field. This flow field has similar behaviors to parallel flow field, a maldistribution and only a few pressure drop occur.

Numerous researches have been conducted to investigate and compare the influence of the designs in cell performance. Hu et al. [25] compared parallel flow field with the interdigitated flow field using three-dimensional, steady-state numerical model. Birgersson and Vynnycky [26] studied the effect of different flow channels; the parallel (run in both co-flow and counter-flow), interdigitated, and porous flow field using CFX software. In porous flow field, the entire surface of the gas flow channel is surrounded by the porous material differs from the others, which contain dead zone between the channels. The results showed that the interdigitated flow fields performed the best in cell performance, followed in descending order by the porous, the parallel (counter-flow), and the parallel (co-flow) flow field, however, the porous provided the most uniform current distribution at the high current density. The effect of flow field designs which are; the serpentine, parallel, multi parallel (see figure 2.2a), and interdigitated flow field, on both steady and transient state cell performance of PEFC was explored by Kumar and Reddy [27] using FLUENT. It was found that in steady state case, which the current density was fixed to 5000 $A/m^2$, the interdigitated

performed the best. However, for transient state case, where the current density was suddenly increased from 5000 A/$m^2$ to 8000A/$m^2$, the parallel flow field performed the best follow by the multi-parallel, serpentine, and interdigitated flow field.

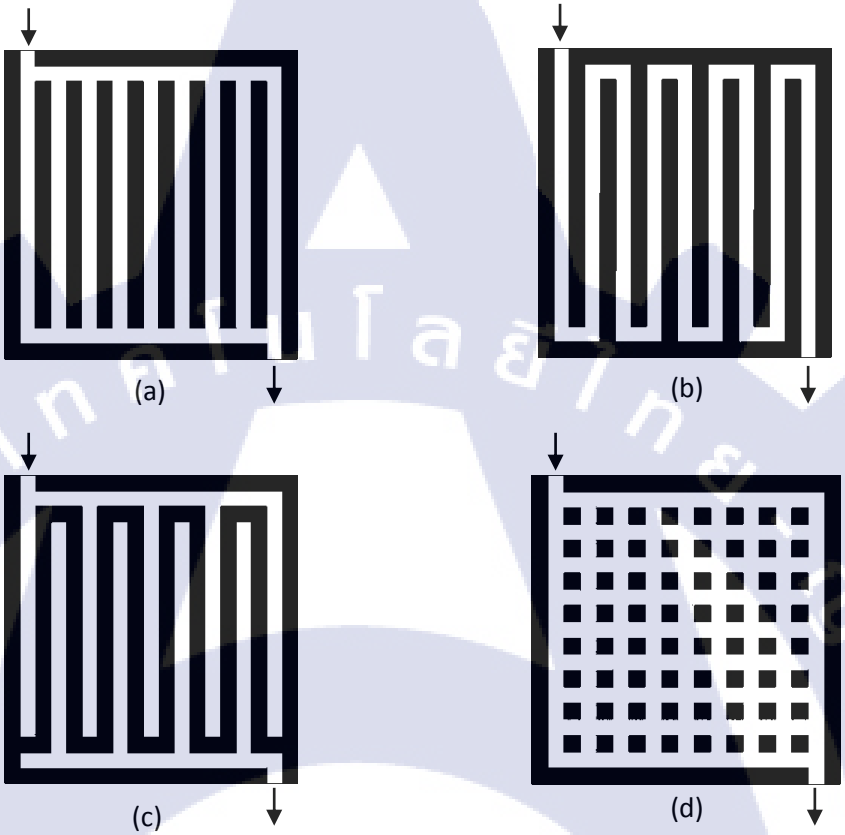


Figure 2.1 Different geometrical configurations of the gas flow field a) Parallel b) Serpentine c) Interdigitated and d) Pin-type flow field

Ferng and Su [28] compared the parallel and serpentine flow field with uniform depth and step-wise depth flow channels. The results showed that the cell performance of the parallel flow field was significantly influenced by the step-wise depth flow channels, on contrary, the serpentine flow field was insensitive to the flow channels with different depth designs. The investigation of the effect on a 10 $cm^2$ serpentine flow field with single channel, double channel, cyclic-single channel and symmetric-single channel (see figure 2.2b, c) patterns was performed by Jeon et al. [8]. The results showed that the double channel flow field had better performance and more

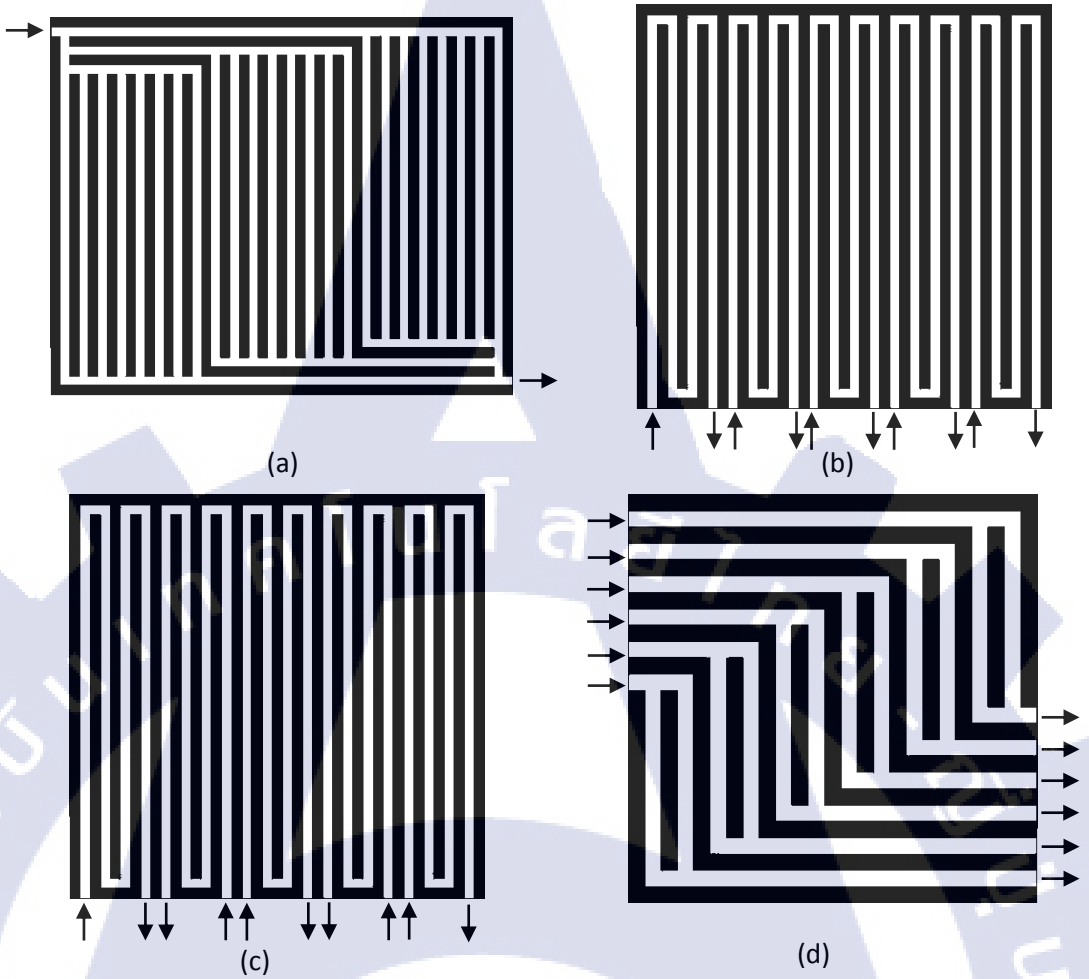


Figure 2.2 Different geometrical configurations of the gas flow field a) Multi-parallel b) Cyclic single channel c) Symmetric single channel and d) Z-type flow field

uniform current distribution at high inlet humidity. However, at low inlet humidity, the four channel serpentine flow field showed an insignificant difference in cell performance. Since the results significantly showed low pressure drop, cyclic-single channel and symmetric-single channel flow-fields were considered as good candidates in large scale system and low inlet humidity operation application. Jang et al. [29] conducted a three-dimensional numerical model of 5 $cm^2$ PEFC with different flow fields; parallel, Z-type (see figure 2.2d) and four channels serpentine flow field, to investigate the influence of the designs on reactants usage, liquid water removal, and cell performance. It was found that the serpentine flow field performed the best in cell performance, while parallel flow field performed the worst, which lead to conclude that

increasing the flow channel length in the conventional flow fields effectively raised the current density and thus, the cell performance.

The comparison of different flow field geometric configuration by using numerical simulation is repeated in several works [30 - 37]. After a study, it can be concluded as follows:

- In high voltage region, the flow field geometric configurations has an insignificant impact on the cell performance. On the other hand, the geometric configuration significantly affects cell performance in a low voltage region where concentration losses take place.
- Generally, the flow fields with low pressure drop, such as the parallel, also have a low cell performance since the maldistribution can easily occur.
- The flow fields with high pressure drop, such as the serpentine and the interdigitated, are having a high cell performance since the designs lead to more uniform reactant distribution.
- One of the main purpose of designing flow field is preventing the liquid water flooding in cathode gas diffusion layer. Therefore, using different flow field design on each side is reasonable since anode side does not need to consider the water flooding

2.2.2.2 Flow direction

Since the reactant gases flow through the flow field while the PEFC is operated, conditions of the reactants; concentration, partial pressure, temperature, relative humidity, and etc., vary as flowing along the channels. Thus, the direction of reactants flowing through the flow field on both sides is also affected the cell performance. Flow directions of the reactants which have been studied most are; co-flow, counter flow, and cross flow as shown in figure 2.3.

Ge and Yi [38] used two dimensional steady state numerical model to investigate the effect of flow mode, including co-flow and counter-flow, on ohmic resistance, water distribution, current density distribution, and the performance. Without the external humidification, the dry reactant gases can be well internally humidified when operated in the counter-flow mode, and thus high performance was

achieved. The counter-flow, however, did not show any advantageous while well humidified reactant gases were feeding.

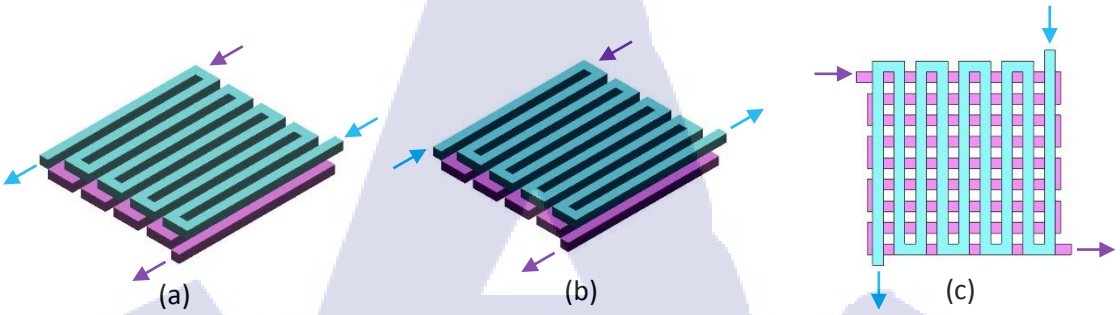


Figure 2.3 Different flow direction schemes a) Counter-flow b) Co-flow c) Cross-flow

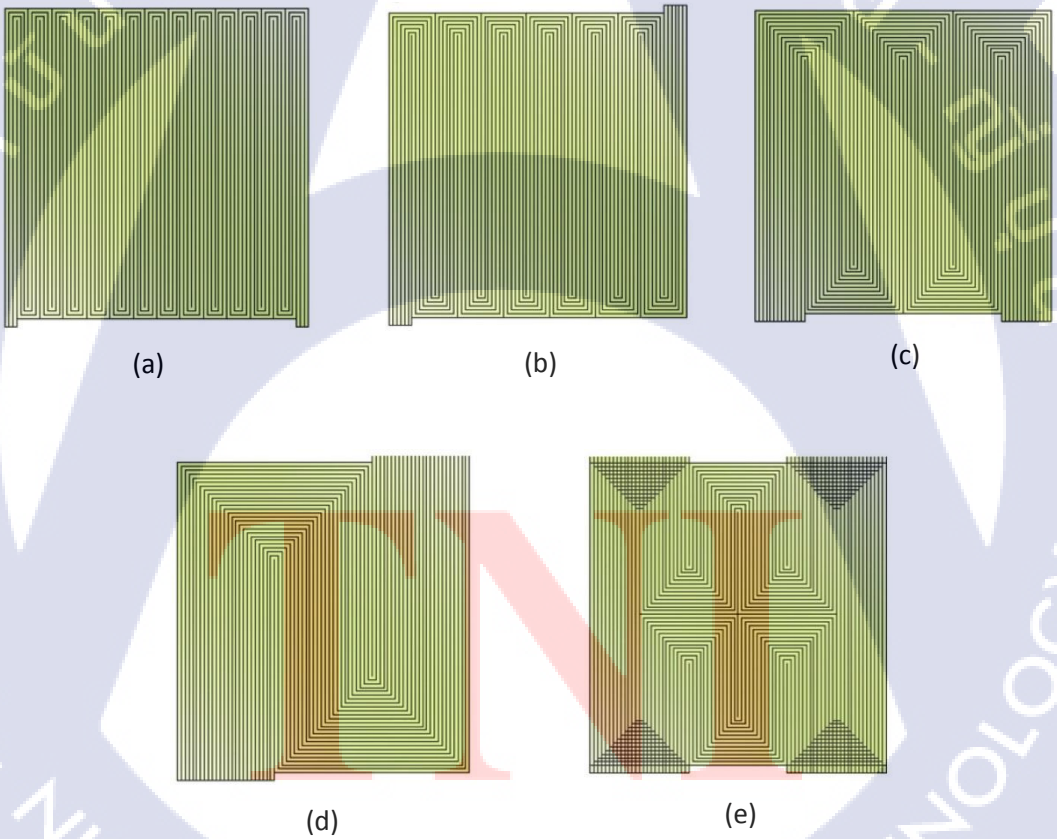


Figure 2.4 Flow field pattern [39] a) 3-channel serpentine b) 6-channel serpentine c) 13-channel serpentine d) 26-channel serpentine and e) 26-channel symmetric serpentine flow field

2.2.2.3 Channel length and number of channels

The channel length and number of channels are considered as one of the most influential parameters on the cell performance and its efficiency. Shimpalee et al. [39] studied the impact of channel path length of PEFC using STAR-CD. 200 $cm^2$ serpentine flow fields with different number of channels, and thus different channel length, were modelled (see figure 2.4). The results showed that the current density of PEFC with shorter path lengths was more uniformly distributed and also lesser condensed liquid water than the longer paths. From a single cell performance, the 13-channel flow field gave the best performance for a 200 $cm^2$ PEFC. The 26-channel flow field, however, was considered as an optimal choice for making a PEFC stack since the current density distribution was more uniform and the pressure drop was much lower. The effect of increasing channel path length on the reactants distribution and cell performance in an interdigitated flow field was explored by Santamaria et al. [40]. The computational model showed that the longer channels lead to a maldistribution, while more uniform distribution was observed in the shorter channels. Experiment also confirmed that the performance of the 5 $cm^2$ interdigitated flow field outperformed the 25 $cm^2$ since the maximum power density of the short interdigitated flow field was 33.9% and 12.7% greater than the long for both normal and excess flow conditions respectively.

2.2.2.4 Use of baffles in the flow direction

As the reactants need to diffuse through gas diffusion layer to reach TPB within the catalyst layers where the electrochemical take places, the proposal of using baffles in the flow direction has been proposed since there are parts of the reactants, which do not react at the TPB, flow away and hence, the unreacted gas is found at the outlet of the flow channel, which is considered as a reduction of the system efficiency. The numerical investigation of the effect of the flow channel design with baffles was explored by Liu et al. [41] concluding that both the reactant transport and cell performance can be enhanced, especially at the low voltage region, by the presence of the baffles in the gas flow channel. Soong et al. [42] investigated the reactant gas transport in a PEFC with the gas flow channel partially blocked by installing baffle plates. It was found that the oxygen flux in cathode catalyst layer would become higher

when the number of baffles in the flow channels is increased, and hence the higher cell performance. However, increasing amount of baffles reduced the overall cell performance due to an increasing of pressure drop, which implies that there is an optimum number of baffles that enhances the overall cell performance. A novel baffled flow field design, as shown in figure 2.5, with a significant better performance than the conventional design was proposed by using three-dimensional numerical model [43]. The results showed that the compressor power needed to overcome the pressure drop of the novel design can be neglected as compared to the cell power output.

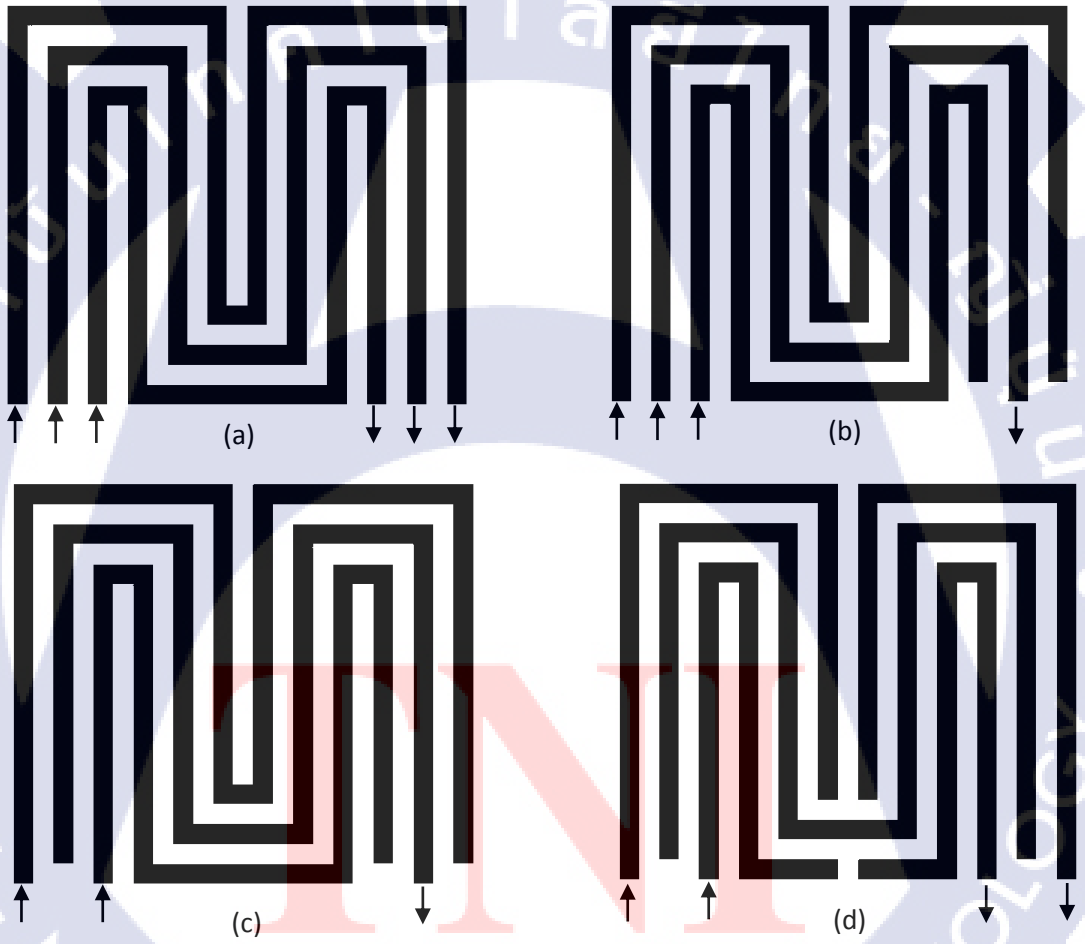


Figure 2.5 Flow field designs [43] a) SFF b) SBFF-1 c) SBFF-2 d) SBFF-3

A two-dimensional numerical model had been conducted to examine the effects of humidity of reactants in the baffled flow field on the transport phenomena and cell performance by Jang et al. [44]. At low voltage region, increasing the relative

humidity of reactant gases in cathode side leads to the reduction of oxygen concentration, and thus the cell performance decreased.

2.2.2.5 Cross-section shape

Although channels with semicircular, trapezoidal, triangular, and others cross-section have been studied, PEFC with rectangular channel cross-section is still mostly used since it can reproduce easily. Kumar and Reddy [45] developed a numerical three-dimensional half-cell (anode) model to investigate the effect of different channel dimensions and shapes on the transport behaviors and cell performance by using FLUENT. It was found that the optimum value of channel width, land width, and channel depth were close to 1.5, 0.5, and 1.5 mm, respectively. Furthermore, triangular and hemispherical cross-section shaped channels, which the land width was close to 0 mm, were also explored. The results showed that both triangular and hemispherical cross-section shaped channels increased hydrogen consumption by 9 % over the rectangular, and thus the better performance was obtained.

Ahmed and Sung [46] investigated the effect of three different channel cross section; rectangular, trapezoidal, and parallelogram, on low voltage region. The results revealed that, when their height were same, the rectangular channel cross-section gave higher power output, while the trapezoidal channel cross-section gave more uniform reactant and current density distributions. The channel and rib width ratio of 1.3-1.4 was suggested as an optimum value for the rectangular. In production process, machining tolerances, tool wear, and different manufacturing process could possibly cause a variations in channel depth, which was expected to affect the performance. The effect of draft angle and etch factor on the cell performance was numerically studied by Shimpalee et al. [47]. The results can be concluded that higher draft angle gave low performance and pressure drop, while the effect of channel radius at the turning was not significant. Consider the effect of non-uniformity channel depth, for well hydrated membrane condition, shallower channels at the outlet gave more uniform distribution as compared to shallower channels at the inlet and uniform channel depth, while, for dry membrane case, the uniform channel depth showed the most uniform distribution. However, the researchers stated that the effect of channel depth on the overall performance is minimal.

2.2.2.6 Channel and rib width

Several researches have studied the influence of channel and rib width, as displayed in figure 2.6, which are considered that the effect of these parameters are more evident in low potential region because of mass transport limitation, and suggested that, in each particular case, the optimal values of those parameters, which enhance the performance, are existed. Sun et al. [48] studied the effect of channel-to-rib width ratio by using an improved two-dimensional model, and the results indicated that increasing channel to rib width, resulting in an improvement of water management and also enhancing the overall ORR rate. Too high ratio, however, lead to worse performance. Ying et al. [49] has performed a numerical simulation using STAR-CD for three cases of different channel width, 2, 3, and 4 mm, while the rib width was fixed to 1 mm and the results showed that the 3 mm channel width gave the best performance.

The effect of the channel design, including the ratio of the number of channels and the channel-to-rib width ratio have been investigated amongst several parameters using Taguchi method by Lee et al. [50]. It was found that the geometric parameters of the flow field mainly contributed an increase of cell performance by affecting concentration loss. Case 3, which cathode channel height to anode channel height ratio, cathode channel-to-rib ratio, anode channel-to-rib ratio, the ratio of number of channels, cathode GDL thickness, anode GDL thickness, cathode GDL permeability, and anode GDL permeability were 2:1, 4:3, 3:4, 1:2, 0.2 mm, 0.2 mm, $10^{-12}$ $m^2$ , and $10^{-12}$ $m^2$, respectively, showed the maximum power, but the pressure drop was high. The obtained set of optimum parameters was in case 18, which those values were 3:1, 3:4, 3:4, 1:1.5, 0.3 mm, 0.25 mm, $10^{-12}$ $m^2$ , and $10^{-8}$ $m^2$, respectively. Shimpalee et al. [51] numerically studied the effect of rib and channel dimension on the performance. The results indicated that, for well hydrated membrane, the narrower channel with wider rib gave a slightly better performance, while, for dry membrane, the wider channel with narrower rib gave a higher performance. However, the authors stated that the channel and rib width effect showed less sensitive to the cell performance as compared to channel path length in the reference [39].

Similar studies were repeated in Scholta et al. [52], which analyzed a model of parallel flow field with counter-flow, and Wang et al. [53], which parallel and interdigitated flow field were modelled.

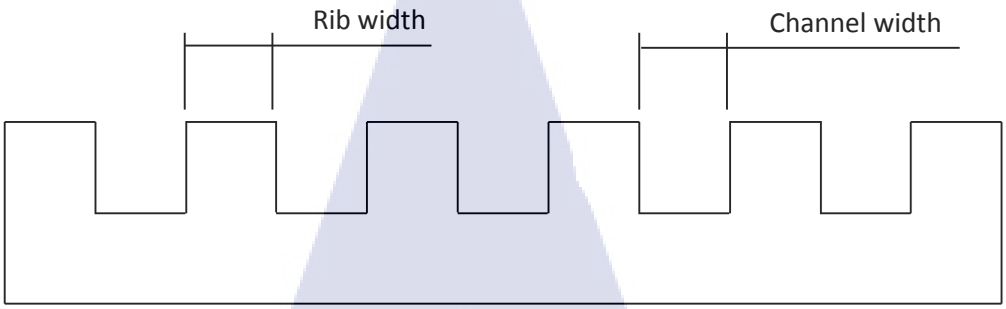


Figure 2.6 Schematic of channel and rib width

2.2.2.7 Channel depth

Although many literatures were found focusing on the analysis of other geometric parameters of flow channel which effected the channel depth (or height), only a few papers have focused in an investigation of the influence of the channel depth on the PEFC cell performance. Yan et al. [54] proposed a novel straight flow channel tapered in height or width (as shown in figure 2.7) enhancing the efficiency of fuel utilization resulting that with the tapered channel design either decreasing height or increasing width, the fuel transport through porous media, fuel utilization, the capability of the liquid water removal, and thus cell performance could be increased. Considering of pressure loss, height taper ratio of 0.5 and weight taper ration of 1.8 was suggested as optimal values. The effects of tapered flow channel on the reactant gas transport and the cell performance were examined in Liu and his co-workers [55]. The authors stated that the effects of the tapered channel were significant in low voltage region since it forced more reactants into gas diffusion layer resulting in a better cell performance.

Yan et al. [56] conducted a three-dimensional numerical model to investigate the effects of reductions of the outlet channel flow area (figure 2.8) on cell performance and transport behaviors. The results showed that with an increasing of the outlet channel height contraction ratio ($H_c/H_0$), the reactant velocities increased significantly around the contracted outlet channel, which improved the cell performance and the outlet channel height contraction ratio of 0.4 was suggested as an optimal value. Moreover, the larger length contraction ratio ($L_c/L_0$) also enhanced the cell performance. Several works of similar study [57], [58] were repeated and found

that the maximum power output can be increased around 9.5-11.9% with an optimal design.

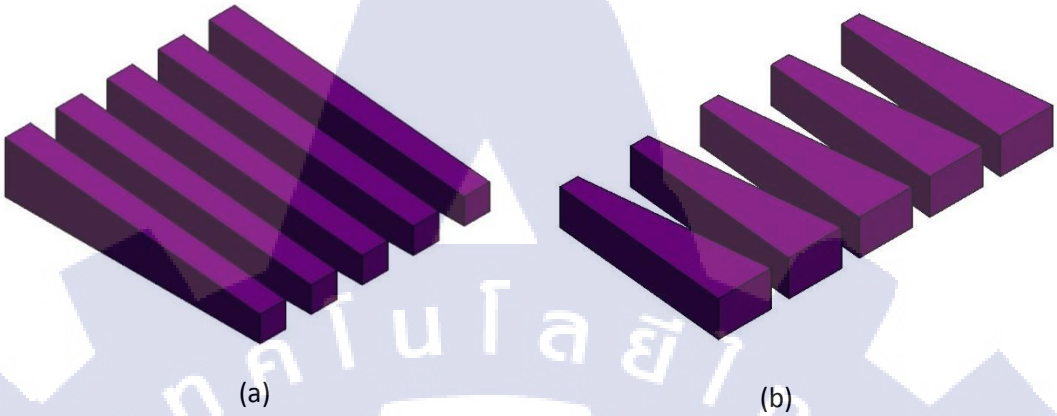


Figure 2.7 Straight flow channel tapered in a) height and b) width [54]

2.2.2.8 Height to width ratio of the channel cross-section

Only a few works interested in the influence of height to width ratio of the channel cross-section on the cell performance. Moreover, they studied only the effects in serpentine channel flow field of both single, and multiple channel. The effects of different channel heights and widths of a 25 $cm^2$ 5 channel 4-turns serpentine flow field were numerically investigated by Choi et al. [59]. The results showed that as the channel height increased, the pressure drop was decreased due to an increase in cross-sectional area of channel flow resulting in an accumulation of liquid water at the outlet, and hence the cell performance was slightly decreased. However, the current distribution remained mostly unchanged. Besides, as the channel width increased, the cell voltage was decreased greatly as compared to an increase in channel height. Additionally, it was found that the wider configuration showed poor water management, and thus membrane dehydration occurred since the formed water was unable to diffuse back to anode side by the back diffusion. Manso et al. [9] observed the influence of the channel cross-section aspect ratio in 10 different cases, varying between 0.07 and 15, on the cell performance. The obtained results showed that the channel cross-section aspect ratio was insignificant in high voltage region. As expected, in low voltage region, the channel cross-section aspect ratio significantly affected the

cell performance. The authors stated that, generally, the models with high aspect ratio gave more uniformity of the current distribution, and thus the overall performance was increased. From this work, the aspect ratio of 10/06 and 12/05, which the first and the second number represent value of height and width, respectively, were suggested as the optimal values.

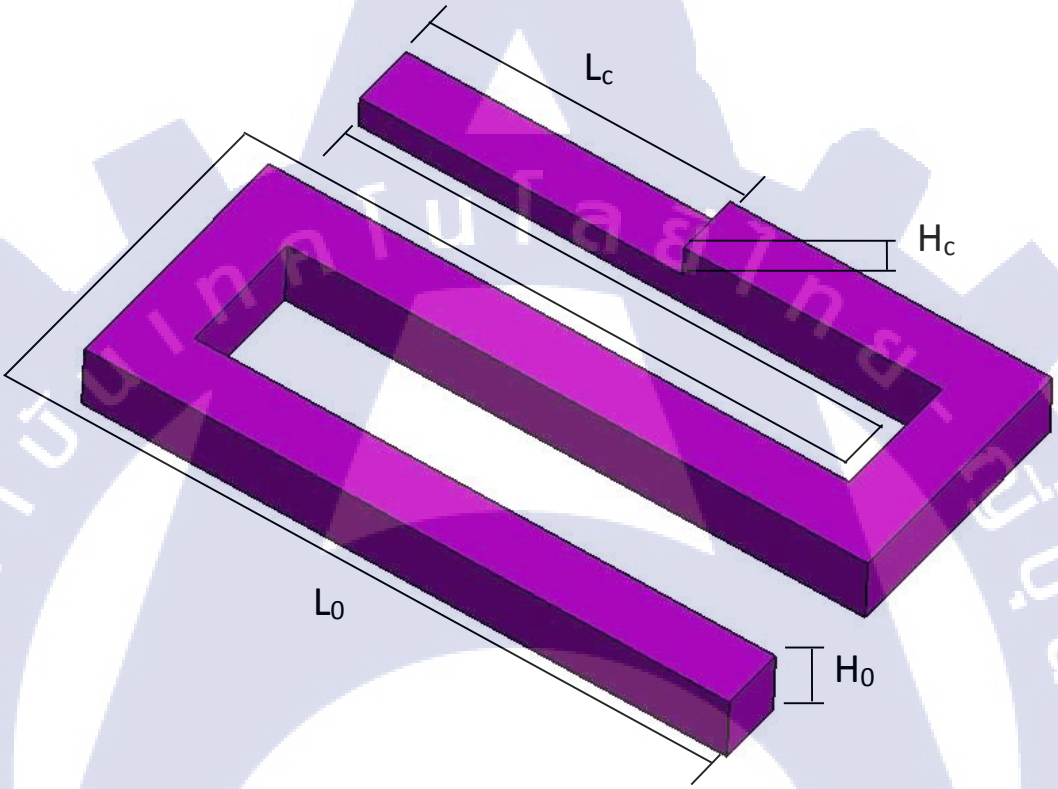


Figure 2.8 Flow field with the reductions at the outlet channel flow area

Apart from the investigation of the influence of the common geometric parameters of the flow fields, numerous studies interested in proposing the new flow field designs, and such a study tend to increase and receive more attention in this recent year. The work of Kuo et al. [60] is a one of the great examples of an attempt to propose a novel flow channel. They conducted a numerical model to investigate the effect of the wave-like flow channel on transport behaviors and the cell performance. The results revealed that the wave-like flow channel significantly improved cell performance as compared to a conventional straight flow channel. Wang et al. [61] proposed a novel biometric flow field which gave higher flow uniformity, lower pressure drop, and hence

a better performance than the conventional serpentine and parallel flow field. The investigation of new flow channel patterns; a leaf design and a lung design (see figure 2.9), was presented by Kloess et al. [62]. The authors stated that these bio-inspired flow channel designs were a combination of advantages of the conventional serpentine and interdigitated flow field. As a result, both the leaf and lung design gave a higher peak power output for 30% more than the conventional design. Furthermore, a lower pressure drop was also investigated. The numerical analysis of new bio-inspired flow field design was conducted by Roshandel et al. [63]. It was found that the design produced 56% and 26% higher than conventional parallel and serpentine flow field, respectively. In two similar works of same research group [64], [65] presented the improvement of cell performance by using annular shaped bipolar plates. However, from our current technologies, the knowledge of producing membrane electrode assembly which is not flat are not existed since membrane electrode assembly are very thin and delicate. Cano-Adrade et al. [66] presented the numerical results of a novel radial flow field design and the authors stated that the design could be a strong candidate in replacing the conventional commercial design in the near future. The analysis of the entropy generation using Fermat's spiral flow distributor and the proposal of a new dimensionless parameter had been presented [67], [68].

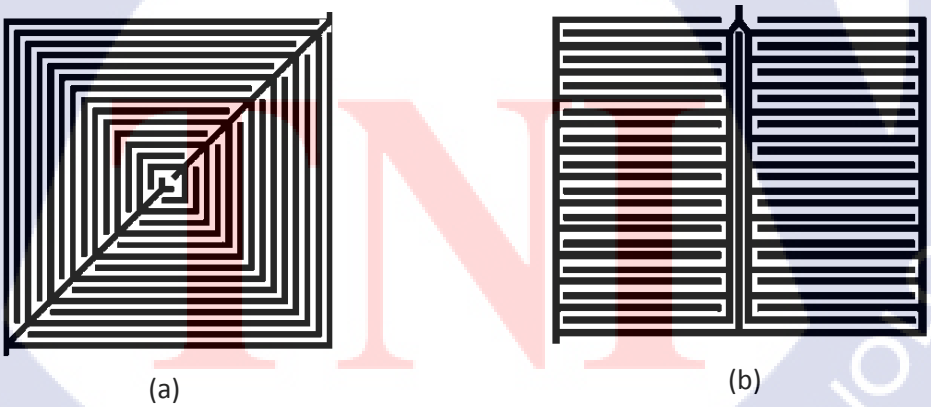


Figure 2.9 Bio-inspired flow fields [62] a) leaf design b) lung design

Note that, in past decades, the single-inlets single-outlet flow fields were mainly focused by researchers since it would be a very difficult task to balance the

amount of the reactants into each inlet of the multi-inlets flow field. However, recently, Toyota motor corporation launched Toyota Mirai, its first commercial fuel cell vehicle, and claimed that the flow field (called 3D fine-mesh), which is the multi-inlets flow field, used in this car contributed a better distribution and water removal.

## 2.3 Related Research

After a study, there are a lot of designs of flow channel configuration in distributing the reactant gases. Serpentine channel configurations are the most widely studied in academic literature since it is a commercial cell, such as the one from Electrochem, which is considered of giving an excellent performance, and in addition, it is one of the simplest designs. Parallel in series flow field design, which is also a 5 $cm^2$ commercial cell of Electrochem, however, received less attention in an investigation of the effects on PEFC cell performance (see figure 1.3). The discussion of the collected research which investigates the transport behaviors of parallel in series flow fields configuration will be presented as follows.

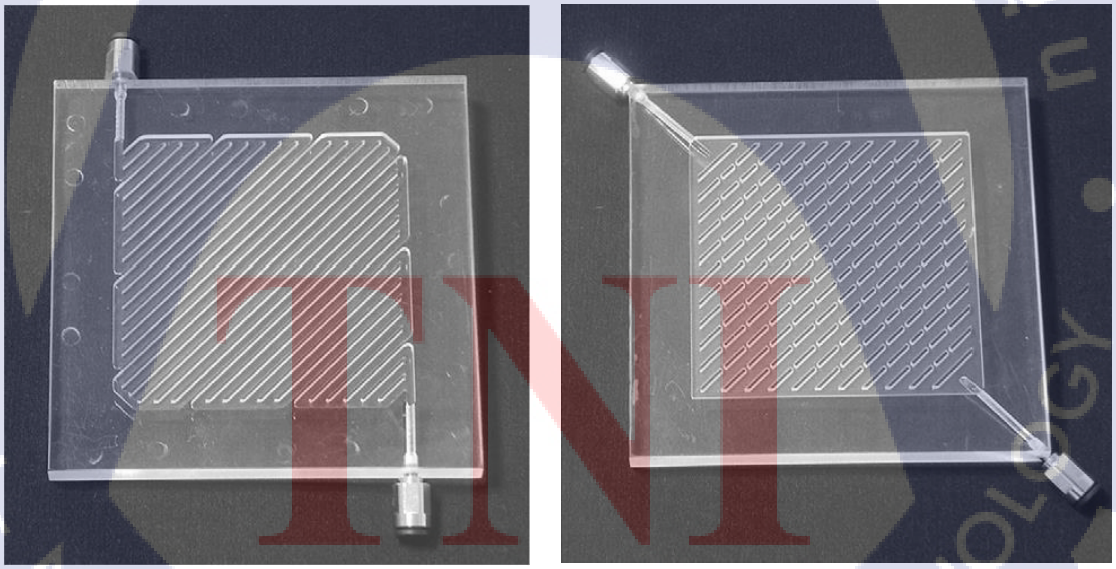

(a) (b)

Figure 2.10 Photographs of transparent bipolar plates [69] a) parallel in series b) cascade-type flow field

Lopez et al. [69] conducted an experiment to observe the water management between two different flow-fields, including parallel in series and cascade type, in PEFC. In order to visualize the processed, the bipolar plates have been created of transparent plastics (see figure 2.10).

Therefore, this fuel cells have been operated at low current density values (below 0.1 A $cm^{-2}$) since bipolar plates were made of plastic, which low thermal and electrical conductivities. The results demonstrated that the pressure was always higher in parallel in series flow field which indicated that a lower overall efficiency was always found in the flow field since more energy was required for operating the cell. It was clearly seen that the amount of water inside the cell was higher in the parallel in series flow field. Furthermore, at high relative humidity which close to 100%, the liquid water flooding has been observed only in parallel in series flow field. As a result, cascade type flow field allowed a better liquid water management as expected. However, it is clearly seen that there are a limitation in experiment, which numerical simulation could play an important role in observing such effects.

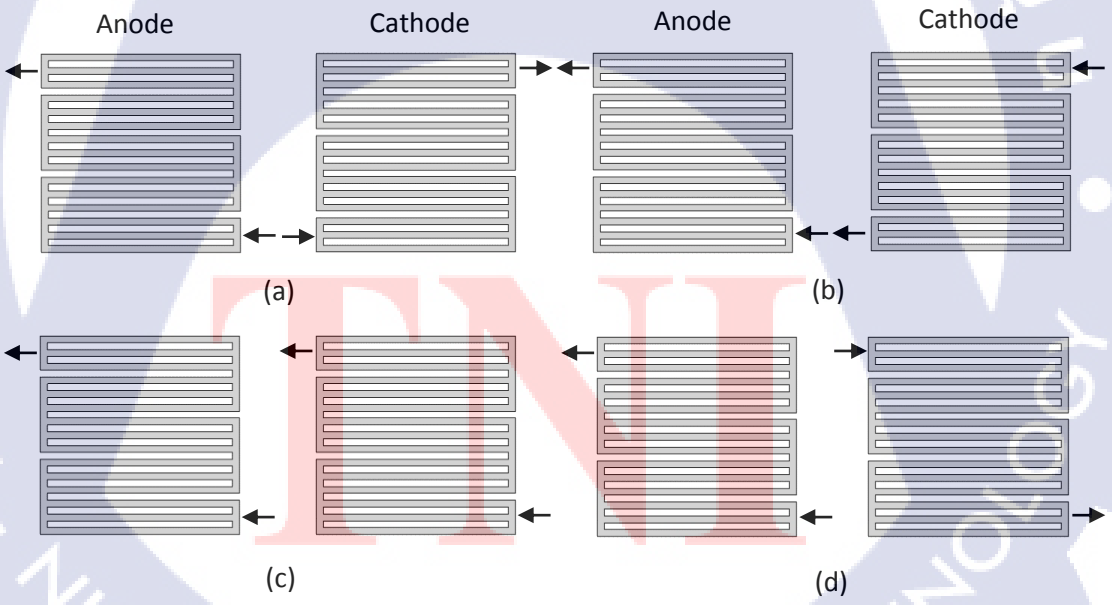


Figure 2.11 Different flow directions [70] a) cross-flow b) non-symmetric flow c) similar flow d) counter-flow

Numerical analysis of the effect of different gas feeding modes (or flow direction), including cross-flow, non-symmetric flow, similar-flow, and counter-flow, which define differently from other papers (see figure 2.11), in a 5 $cm^2$ parallel in series flow field design commercial cell of Electrochem was conducted using ANSYS FLUENT by Sierra et al. [70]. The mode of feeding gases that showed the most uniform current distribution was similar flow. From the polarization curve, however, the co-flow mode gave the best performance as shown in higher current density.

Lu and Reddy [71] studied the performance of micro-PEFC with 4 different flow field designs, including three channels parallel in series, single channel serpentine, two channels parallel in series, and z-type multi-parallel flow field. The results showed that at the high gas flow rate, the flow field with a narrow channel width and long channel length gave an excellent performance. However, with the lower gas flow rate, the flow field with a narrow channel width and long channel length performed badly due to the liquid water flooding effect. The authors suggested that the micro PEFC should use the flow field with a mixed of multi-channel and long channel design, which is clearly seen from the polarization curve that two channels parallel in series flow field gave the best performance.

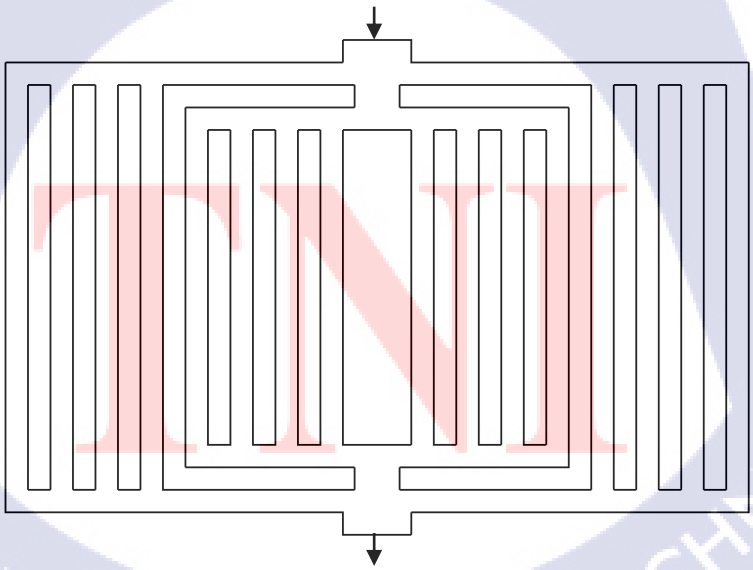

Figure 2.12 Schemetic illustration of multiple-U parallel flow field [11]

Development of an algorithm to investigate the pressure drop and flow distribution in various flow field configurations, including serpentine, parallel, multiple-U type parallel (see figure 2.12), and multiple-Z type parallel (or parallel in series) flow field, has been performed by Maharudrayya et al. [11]. The results had been validated against the obtained results from three-dimensional CFD simulations. As expected, serpentine flow field significantly showed higher pressure drop while parallel flow field gave non-uniformity of flow distribution. To reduce the latter problem, with insignificant increasing in pressure drop, multiple-U type parallel flow field had been proposed. Although multiple-Z type parallel gave the best in uniformity of flow distribution, the pressure drop were much higher.

Since a good flow field design gives a uniform distribution, low material and cell degradation are hypothetically expected, current distribution measurement are one of the tools which is used to investigate the characteristics of flow field designs. Lobato et al. [72] performed a study of flow field in high temperature PEFC using the measurement. It was found that the parallel in series and pin-type flow field gave better current distribution amongst others two flow fields. Furthermore, when using pure oxygen on cathode side, the flow fields performed 25 % higher in power output. When using air on the cathode side, however, interdigitated flow field performed as well as the flow fields. The variation of channel width and height of parallel in series flow field has also performed. The results showed that wider channel slightly gave a better performance in low voltage region, while higher channel have an insignificant effect. It should be noted that although interdigitated flow field gave a good performance when using air as oxidant, the flow fields, especially the pin-type, were required much lower operating power to compensate the pressure drop.

Lobato et al. [73] also performed a numerical investigation of the influence of flow field designs, including parallel in series, parallel, and pin-type flow field, in high temperature PEFC. The results demonstrated that using parallel flow field gave a bad uniformity of current distribution, while parallel in series performed best, although the difference between pin-type and parallel in series flow field can only be observed at low voltage region.

The key findings in the previous studies mentioned above are summarized in Table 2.1. The details of the research methodology of this research are presented in chapter 3.

Table 2.1 Summary of literature study

| Researchers | Year | EA/NS | Study | Results | Notice |
|---|---|---|---|---|---|
| CFCD Role in PEFC Research | | | | | |
| Iranzo et al. [1] | 2010 | EA/NS | Model Validation | Their models are validated in several boundary condition by using model parameters which obtained from technical data sheets, literature review and experimental measurement | **Best practice guidelines** |
| Arvay et al. [2] | 2012 | NS | Convergence criteria | Minimum 15,000 iterations are required to achieve an error within 5% of current density | Basic analysis has to be performed in case by case to ensure the quality of PEFC CFD modelling |
| Kamarajugadda and Mazumder [3] | 2008 | NS | Investigation of the accuracy and efficiency in different membrane model | Grid independence analysis to suggest the optimum value of computational cells across each layer of the model concluding that 10, 5, 40 computational cells across the layers is needed for gas diffusion layer, catalyst layer, and membrane, respectively. | |

Table 2.1 Summary of literature study (Continued)

| Researchers | Year | EA/NS | Study | Results | Notice |
|---|---|---|---|---|---|
| Shimpalee et al. [4] | 2004 | NS | Water and current distribution | The patented flow-field gives no significant difference in power output between humidified cathode and dry cathode cases | **Transport Simulation**<br><br>CFD has been a powerful tool to study the problem of water, current density, temperature and pressure distribution inside a PEFC for a decade or more |
| Shimpalee et al. [6] | 2007 | NS | Flooding effects using a simplified technique | A simplified approach, a homogenous and stationary liquid water phase inside gas diffusion layer, gave the results which showed a good agreement with the experimental data | |
| He et al. [5] | 2010 | NS | Heat transfer of anisotropic GDL thermal conductivity | The isotropic gas diffusion layer is better than the anisotropic for several reasons | |
| Zhou et al. [24] | 2013 | NS | The effect of assembly force | Thick gas diffusion layer can sustain a larger assembly force without the risk of water flooding in gas diffusion layer and yield a less sensitivity cell performance to the assembly force | |
| Manso et al. [10] | 2012 | - | Review the influence of geometric parameters | They classified geometric parameters into 8 categories and the flow field design is the most important factor | **Review**<br><br>Flow field design was a major issue in the study, however, parallel in series flow field has received a low attention |

Table 2.1 Summary of literature study (Continued)

| **Researchers** | **Year** | **EA/NS** | **Study** | **Results** | **Notice** |
|---|---|---|---|---|---|
| Flow field designs | | | | | |
| Cha et al. [35] | 2004 | NS | Comparison of 3 different flow fields | • In low voltage region, the flow field geometric configurations has a significant impact to cell performance while in high voltage region, their effects are insignificant.<br>• The flow fields with low pressure drop generally have a worse cell performance as compare to the higher pressure drop since the maldistribution can easily occurs.<br>• Using different flow field design in each sides is reasonable | None of these has focused on parallel in series |
| Jang et al. [29] | 2008 | NS | | | |
| Wang et al. [31] | 2009 | NS | | | |
| Ramos-Alvarado et al. [34] | 2012 | NS | | | |
| Birgersson and Vynnycky [26] | 2006 | NS | Comparison of 4 different flow fields | | |
| Kumar and Reddy [27] | 2006 | NS | | | |
| Boddu et al. [32] | 2009 | NS | | | |

Table 2.1 Summary of literature study (Continued)

| Researchers | Year | EA/NS | Study | Results | Notice |
|---|---|---|---|---|---|
| Hu et al. 25] | 2004 | NS | Comparison of parallel and interdigitated flow fields | • In low voltage region, the flow field geometric configurations has a significant impact to cell performance while in high voltage region, their effects are insignificant.<br>• The flow fields with low pressure drop generally have a worse cell performance as compare to the higher pressure drop since the maldistribution can easily occurs.<br>• Using different flow field design in each sides is reasonable | None of these has focused on parallel in series |
| Ferng and Su [28] | 2007 | NS | Comparison of parallel and single serpentine flow fields | | |
| Jeon et al. [8] | 2008 | NS | Comparison of different serpentine flow field designs | | |
| Zhang et al. [30] | 2009 | NS | Comparison of different parallel flow field designs | | |
| Lee et al. [33] | 2011 | NS | Comparison of multi and single inlet serpentine flow field | | |
| Wang et al. [36] | 2011 | NS | Transient state comparison of parallel and interdigitated flow fields | | |
| Li et al. [37] | 2011 | NS | Transient state comparison of 3 different flow fields | | |

Table 2.1 Summary of literature study (Continued)

| Researchers | Year | EA/NS | Study | Results | Notice |
|---|---|---|---|---|---|
| Flow direction | | | | | |
| Ge and Yi [38] | 2003 | NS | Comparison of different flow modes | The dry reactant gases can be well internally humidified when operated in the counter-flow mode. However, The counter-flow did not show any advantageous while well humidified reactant gases were feeding | Although, while well humidified reactants were used, the result showed insignificant different, the counter-flow showed the best performance. |
| Channel length and number of channels | | | | | |
| Shimpalee et al. [39] | 2006 | NS | Comparison of different channel length of serpentine flow fields | The 13-channel flow field gave the best performance. However, The 26-channel flow field were considered as an optimal choice for making a PEFC stack due to their lesser pressure drop | The effect of the channel path length has been observed only in serpentine design. |
| Santamaria et al. [40] | 2013 | NS | Comparison of different channel length of interdigitated flow fields | The longer channels leads to a maldistribution | The effect of the channel path length has been observed only in interdigitated design. |
| Use of baffles in the flow direction | | | | | |
| Liu et al. [41] | 2005 | NS | The effect of the flow channel design with baffles | In low voltage region, the performance can be enhanced by using the baffles | |

Table 2.1 Summary of literature study (Continued)

| Researchers | Year | EA/NS | Study | Results | Notice |
|---|---|---|---|---|---|
| Soong et al. [42] | 2005 | NS | The effect of the partial blocked flow channel design | When increasing the number of baffles in the flow channels, the higher cell performance is obtained. However, increasing amount of baffles reduced the overall cell performance due to an increasing of pressure drop | The parallel in series flow field can be considered as parallel flow field with fully blocked baffles |
| Dong et al. [43] | 2007 | NS | Study the behaviour of their novel serpentine-baffle flow field design | The compressor power needed to overcome the pressure drop of the novel design can be neglected as compared to the cell power output | |
| Jang et al. [44] | 2006 | NS | The effect of the flow channel design with baffles | Increasing inlet relative humidity in the cathode at lower operating voltages leads to insufficient mass concentration and furthermore, more liquid water produced and filled the pore in the porous media. Thus, the cell performance was decreased with and increasing of baffles | |
| Channel cross-section | | | | | |
| Kumar and Reddy [45] | 2003 | NS | The effect of the channel cross-section | Both triangular and hemispherical cross-section shaped channels increased Hydrogen consumption by 9 % over the rectangular. However rectangular cross-section showed a significant lower pressure drop | Even though the effect of different channel cross-sections have been studied, the rectangular is used in commercial cell. |

Table 2.1 Summary of literature study (Continued)

| Researchers | Year | EA/NS | Study | Results | Notice |
|---|---|---|---|---|---|
| Ahmed and Sung [46] | 2006 | NS | The effect of three different channel cross section | The rectangular channel cross-section gave higher power output, while the trapezoidal channel cross-section gave more uniform reactant and current density distributions | Even though the effect of different channel cross-sections have been studied, the rectangular is used in commercial cell. |
| Shimpalee et al. [47] | 2011 | NS | The effect of draft angle and etch factor on the cell performance | Higher draft angle gave low performance and pressure drop | |
| Channel and rib width | | | | | |
| Sun et al. [48] | 2005 | NS | The effect of channel-to-rib width ratio | Increasing channel to rib width resulted in an improvement of water management. However, too high ratio lead to worse performance. | The channel and rib width effect showed less sensitive to the cell performance as compared to channel path length |
| Ying et al. [49] | 2005 | NS | The effect of different channel width | The 3 mm channel width gave the best performance | |
| Lee et al. [50] | 2008 | NS | Channel-to-rib width ratio has been investigated amongst several parameters using Taguchi method | Taguchi method can be useful to get the optimal combination between design parameters in the system design | |

Table 2.1 Summary of literature study (Continued)

| Researchers | Year | EA/NS | Study | Results | Notice |
|---|---|---|---|---|---|
| Shimpalee and Van Zee (2007) [51] | 2007 | NS | The effect of different rib and channel dimension | For well hydrated membrane, the narrower channel with wider rib gave a slightly better performance, while, for dry membrane, the wider channel with narrower rib gave a higher performance. | The channel and rib width effect showed less sensitive to the cell performance as compared to channel path length |
| Scholta et al. (2006) [52] | 2006 | NS | The effect of different rib and channel dimension in parallel flow field | Narrow channel dimensions are preferred for high current densities, whereas wider dimensions are better at low current densities | |
| Wang et al. (2007) [53] | 2007 | NS | The effect of different rib and channel dimension in parallel and interdigitated flow field | In parallel flow field, the cell performance improved as the increasing of the flow channel area ratio. For interdigitated flow field, however, the effect was insignificant. | |
| Channel depth and Height to width ratio of the channel cross-section | | | | | |
| Yan et al. (2006) [54] | 2006 | NS | Proposed a novel straight flow channel tapered in height or width | Both decreasing height and increasing width positively affect the cell performance | There is a difficulty in producing the flow fields, and it cannot be commercial cell in the near future. |
| Liu et al. (2006) [55] | 2006 | NS | The effects of tapered flow channel | The effects of the tapered channel were significant in low voltage region | |

Table 2.1 Summary of literature study (Continued)

| Researchers | Year | EA/NS | Study | Results | Notice |
|---|---|---|---|---|---|
| Yan et al. [56] | 2008 | NS | The effects of reductions of the outlet channel flow area | The outlet channel height contraction ratio of 0.4 was suggested as an optimal value | There is a difficulty in producing the flow fields, and it cannot be commercial cell in the near future. |
| Wang et al. [57] | 2010 | NS | Propose the flow field with varying channel heights | The maximum power output can be increased 11.9% with the design | |
| Fontana et al. [58] | 2011 | NS | The effects of flow channel tapered in height | The peak current density can be increased 9.5 with an angle of 0.75º | |
| Choi et al. [59] | 2011 | NS | The effects of different channel height and width ratio | As the channel height increased, the pressure drop was decreased and the cell performance was also slightly decreased. However, as the channel width increased, the cell voltage was decreased greatly | |
| Manso et al. [9] | 2011 | NS | The effects of different channel height and width ratio | The models with high aspect ratio gave more uniformity of the current distribution, and thus the overall performance was better. | |

Table 2.1 Summary of literature study (Continued)

| Researchers | Year | EA/NS | Study | Results | Notice |
|---|---|---|---|---|---|
| New flow field designs | | | | | |
| Kuo et al. [60] | 2008 | NS | Wave-like flow channel | The channel showed significant improved cell performance as compared to a conventional straight flow channel | From our current technologies, there are several barriers in producing such flow fields and also the knowledge of producing membrane electrode assembly which is not flat are not existed |
| Wang et al. [61] | 2010 | NS | Novel biometric flow field | The flow field could give higher flow uniformity, lower pressure drop, and hence a better performance than the conventional serpentine and parallel flow field. | |
| Kloess et al. [62] | 2009 | NS | A leaf design and a lung design flow field | Both the leaf and lung design gave a higher peak power output for 30% more than the conventional design. Furthermore a lower pressure drop was also investigated. | |
| Roshandel et al. [63] | 2012 | NS | New bio-inspired flow field design | The design produced 56% and 26% higher than conventional parallel and serpentine flow field, respectively. | |
| Khazaee and Ghazikhani [64] | 2011 | NS | Annular shaped bipolar plates | The cell performance wass increased as the number of connections between GDL and bipolar plate increased | |
| Khazaee et al. [65] | 2012 | NS | Annular shaped bipolar plates | Differently from conventional PEFC, the performance enhanced in an increasing of the thickness and a decreasing of the porosity of GDL. | |

Table 2.1 Summary of literature study (Continued)

| **Researchers** | **Year** | **EA/NS** | **Study** | **Results** | **Notice** |
|---|---|---|---|---|---|
| Cano-Andrade et al. [66] | 2010 | NS | Novel radial flow field design | The design could be a strong candidate in replacing the conventional commercial design in the near future | From our current technologies, there are several barriers in producing such flow fields and also the knowledge of producing membrane electrode assembly which is not flat are not existed |
| Rangel-Hernandez et al. [67] | 2011 | NS | Fermat's spiral | A new dimensionless parameter has been presented | |
| Juarez-Robles et al. [68] | 2011 | NS | Fermat's spiral | 4-channel Fermat's spiral is the best option since It gave the best performance | |
| Parallel in series research | | | | | |
| Lopez et al. [69] | 2009 | EA | Water management | Lower overall efficiency was always found in the flow field as compared to cascade type. | They observed in high voltage region, however, water generation showed significant effect in low voltage region |
| Sierra et al. [70] | 2011 | NS | Flow direction | The mode of feeding gases that showed the most uniform current distribution was similar flow | They did not compare the results with other types of flow field designs |
| Lu and Reddy [71] | 2010 | EA | Performance comparison of 4 different flow fields | With lower gases flow rate, the parallel in series flow fields perform better than serpentine flow field | The did not carefully control the geometric parameters of the flow fields |

Table 2.1 Summary of literature study (Continued)

| **Researchers** | **Year** | **EA/NS** | **Study** | **Results** | **Notice** |
|---|---|---|---|---|---|
| Maharudrayya et al. [11] | 2006 | NS | Pressure drop and flow distribution using analytical approach | Parallel in series gave the best in uniformity of flow distribution but the pressure drop were much higher as compared to the others | Others behaviors have not been investigated excepted pressure drop and flow distribution since they used analytical approach |
| Lobato et al. [72] | 2011 | EA | Current distribution | When using pure oxygen as oxidant, parallel in series flow fields performed 25 % higher than the others in power output. | It's HT-PEMFC and they compare only current density distribution |
| Lobato et al. [73] | 2010 | NS | Comparison between 3 different flow fields | Parallel in series performed best in uniformity of current distribution | It's HT-PEMFC. Therefore, water management is not their interest |
| Iranzo et al. [1] | 2010 | EA/NS | Model validation | Model validation using model parameters which obtained from technical data sheets, literature review and experimental measurement | They did not compare the characteristics of distribution between both 2 flow fields |
| Iranzo et al. [74] | 2014 | EA/NS | Model validation against local liquid water distributions | Their model cannot reproduce the liquid water accumulated in the channels | Although the absolute values are different, their model can gave the trend. Therefore, the model could give a superficial understanding |

# Chapter 3
# Research Methodology

This chapter presents a research methodology which is described by the following flow diagram.

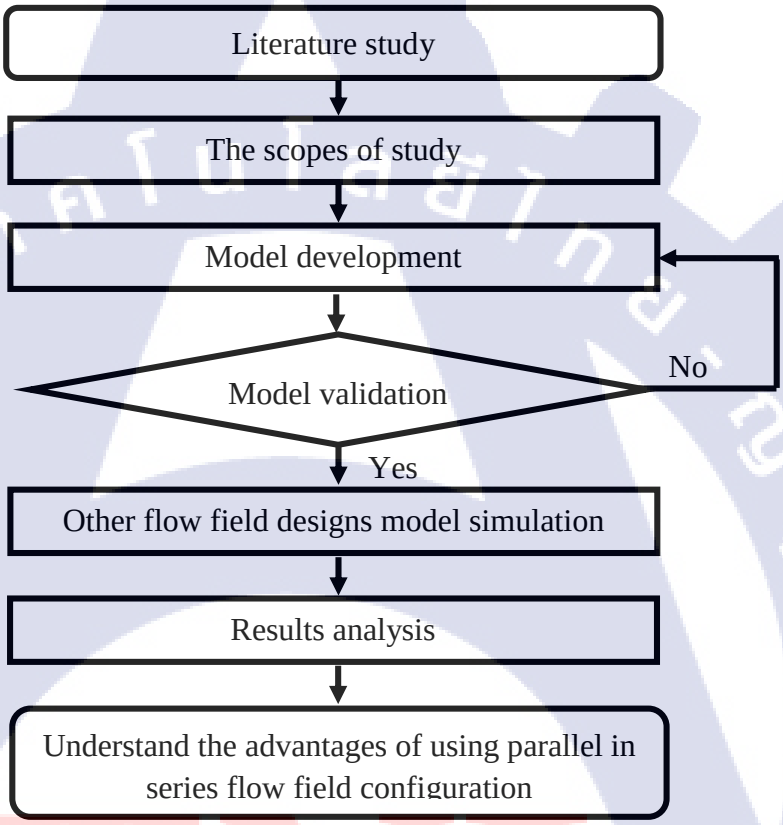


Figure 3.1 Flow diagram of research process

Since the literature study has been presented in the previous chapter, in this chapter, the discussion of selecting the scopes of study will be presented in section 3.1. In section 3.2, the model creation is described. The processes of the model validation will be described in section 3.3. Once the model is validated, the other interested designs will be modelled, and this process will be discussed in section 3.4. Section 3.5 presents the process of results analysis.

## 3.1 The scopes of study

After several academic literatures had been reviewed in chapter 2, it is found that there are numerous designs of gas flow channel configuration, which present different advantages in each condition. Both single and multiple serpentine channel configurations have received the highest attention in both numerical and experimental studies (see figure 1.1) since their designs are simple, which are easy to get a converged solution when models numerically, and they are commercial cells, which are easy to get for experimental study. However, parallel in series flow channel configuration, which is also sold by Electrochem in 5 $cm^2$ PEFC stack, has received very low attention. Therefore, the broad objectives of this work are to investigate transport behaviors and cell performance of the parallel in series flow field configuration. Six different flow fields with minimal change in each will be studied, in order to understand the behaviors. Since experimental approaches are time-consuming, expensive and highly uncertain, CFD has become an important tool for studying the PEFC. Therefore, in this present work, the study will be conducted by using commercial ANSYS FLUENT software, which is one of the most famous CFD software in PEFC study.

## 3.2 Model development

There are three basic steps involving in modeling and simulating PEFC using ANSYS FLUENT.

1. Creating the geometry
2. Meshing the computational surface and volume elements
3. Defining the parameter values and models used

Creating the geometry can be done by using different computer aided design (CAD) software, such as CATIA, ANSYS, and SolidWorks. The purpose of this step is to define the physical dimension of the components and their relation to one another, which is a vital step since all physical parameters are related to the cell performance, therefore creating wrong size physical dimension may lead to wrong solutions. The first flow field, which will be used in validation against experimental data, will be modelled in single serpentine channel configuration. The geometries of 5 $cm^2$ PEFC were created in ANSYS WORKBENCH, including bipolar plates (BPs), gas flow channels (GFCs), gas diffusion layers (GDLs), catalyst layers (CLs), and membrane. The geometries

dimension of the model is shown in table 3.1 and figure 3.2 in which their dimensions are the real geometries after compression obtained from Limjeerajarus et al. [75].

Table 3.1 Model geometries dimension.

| **Parameter** | **Value** | **Unit** |
|---|---|---|
| Channel height | 0.8 | mm |
| Channel width | 0.8 | mm |
| Rib width | 0.8 | mm |
| Bipolar plate thickness | 0.8 | mm |
| Cell active area | 510 | $mm^2$ |
| Gas diffusion layer thickness | 0.190 | mm |
| Catalyst layer thickness | 0.015 | mm |
| Membrane thickness | 0.050 | mm |

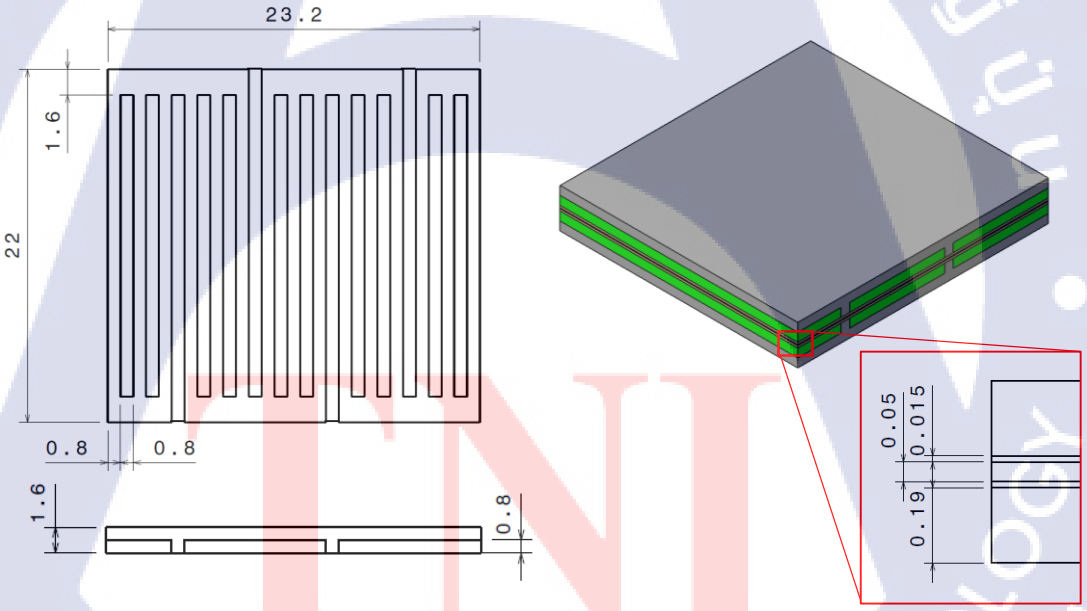


Figure 3.2 The model geometries dimension

ANSYS FLUENT is based on finite volume techniques, hence the created geometry is required to break down into small volume elements. This process can be done by using different software, such as meshing through ANSYS Workbench,

GAMBIT, and ICEM CFD. Since the phenomena in PEFC are very complex, high quality of generated meshes is needed to receive a converged solution, and lower computational time. Hexahedral volume elements and quadrilateral faces are suggested as the best meshing since they do not create highly skewed elements, which will lead to the divergent solution. Although a very fine meshing, a numerous amount of computational cells, leads to accurate results, long computational time is required. The balance between accurate results and computational time have to be carefully considered, thus the basic analysis, such as mesh independent analysis has to be done to ensure the quality of the results. In this work, the meshing process will be done using ANSYS ICEM CFD.

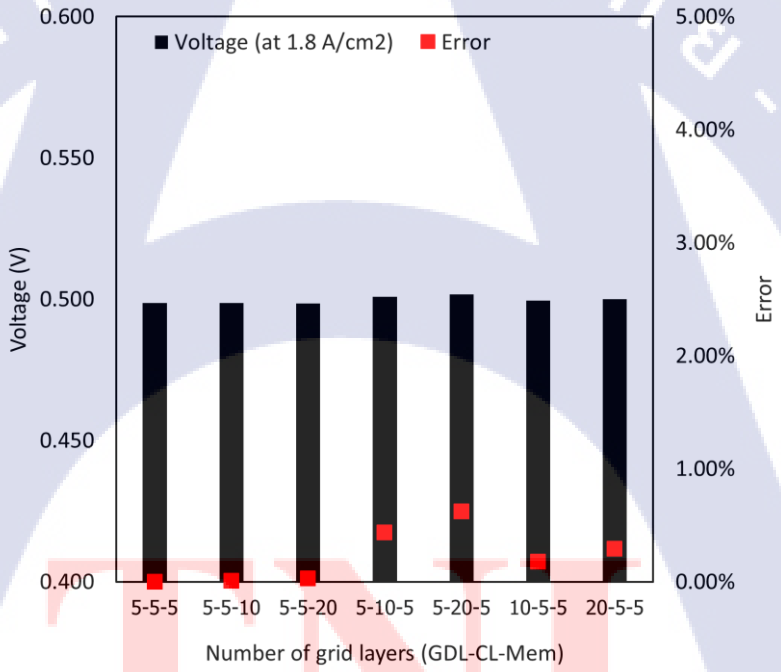


Figure 3.3 Comparison of grid independent analysis

In this present work, the grid independent analysis of each layer of the MEA (i.e., GDL, CL, and membrane) was performed. At the first stage, 5 cells lined in the deep of the through-plane direction were used across each layer of the MEA. After the results were obtained, the variation of the number of cells lined in the deep (5, 10, 20 cells in each layer) was done to investigate the grid independency. It was found that the

maximum difference of the cell voltage obtained from the different cell numbers is within 1% of each other, as seen in figure 3.3. However, the computational time required for the higher number of cell cases were also much higher and moreover, the convergence solution was more difficult to obtain and the convergence rate was much higher since the computational cells were too many [76]. Thus, the number of cells lined in the deep, in all GDL, CL, and membrane used in the models were 5, resulting in the total of 681,164 hexahedral cells with a maximum aspect ratio of 94 (see figure 3.4).

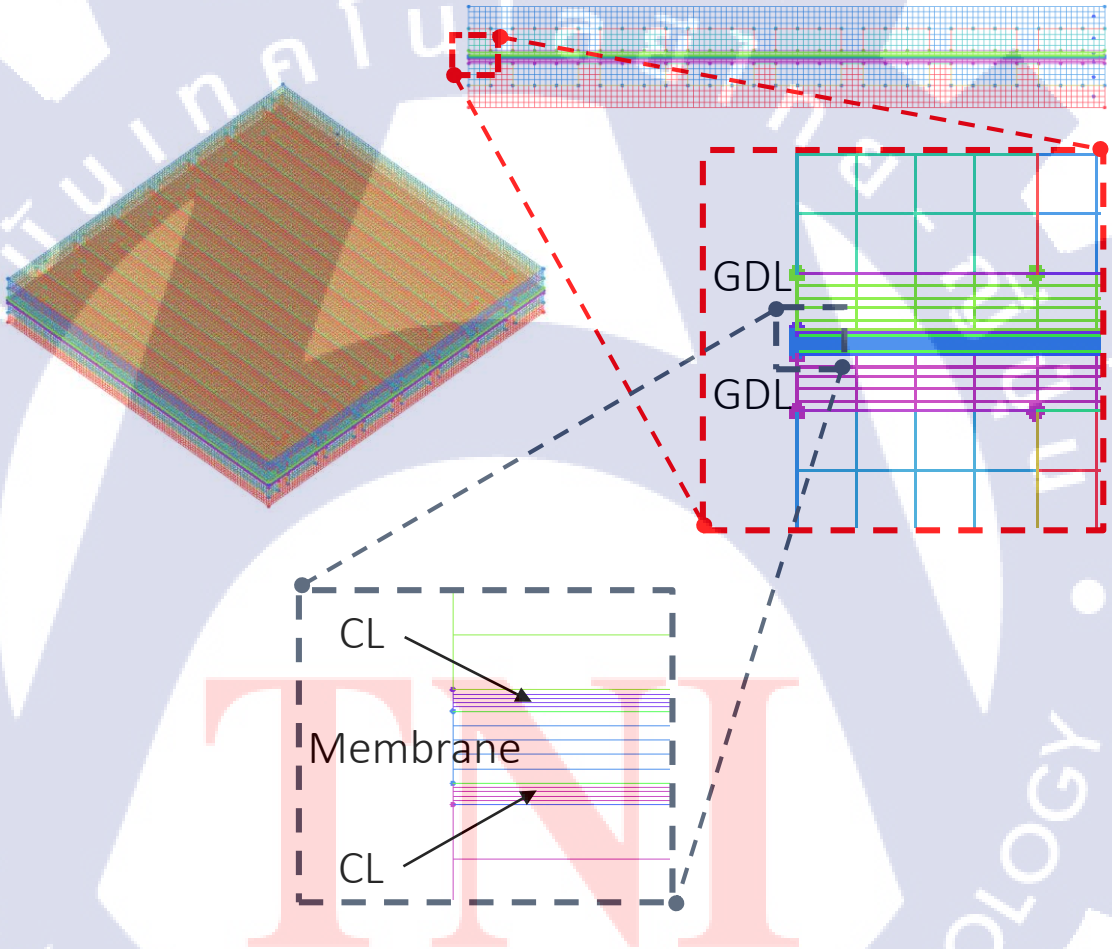


Figure 3.4 Computational grids

One of the main issues in PEFC modeling is, finding the correct values for the parameters. After a review through several literatures, the used parameters vary in high range. Hence, the properties and parameters used in this 3-D modelling were the

realistic material and reaction parameters obtained from Limjeerajarus et al. [75], as displayed in table 3.2.

Table 3.2 Material and reaction parameters

| **Physical parameters** | **Value** | **Units** | **Ref** |
|---|---|---|---|
| **GDL** | | | |
| Wall contact angle | 110 | Degree | [77] |
| Porosity | 0.6 | | [75] |
| **CL** | | | |
| Porosity | 0.4 | | [75] |
| Surface to volume ratio | $1.127 \times 10^{7}$ | $m^2$-pt $m^{-3}$-electrode | [75] |
| **Membrane** | | | |
| Thermal conductivity | 0.16 | W $m^{-1}$ $K^{-1}$ | [78] |
| Dry membrane density | 1,980 | kg $m^{-3}$ | [79] |
| Equivalent weight of dry membrane | 1,100 | kg $kmol^{-1}$ | [79] |
| **Reaction parameters** | | | |
| Open circuit voltage | 1.05 | V | [75] |
| Reference concentration | 0.0008814 | Kmol $m^{-3}$ | [75] |
| Anode charge transfer coefficient | 1 | | [75] |
| Anode exchange current density | 7.17 | A $m^{-2}$-pt | [75] |
| Cathode charge transfer coefficient | 1 | | [75] |
| Cathode exchange current density | $7.17 \times 10^{-5}$ | A $m^{-2}$-pt | [75] |

There are several options in simulating PEFC using ANSYS FLUENT, including joule heating, reaction heating, electrochemistry sources, Butler-Volmer rate, membrane water transport, multiphase, multicomponent diffusion, and anisotropic e-

conductivity in porous electrode. Only this following six options will be included in the model in which oxygen was used as the oxidant. The joule heating option is an option which takes ohmic heating into account, while the heat generated by electrochemical reaction is included in the reaction heating option. Normally, the electrochemistry sources option is turned on but if the basic flow throughout the cells is an only interest, this option can be turned off. The Butler-Volmer rate is used in computing the transfer currents inside the catalyst layer. The transport of water across the membrane can be modelled by the membrane water transport option. The multiphase option will enable the formation of liquid water in gas diffusion layers. However, for taking the nitrogen specie into account when used air as an oxidant, the seventh option of multicomponent diffusion is enabled.

In this study, the considered cell temperature was 60ºC in which the BPs were set to maintain at 60ºC. The system operating pressure was set at 1 atm on the outlet of GFCs. The stoichiometric flow rates of 1.1/10.6 at 60ºC with 90% RH in both $H_2/O_2$ inlets were used in the model validation and cell performance evaluation. Since, generally, the real application uses air as oxidant due to its convenience in which no space is required for the storage, the stoichiometric number of 1.1/1.1 at 60ºC with 90% RH in both $H_2$/Air inlets were also used to investigate the transport behaviors and cell performance. The stoichiometric number mentioned earlier was calculated based on the reference current density of 1.8 A/cm$^2$. All of the boundary conditions used in the simulations are summarized in table 3.3.

The computational time varies significantly in different cases, and also between the first point of IV performance curve and the others. Typically, the required time for achieving a convergence solution in the higher flow rate case was about 2 times lower than that in the lower flow rate case. The higher computational time was happening since the lower flow rate case included the Stefan-Maxwell equation in the model instead of Fick's law which added the complexity to the model, and therefore the under-relaxation factors were set at a low value for the calculation stability.

To ensure that the model is fully converged, the following 4 ways for judging convergence are used.

1. Residual levels monitoring
2. Consistency of the calculated voltage

3. Comparison of the calculated current and the fixed current
4. The convergence of the average water saturation in the cathode CL

As suggested by ANSYS [14], the default convergence criteria in FLUENT are sufficient for most problems in which the criteria require that the residuals of all equations has to drop lower than $10^{-3}$ except the energy equation in which $10^{-6}$ is recommended. However, in PEFC modelling, the mentioned criteria are not sufficient to ensure that the model is fully converged as the default setting in ANSYS FLUENT for terminating the calculation when the convergence criteria is achieved is automatically disable during which the fuel cell add-on module is loaded into ANSYS FLUENT via the text user interface.

Differently from Arvay et al. [2], this model used the fixed current as the boundary condition at the cathode terminal and thus, a cell voltage is calculated during each iteration instead of current density. The consistence of the reported cell voltage was also used to be another aspect for judging convergence.

To ensure that the solution is converged, the third way which used species mass conservation for another part of the convergence criteria is introduced by Arvay et al. [2] in which the consumed species mass obtained from simulation has to be satisfied the reported current flux. However, the fixed current density was used as the boundary condition instead of the cell voltage. Hence, in this work, the consumed species mass of the fixed current flux was used to be compared with the consumed species mass obtained from the simulation. The relation between the species mass flow and current can be expressed by this following equation.

$$I = \frac{mnF}{MM} \tag{4.1}$$

Where,

| | | | |
|---|---|---|---|
| $I$ | = | the current | unit: A |
| $m$ | = | the species mass flow rate | unit: kg/s |
| $n$ | = | the number of electrons transferred | |
| $F$ | = | the Faraday constant | unit: C/kmol |
| $MM$ | = | the molar mass | unit: kg/kmol |

However, besides these 3 ways of judging convergence, it is widely known that the multiphase flow and membrane water transport model is very difficult to achieve the convergence in PEFC modelling in which the typical solver generally uses very low under-relaxation factors for preventing a diverging of the solution which may sometimes mislead the users to consider that the solution is fully converged. Thus, the careful monitoring on the average scalar quantity of water saturation and water content in the cathode CL and the membrane are needed to ensure a good quality of the solution and that the model is fully converged.

Table 3.3 Boundary conditions

| | **$H_2/O_2$** | **$H_2$/Air** | **Unit** |
|---|---|---|---|
| **Anode** | | | |
| Volume flow rate | 100 | 100 | mL/min |
| Inlet temperature | 60 | 60 | ºC |
| Inlet relative humidity | 90 | 90 | % |
| **Cathode** | | | |
| Volume flow rate | 500 | 250 | mL/min |
| Inlet temperature | 60 | 60 | ºC |
| Inlet relative humidity | 90 | 90 | % |
| Anode voltage | 0 | 0 | V |
| Cathode current density | 0.0025-1.8000 | 0.0025-1.8000 | $A/cm^2$ |
| Outlet Pressure | 101,325 | 101,325 | Pa |
| Cell temperature | 60 | 60 | ºC |

## 3.3 Model validation

The CFCD modeling results are needed to validate carefully against the experimental results. There are several ways of validation such as using local liquid water distribution with neutron imaging [74], using current distribution [80], and using the polarization curve which is the most popular way. Thus, in this present work, the models will be validated against the experimental data of our laboratory previous work [75], the polarization curve.

### 3.4 Other flow field designs model creation

There are eight geometric parameters of flow field which affect the cell performance and transport phenomena, and hence the variation of parameters in investigating the difference in each flow field design needs to be carefully checked since some parameters may affect the others, such as number of channels, which could reduce the channel and rib width. To prevent those problems, the channel density of single serpentine, which is used in the validation, and three channels parallel in series flow field, which is the main purpose of this study, will be used, and thus six different flow fields which used in this work are presented in figure 3.5.

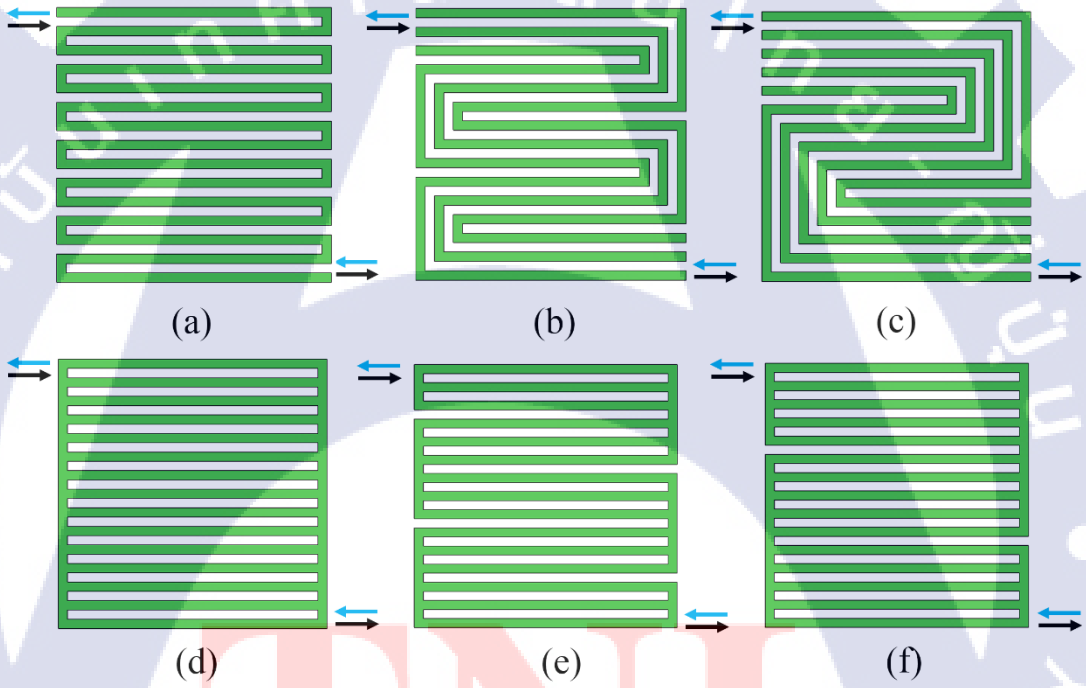


Figure 3.5 Flow fields used in this work a) single channel serpentine b) three channels serpentine c) five channels serpentine d) conventional parallel e) three channels parallel in series and f) five channels parallel in series flow field (↗) Anode and (↗) Cathode flow directions

To eliminate the other parameters, flow direction will be fixed as counter, which is used in our laboratory previous work and furthermore, it is considered that in most cases this gas feeding mode performs the best. The channel cross-section shape,

channel and rib width, and channel depth are fixed as rectangle, 0.8 and 0.8 mm, and 0.8 mm, respectively, as mentioned earlier. Hence, only two geometric parameters, i.e. flow field designs and channel path length, remain affecting the cell performance and transport behaviors. These two remaining geometric parameters were selected to be investigated for clarifying the doubtfulness of how the cell performance and transport behaviors are different among parallel in series, serpentine, and parallel flow field and also how the number of channels of the parallel in series and serpentine flow field would affect the cell performance and transport behaviors.

### 3.5 Results Analysis

Since ANSYS FLUENT can give us an observation in $H_2$ concentration, $O_2$ concentration, temperature distribution, liquid water content in the membrane, protonic conductivity, water saturation in gas diffusion layer, current density distribution, and static pressure distribution, all of these results in every flow field will be presented and discussed in results analysis section along with the polarization curve.

# Chapter 4
# Results and discussion

The results obtained from the simulation are presented and discussed in this chapter as follows.

4.1. Model validation

4.2. Using oxygen as oxidant

4.3. Using air as oxidant

## 4.1 Model validation

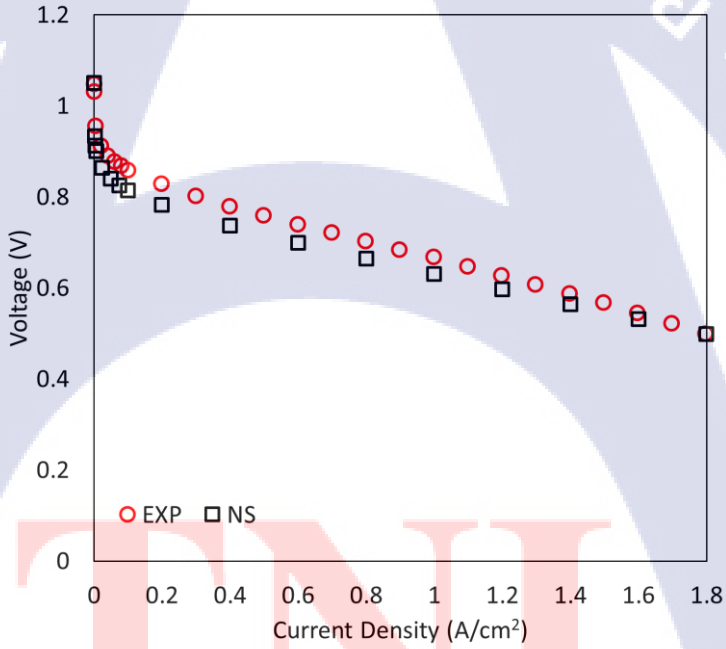


Figure 4.1 Validation of the model and its simulation parameters for the single channel serpentine flow field

A reasonable agreement between experimental data and numerical solutions are clearly seen at all current density in Fig. 4.1. Note that the small discrepancy between those results in the high-potential region was caused by the limitation of the ANSYS FLUENT software, which is based on the finite volume method itself since the

finite volume method is not effective in responding to microscopic reaction phenomena. To solve such a problem, microscopic simulation which required the other developed program is needed.

Nevertheless, in overall, it is adequate to use the developed model and its simulation parameters for investigating the macroscopic transport behaviors and cell performance of the PEFC in other five different flow field designs.

## 4.2 Using oxygen as oxidant

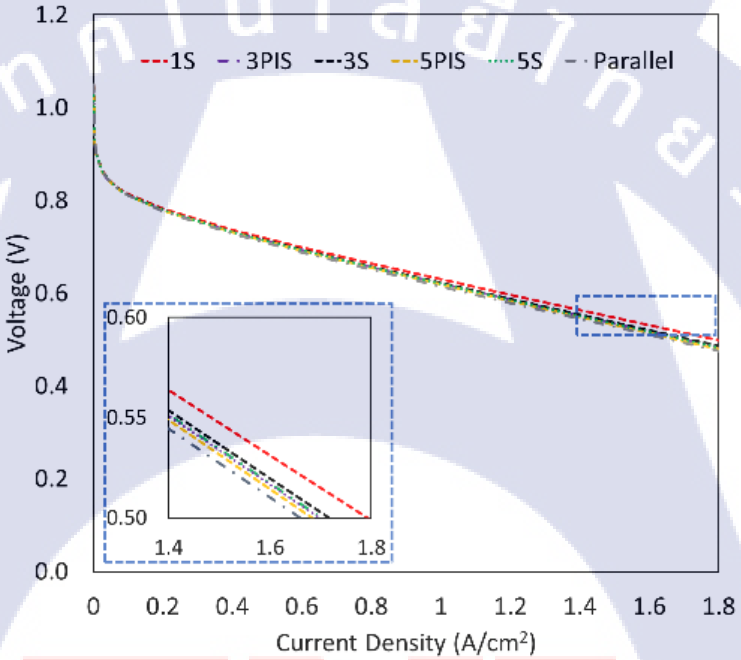


Figure 4.2 The IV performance curves of the six different flow fields with the conditions of 1.1/10.6 stoich at 60ºC 1 atm with 90% RH in both $H_2/O_2$ inlet

The numerical results of the six different flow field designs when using pure $O_2$ as the oxidant are shown in Fig. 4.2. From the polarization curve, the single channel serpentine (1S) flow field showed the best performance followed by three channel serpentine (3S), three channel parallel in series (3PIS), five channel serpentine (5S), five channel parallel in series (5PIS) and parallel flow field, respectively, which coincided with the experiment of Lu and Reddy [71]. A further investigation on the

distributions when current density was 1.0 A/cm$^2$ (approximately at 0.6 V) was conducted and discussed since most PEFC stacks operate at around 0.6 V in practice [79], [81 - 84].

Fig. 4.3a–f shows the hydrogen mass fraction distribution on the anode CL/GDL interface of the 1S, 3S, 5S, parallel, 3PIS, 5PIS flow fields, respectively. As expected, the 1S flow field gave the best uniformity in distributing the hydrogen, while the parallel flow field performed worst. The PIS flow fields distributed the hydrogen quite better than the multi-channel S flow fields (i.e., 3PIS and 5PIS), as seen by the contour in the first corner. In addition, the hydrogen concentration at the inlet was lower than that at the outlet as the water was mostly absorbed into the CL around the inlet area.

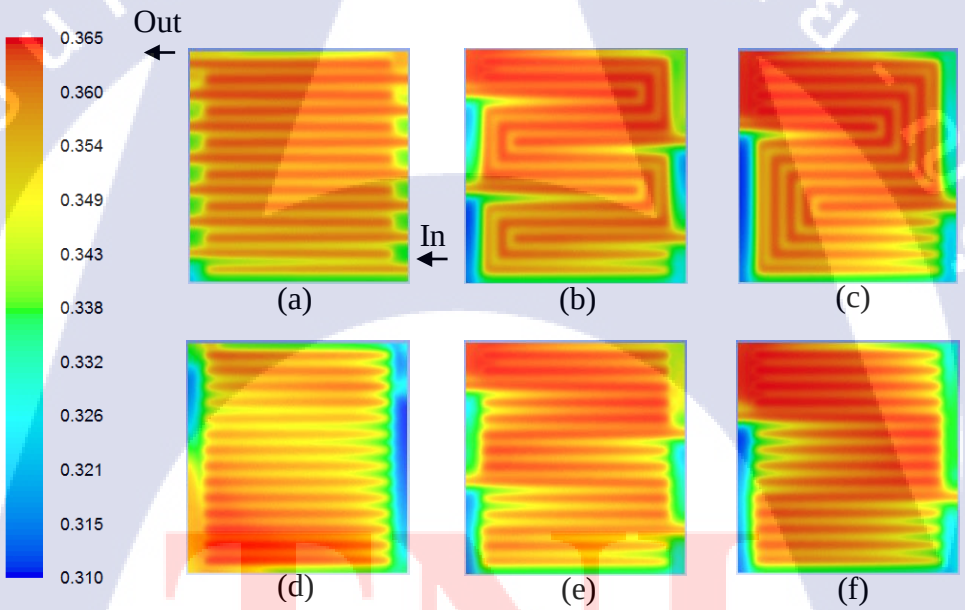


Figure 4.3 Hydrogen mass fraction distribution at 1.0 A/cm$^2$ of a) 1S b) 3S c) 5S d) parallel e) 3PIS and f) 5PIS flow fields when using oxygen as oxidant

The oxygen mass fraction distribution on the interface of CL/GDL at the cathode side is displayed in Fig. 4.4. The oxygen gradually reduced along the flow channels from the inlet to the outlet, which was opposite to the behavior of the hydrogen at the anode side. For such a high flow rate, i.e., 10.6 stoich, the difference among the different flow fields in distributing the oxygen cannot be observed with clarity.

However, as expected, the parallel flow field still performed worst as it distributed the oxygen non-uniformly. It should be noted that the lower oxygen concentration areas had, at the same time, the high water mass fraction.

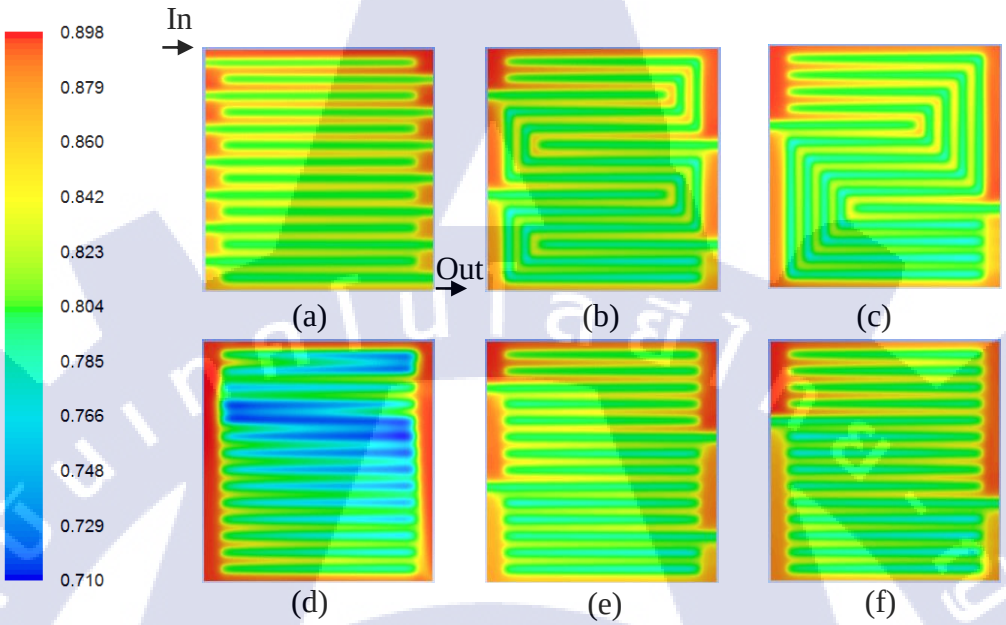


Figure 4.4 Oxygen mass fraction distribution at 1.0 A/cm$^2$ a) 1S b) 3S c) 5S d) parallel e) 3PIS and f) 5PIS flow fields when using oxygen as oxidant

Since it has been widely known that a uniform distribution of water content leads to a better cell durability, many researchers have tried to develop the flow fields which give the uniform distribution of membrane water content. Fig. 4.5 presents an information of local water content distribution on CL/MEM at the cathode side. The 1S flow field provided the best uniformity of the membrane hydration, while the parallel gave the worst uniformity. As seen in Fig. 4.5, the area of high water content was the same with the area of low oxygen mass fraction in Fig. 4.4 which confirmed that the lower oxygen concentration areas were full of water. Furthermore, the results also indicated that the MEA, especially membrane, was full of liquid water since a maximum value of membrane water content is higher than 14, which is the value when equilibrated with saturated water vapor [20]. Although the higher water content leads to the higher proton conductivity, the too-high water content (higher than 14) can cause water flooding which is an explanation of the lower cell performance of other flow

fields as compared to that of the 1S flow field. Therefore, apart from its uniformity, the membrane water content should not exceed 14 during the operation.

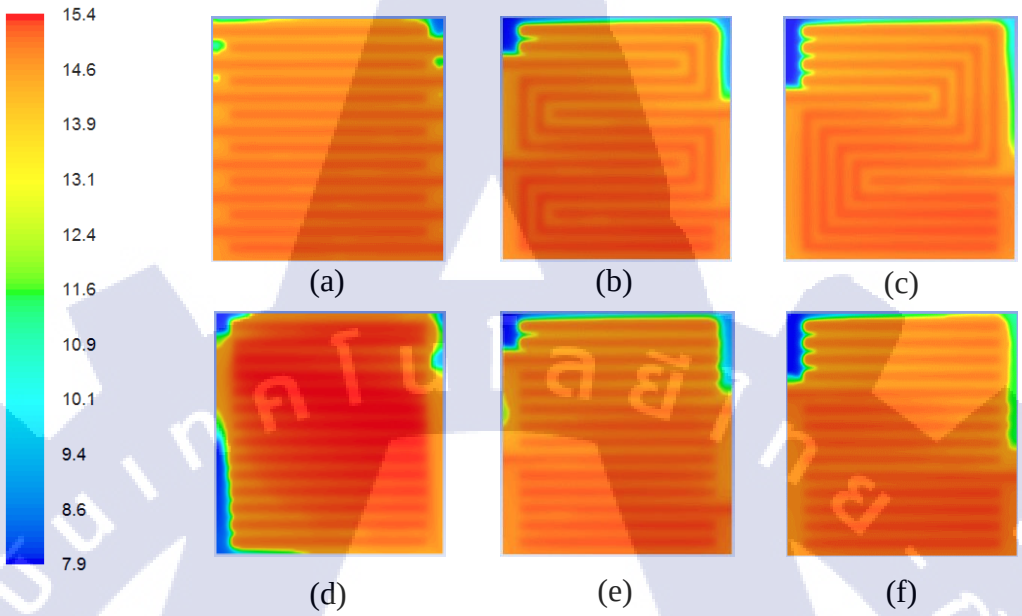


Figure 4.5 Water content distribution at 1.0 A/cm$^2$ of a) 1S b) 3S c) 5S d) parallel e) 3PIS and f) 5PIS flow fields when using oxygen as oxidant

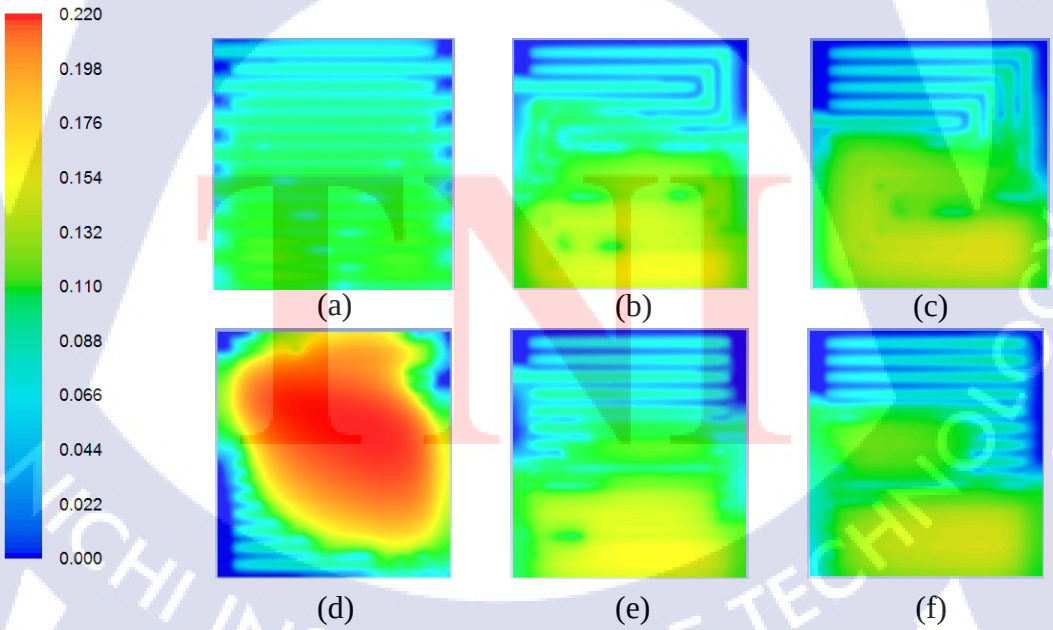


Figure 4.6 Water saturation distribution at 1.0 A/cm$^2$ of a) 1S b) 3S c) 5S d) parallel e) 3PIS and f) 5PIS flow fields when using oxygen as oxidant

The existence of liquid water in the MEA was also confirmed by the water saturation distribution, as depicted in Fig. 4.6, in which the pore in cathode GDL of the parallel flow field was full with the volume of liquid water (higher values of water saturation). Since the 1S flow field consisted only one flow path, the reactants were forced down to eliminate the liquid water in GDL out through the channel, and thus the 1S performed best in both cell performance and water management. On the contrary, the parallel flow field could not handle the liquid water flooding since it could not distribute the reactants uniformly when the flooding occurred, resulting in the lowest cell performance.

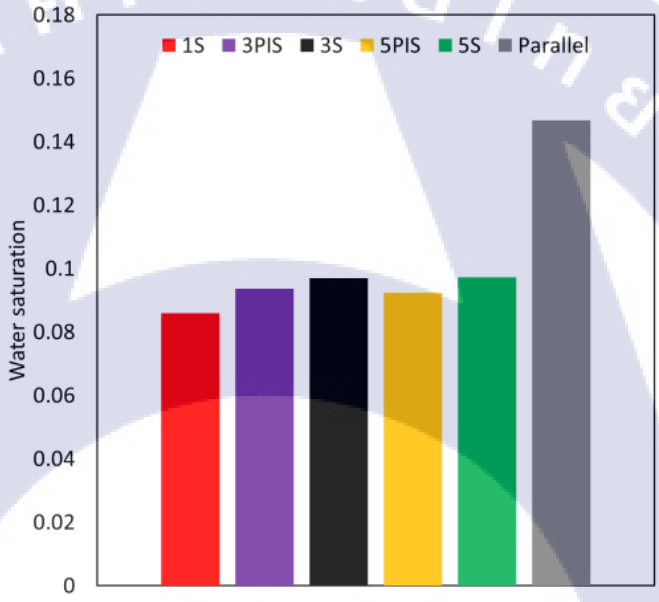


Figure 4.7 Water saturation in cathode gas diffusion layer at 1.0 A/cm$^2$ when using oxygen as oxidant

However, from the experiment of Wang and Van Nguyen [85], it was observed that the performance would be unstable when the average water saturation level reached 0.2. Therefore, considering the amount of water saturation in cathode porous layer (see Fig. 4.7), the cell voltage of all flow fields was still stable, although it was found that the liquid water in the parallel flow field was very high as compared to that of the others.

Moreover, the PIS flow fields tend to handle the flooding situation slightly better than the S flow fields while keeping the membrane hydrated.

The current distribution in the in-plane direction is shown in Fig. 4.8. It was observed that the trend of the distribution was the same in all flow fields in which the current mostly generated under the ribs. The different rates of current generation were caused by the hydrogen distribution (see Fig. 4.3) and the membrane water content (see Fig.4.5) which mostly higher under the ribs. Furthermore, the results implied that the 1S provided the best uniformity in current distribution while the others were almost the same.

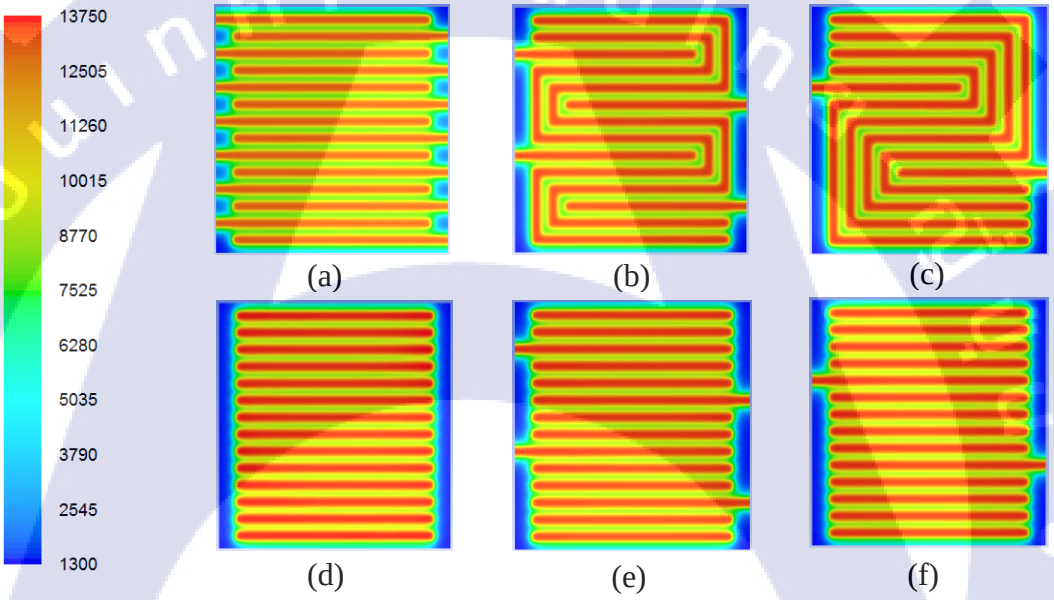


Figure 4.8 Current density distribution ($A/m^2$) at 1.0 $A/cm^2$ of a) 1S b) 3S c) 5S d) parallel e) 3PIS and f) 5PIS flow fields when using oxygen as oxidant

The temperature distribution at the interface where electrochemical reaction occurs is depicted in Fig. 4.9. As expected, the 1S flow field provided the most uniform in temperature distribution. Since the amount of water in the PIS flow fields was slightly lower than that in the multi-channel S flow fields, the temperature in the PIS flow fields was found higher as compared to the multi-channel S flow fields with the same number of channels. Although the maximum temperature differences were approximately within 2.5 K, a safety limit for ensuring that the temperature differences would not

affect the MEA durability is approximately 5 K in general [86]. Therefore, those differences were considered as a very small value. The differences were small and provided an insignificant effect on the cell durability due to the small size MEA and the thin membrane. However, the temperature variation did play an important role on the MEA durability in the MEA which has a large cell area and used the thick membrane since the water distribution is hardly uniform.

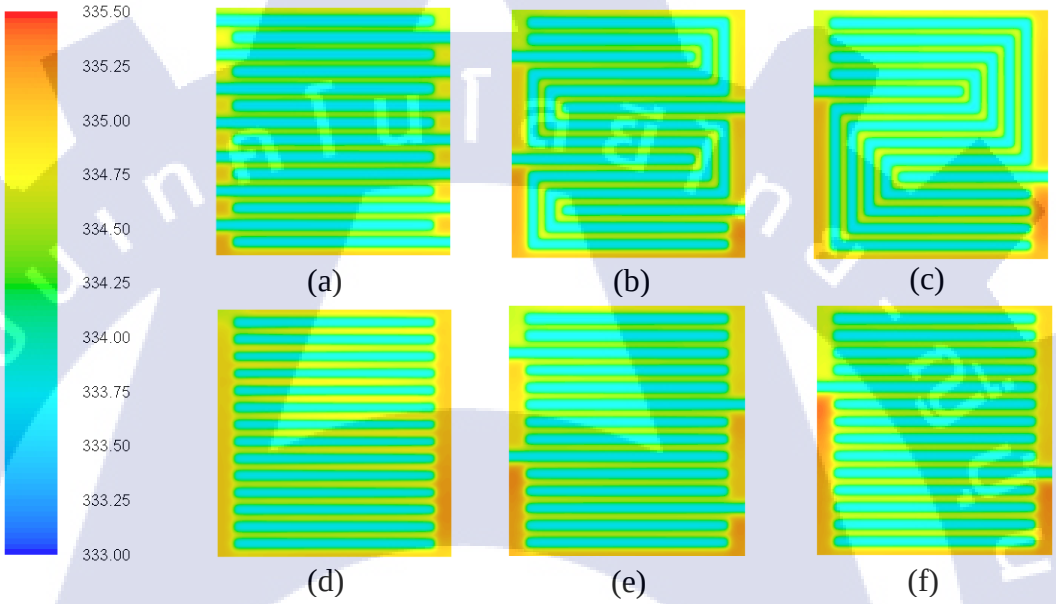


Figure 4.9 Temperature distribution (K) at 1.0 A/cm$^2$ of a) 1S b) 3S c) 5S d) parallel e) 3PIS and f) 5PIS flow fields on the cathode CL/MEM interface when using oxygen as oxidant

In a PEFC system design, the pressure drop is one of the important aspects as it defines the required power for the flowing of the reactants which reduces the overall system performance. Although the 1S flow field was the best in cell performance and water management, the required power for compensating the pressure drop is approximately 10 times higher than the 3S and 3PIS flow fields and approximately 20 times higher than the 5S and 5PIS flow fields (see Fig 4.10). It was also observed that the PIS flow fields produced the higher pressure drop as compared to the multi-channel S flow fields since the PIS flow fields consisted only one flow path for connecting the parallel flow field in the series while the multi-channel S flow fields could flow through

many flow paths simultaneously. Considering all aspects in this given operating condition, it can be concluded that the 1S flow field would be the optimal choice for making a stack with a 5 $cm^2$ PEFC which could be useful for a small application (such as a small stack or lab scale experimentation) due to its reasonably high cell performance, more reactants uniformity and lower water saturation. Although the pressure drop is very high, from the user point of view, the PEFC used oxygen as oxidant does not required any power to force the reactants through the channel since the pure oxygen is generally stored in a high pressure tank and the required power to pressurize the oxygen does not supply by the user. However, commercial PEFC stacks in a real application used air as the oxidant due to its convenience that no space is required for the oxidant storage. Therefore, a further study on the transport behaviors and cell performance of the different flow fields with air as the oxidant was conducted and discussed in the next section.

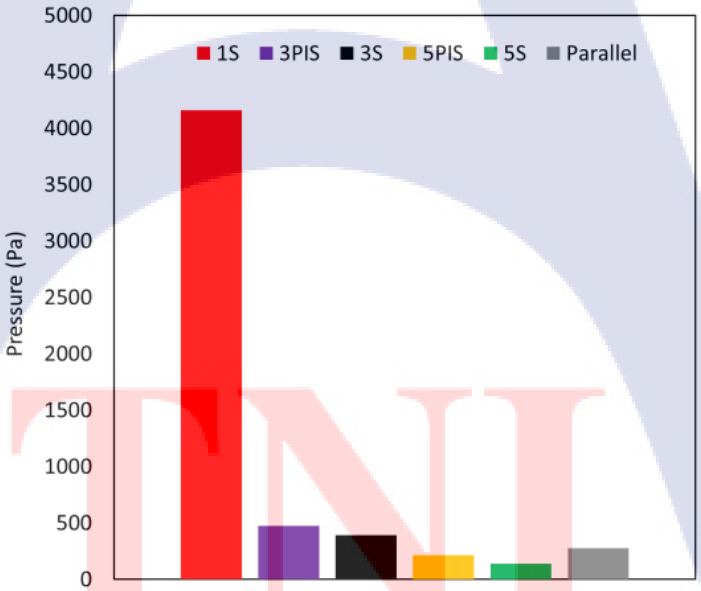


Figure 4.10 Pressure drop at 1.0 A/$cm^2$ when using oxygen as oxidant

## 4.3 Using air as oxidant

When air mixture is used as the oxidant, Fig. 4.11 shows the simulation results of the six different flow field designs. From the I-V performance curve, in high voltage

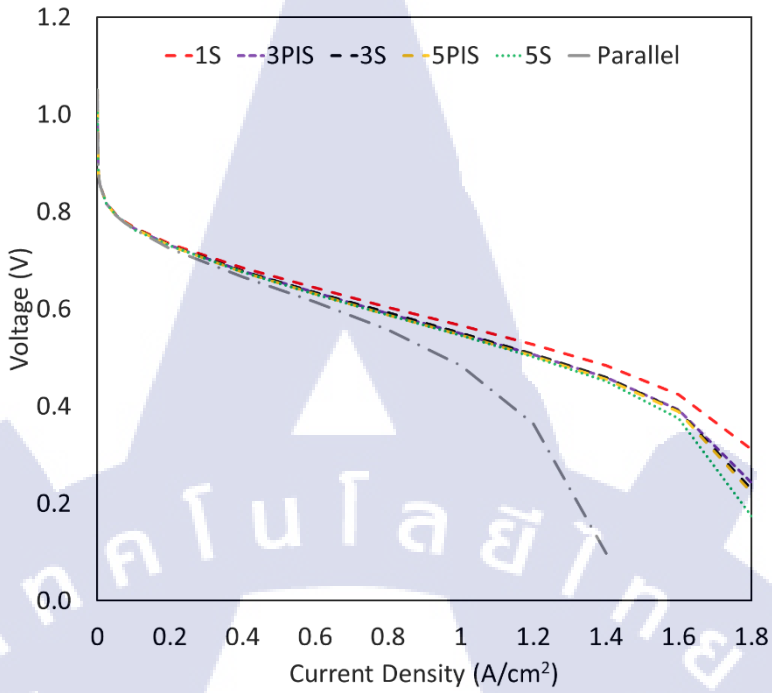


Figure 4.11 The IV performance curves of the six different flow fields with the conditions of 1.1/1.1 stoich at 60ºC 1 atm with 90% RH in both $H_2$/Air inlet

region (above 0.7 V) [87], the 1S flow field showed the best performance followed by 3S, 3PIS, 5S, 5PIS and parallel flow field, respectively, which is in concurrence with when using oxygen as oxidant. In the low potential region (below 0.7 V), with the same number of channel, the PIS flow fields performed better than the multi-channel S flow fields. The higher performance in low potential region indicated that the PIS flow fields could deal with the water flooding problem better than the multi-channel S flow fields. Same as using oxygen as oxidant, these results are in concurrence with the developed 2.25 $cm^2$ PEFC experiment of Lu and Reddy [71] in which, with a high gas flow rate, the long channel flow field (i.e. 1S) provided the best performance as compared to PIS and z-type multi-parallel flow field since the high gas flow rate enhanced the under-rib mass transport and thus the liquid water removal. Even though the PIS fields did not present a performance in the low voltage region higher than the 1S as expected, the PIS flow fields perform slightly better than the multi-channel S flow fields with the same number of channels. Furthermore, the performances tended to decrease as the number of channels were increased. Note that it is considered as a high flow rate case since the

stoichiometric flow rate of 1.1 was calculated based on the current density of 1.8 A/cm$^2$. This result of the effect of number of channel was contradictory to the results obtained from the 200 cm$^2$ PEFC simulation by Shimpalee et al. [39] in which, in low voltage region, the flow fields which had a lower number of channel tended to perform worse. This result may imply that the PEFC performance and transport behaviors also changed significantly with a different MEA and a PEFC size due to its non-linear behaviors.

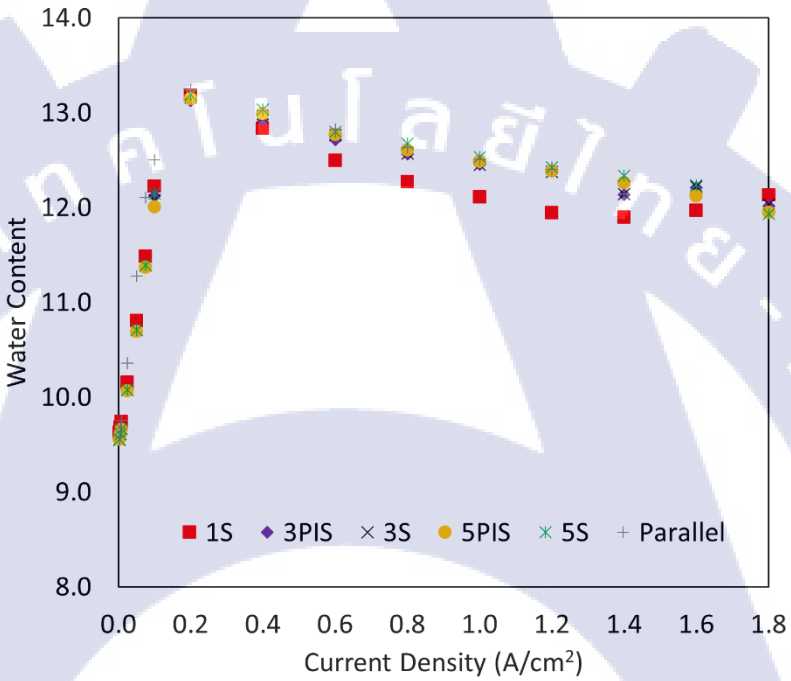


Figure 4.12 Average membrane water content of each current density

Since the PEFC performance is directly proportional to the protonic conductivity and so the water content of the membrane as long as there is no water flooding, the average membrane water content at each current density of each flow field was investigated to clarify this ambiguity. As displayed in Fig. 4.12, the results revealed that the water content increased with the current density in the region before 0.2 A/cm$^2$ (in the high-potential region) while in the region beyond 0.2 A/cm$^2$ (in the low-potential region), the water content decreased as the current density increased. This indicated that, in the high-potential region, the water content increased due to the increasing amount of generated water and thus the domination of back diffusion while, in the low-

potential region, the water content decreased (drying of the membrane) due to the domination of the electro-osmotic drag, as the current density increased [84].

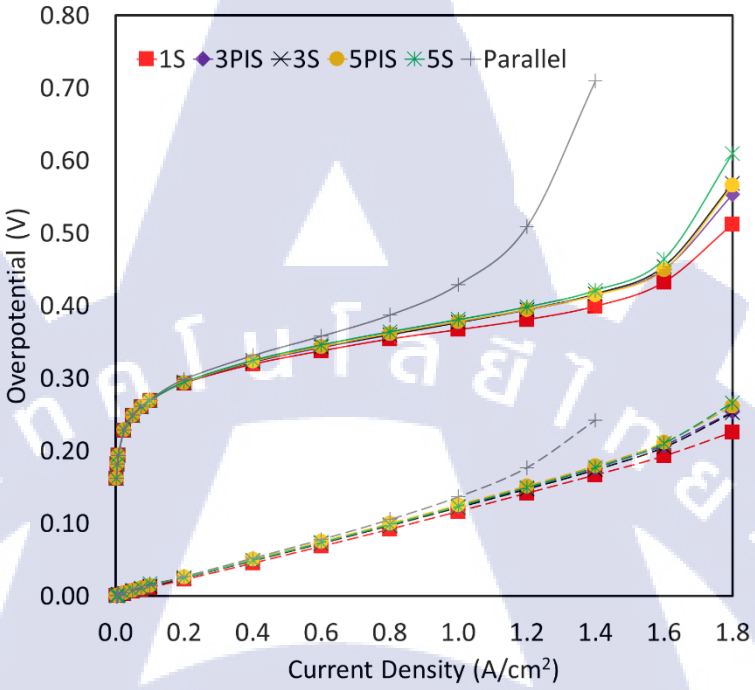


Figure 4.13 The activation and concentration overpotentials (solid line) and ohmic overpotential (dash line) of each current density

Since the amount of fed water and rate of generated water were same in each flow field, the difference in average membrane water content indicated that there was a difference in the water transport in the membrane and thus the uniformity of the water distribution. From Fig. 4.12, in the high potential region, the parallel flow field provided the higher water content than the others while the lower number of channel flow field contributed a slightly lower water content in the low potential. The result was not in concurrence with the statement mentioned earlier since the 1S flow field gave the best performance in an entire current density but the lowest water content in the low potential region. Note that the average water content results are opposite to the results of Shimpalee et al. [39] in which the fewer number of channel flow fields tend to have a higher membrane water. However, the average water content was only slightly different among the flow fields due to the performance of electrode, the thickness of

membrane and the size of PEFC. Hence, the higher water content does not always reflect in the better performance since there are plenty of factors remained affecting the cell performance.

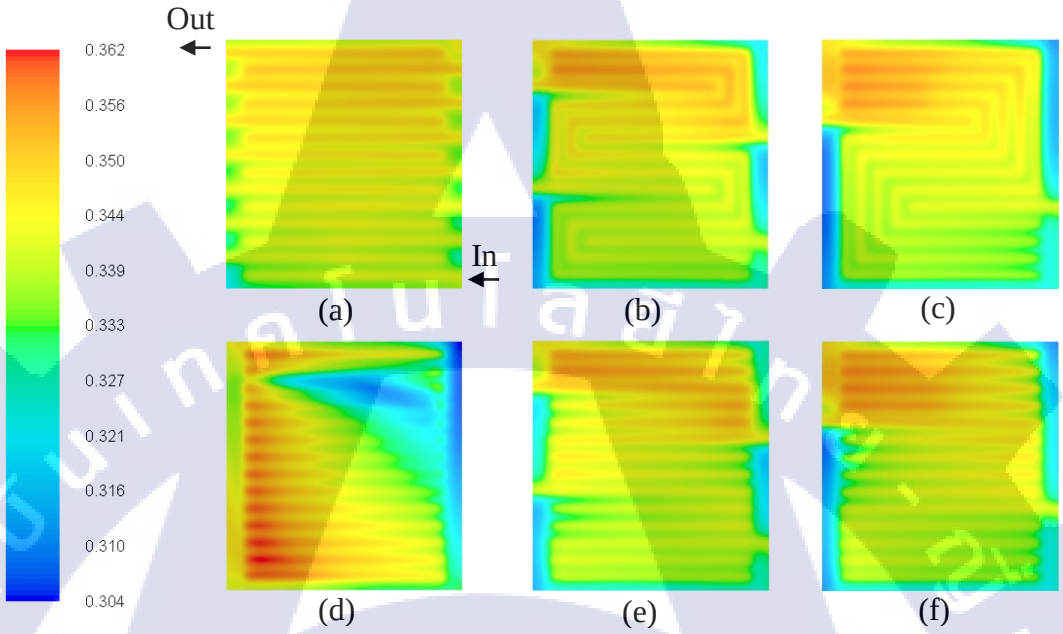


Figure 4.14 Hydrogen mass fraction distribution at 0.8 A/cm$^2$ of a) 1S b) 3S c) 5S d) parallel e) 3PIS and f) 5PIS flow fields when using air as oxidant

The membrane water content can also be described in a form of voltage or power loss which is widely known as the overpotential. However, the overpotential consist of 4 types, i.e., activation overpotential, ohmic overpotential, concentration overpotential, and fuel cross over overpotential. Since the contact resistance was not considered in this model, the remaining effects in ohmic overpotential are then the ionic and electronic overpotential, which were almost the same in each flow field due to the insignificant difference in average water content. Moreover, the fuel cross over and internal current were already taken into account in the open circuit voltage, as seen in Fig. 4.13. Since the activation overpotential only depends on the reaction parameters of the MEA, not a flow field, therefore only the concentration overpotential remains affected the difference in IV performance curve, especially in the low potential region. Note that although the 1S flow field provided the lowest average membrane water

content, the ohmic overpotential was also found lowest. This can be interpreted that the 1S flow field gave a better water content uniformity. A further investigation on the distributions when current density was 0.8 A/cm$^2$ (approximately at 0.6 V) was conducted and discussed since the operating voltage of the single cell PEFC application was around 0.6 V in practice [79], [81 - 84].

The hydrogen mass fraction distribution at the anode Cl/GDL interface of 6 different flow fields is shown in Fig.4.14a-f. Same as when using oxygen as oxidant, the 1S flow field distributed the hydrogen the most uniform, while the worst flow field in distributing the hydrogen was parallel. The PIS flow fields performed slightly better than the multi-channel S flow fields in distributing the hydrogen, as expected. The results also revealed that most of the flow field, except the parallel flow field, provided almost the same contour as using oxygen as oxidant, although the magnitude was slightly different which may cause by a different investigated current density. From this result, it can be concluded that the distribution on the anode side did not depend on the flow condition of the anode side alone since the transport behavior of the anode side changed dramatically when the flow condition of the cathode side was changed.

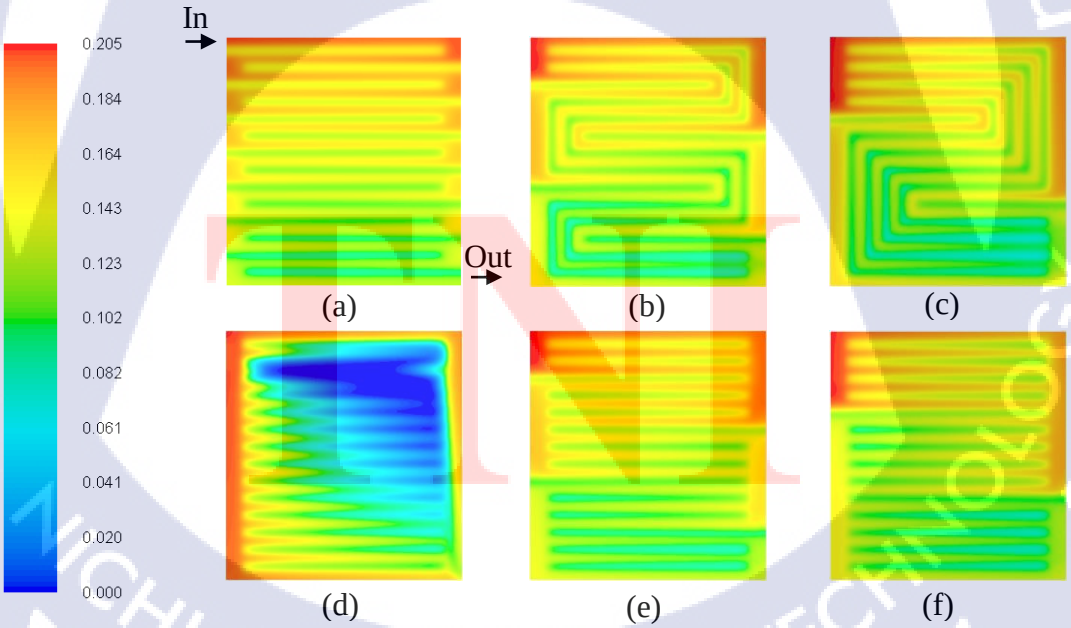


Figure 4.15 Oxygen mass fraction distribution at 0.8 A/cm$^2$ of a) 1S b) 3S c) 5S d) parallel e) 3PIS and f) 5PIS flow fields when using air as oxidant

The phenomenon in which the hydrogen mass fraction at the inlet was lower than that at the outlet, which was found when using oxygen as oxidant, was also found in the cathode side when air is used as oxidant, as depicted in Fig. 4.15a-f. However, from Fig. 4.15a-f, it could not be concluded that the low oxygen mass fraction area is full of water since there were 3 species included in cathode side ($O_2$, $N_2$, $H_2O$), while there were only 2 species in anode side ($H_2$, $H_2O$). Therefore, the water mass fraction needs to be investigated along with the oxygen mass fraction to clarify whether the reactive site is full of water. Fig. 4.16a-f presents the water mass fraction of the six different flow field in which it was found that, except the parallel, the water mass fraction at cathode side of all flow fields is exactly opposite to the oxygen mass fraction since the water was generated and removed along the channels and thus the water mass fraction was increased. The area with low oxygen mass fraction of the parallel flow field did not show a high water mass fraction. Thus, the area in cathode side which showed both oxygen and water in low mass fraction is an unreactive area where no water was generated.

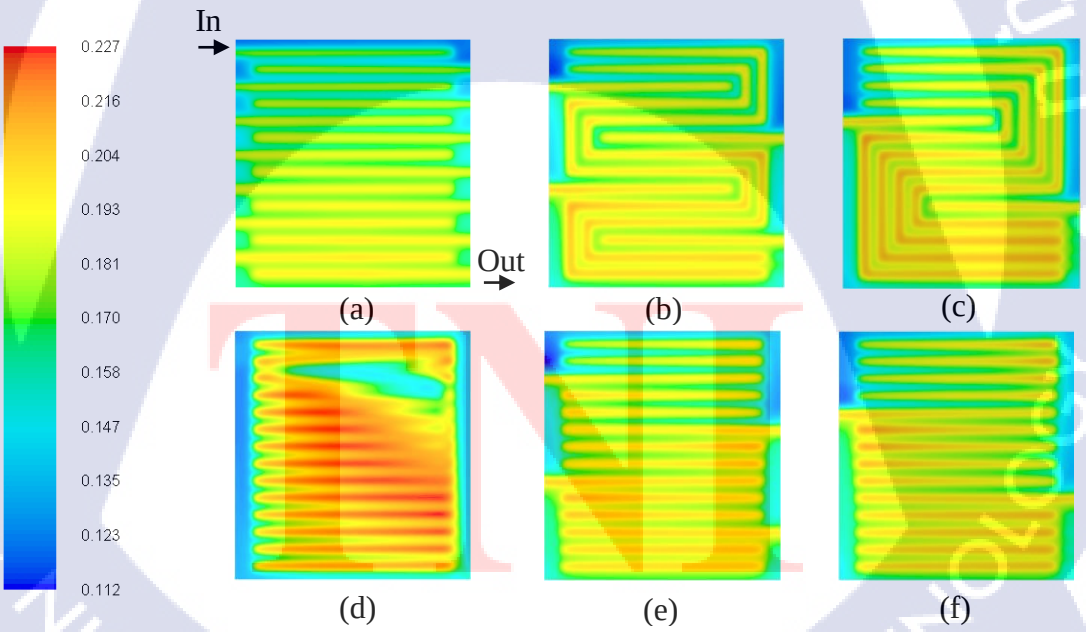


Figure 4.16 Water mass fraction distribution at 0.8 A/cm$^2$ of a) 1S b) 3S c) 5S d) parallel e) 3PIS and f) 5PIS flow fields when using air as oxidant

As mentioned earlier that a uniform distribution of water content leads to a better cell lifetime since uniform distribution of water content could reduce a local hot spot and water flooding and thus the mechanical stress. In addition, it has been also known that the cathode side of the PEFC associates with the water flooding problem, and hence Fig. 4.17a-f presents an information of local water content distribution on CL/MEM interface at the cathode side. Same as when using oxygen as oxidant, the 1S flow field provided the most uniform distribution of the membrane water content, while the parallel performed worst. It can also be observed that the PIS flow fields performed slightly better than the multi-channel S flow fields in the uniformity of membrane water content. Furthermore, the lower number of channels tended to give the better uniformity in both S and PIS flow fields. It was clearly seen that the distribution of water content shared the same contour with the water mass fraction in Fig. 4.16 in which the water gradually increased along the channel. Due to the effect of the water removal, at the inlet of the S (Fig. 4.17b-c), the parallel (Fig. 4.17d) and the PIS (Fig. 4.17 e-f) flow fields, the water content was found very low as compared to the other parts.

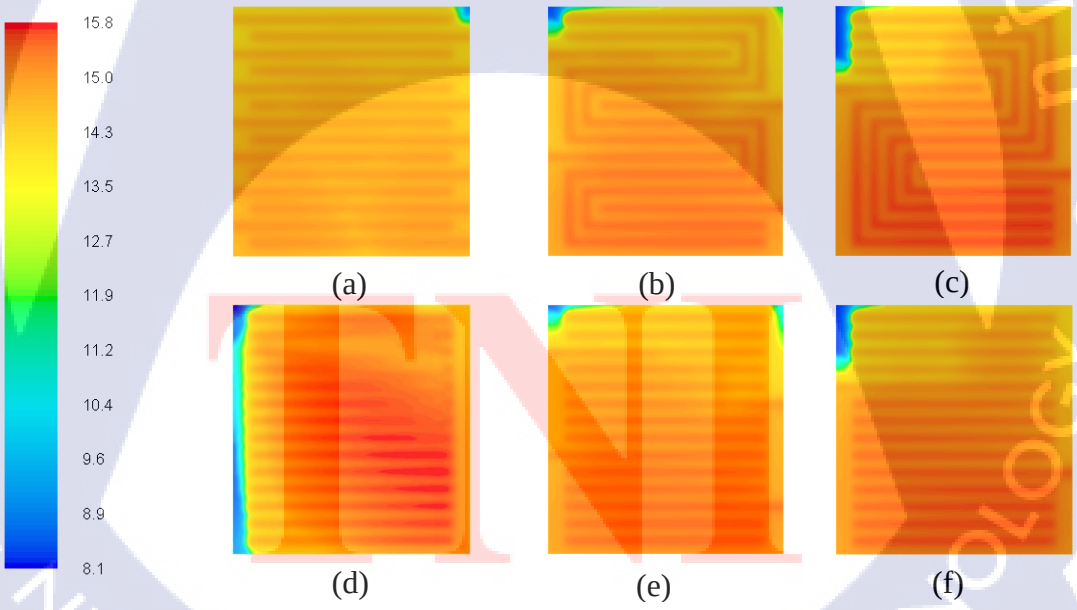


Figure 4.17 Water content distribution at 0.8 A/cm$^2$ at the cathode side of a) 1S b) 3S c) 5S d) parallel e) 3PIS and f) 5PIS flow fields when using air as oxidant

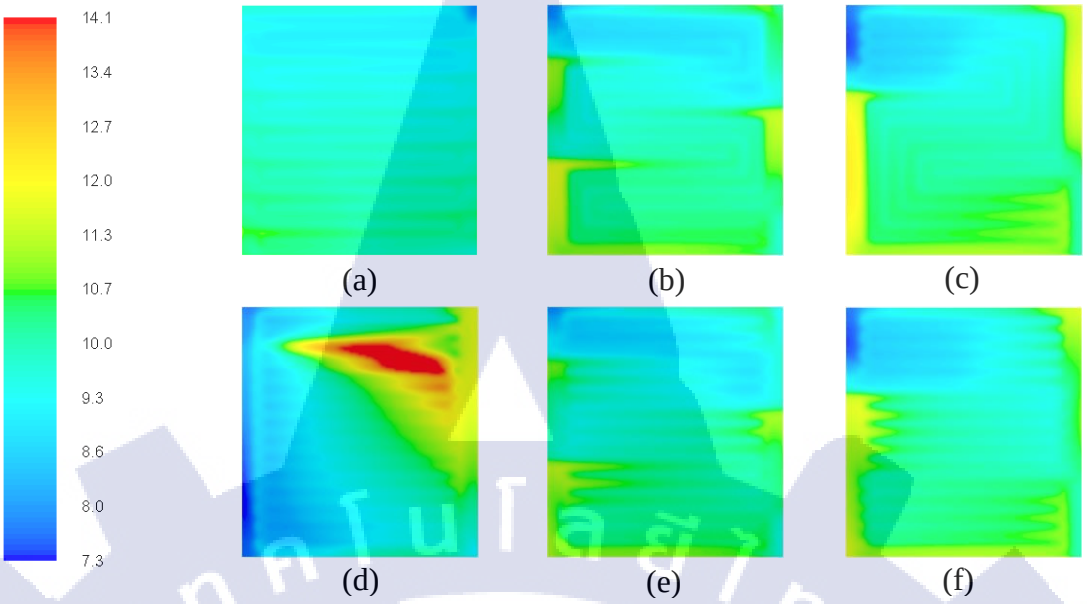


Figure 4.18 Water content distribution at 0.8 A/cm$^2$ at the anode side of a) 1S b) 3S c) 5S d) parallel e) 3PIS and f) 5PIS flow fields when using air as oxidant

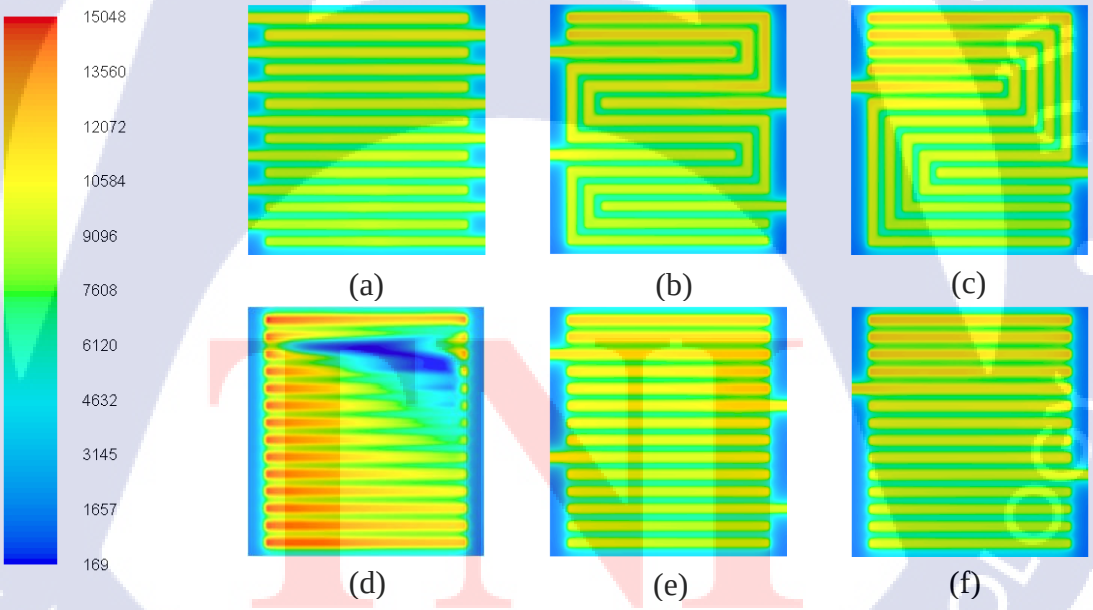


Figure 4.19 Current density distribution (A/m$^2$) at 0.8 A/cm$^2$ a) 1S b) 3S c) 5S d) parallel e) 3PIS and f) 5PIS flow fields when using air as oxidant

While the cathode side of the MEA has to deal heavily with the water flooding problem, the anode side has a problem of the protonic resistance of the membrane due to the membrane dehydration. Hence, the membrane water content on the anode CL/MEM interfaces are shown in Fig. 4.18a-f. Whereas the water content on the cathode side is hardly seen the differences in the uniformity, the anode side showed a better view. As seen in Fig. 4.18, the better uniformity in the membrane hydration can be observed in the flow fields with the lower number of channels. With the same number of channel, the PIS flow fields contributed a more uniform distribution as compared to the multi-channel S flow fields, as discussed earlier. However, while other flow fields had the water content on the same level, the parallel flow fields had a very peak water content at around 14 on the interface. This non-uniform distribution occurred since the fuel cannot not reach the catalyst layer at that area (see Fig. 4.14d). Hence, there are no transferring protons to drag the water molecules from the anode to cathode resulting in a very high and low water content at that area on the anode and cathode side, respectively. This could be implied that the area of higher water content on the anode side would provide a lower current due to the low electro-osmotic drag effect. Furthermore, the distribution on the anode side in which the water was found to accumulate at the inlet occurred since the fed water was mostly absorbed into the CL at that area. Although the counter flow configuration provided the highest cell performance, the non-uniform distributions are the major drawback of this type of flow configuration which is in concurrence with the numerical result of Sierra et al. [70]. To achieve more even distribution, the similar-flow configuration should be used instead. However, the similar flow configuration provided the lowest cell performance among the different gas feeding modes. Therefore, selecting the gas feeding mode has to be considered carefully depending on the applications.

A confirmation, of which the anode high water content area contributed to a lower current, is shown by the local current density distribution in a through-plane direction on cathode CL/GDL interface of each flow field, as displayed in Fig. 4.19a-f. The parallel flow field clearly gave a non-uniform distribution due to the unreactive area while the 1S flow field gave the best uniformity. Thus, mechanical stress due to the non-uniform variation of temperature and water distribution was likely to occur in the parallel as compared to other designs.

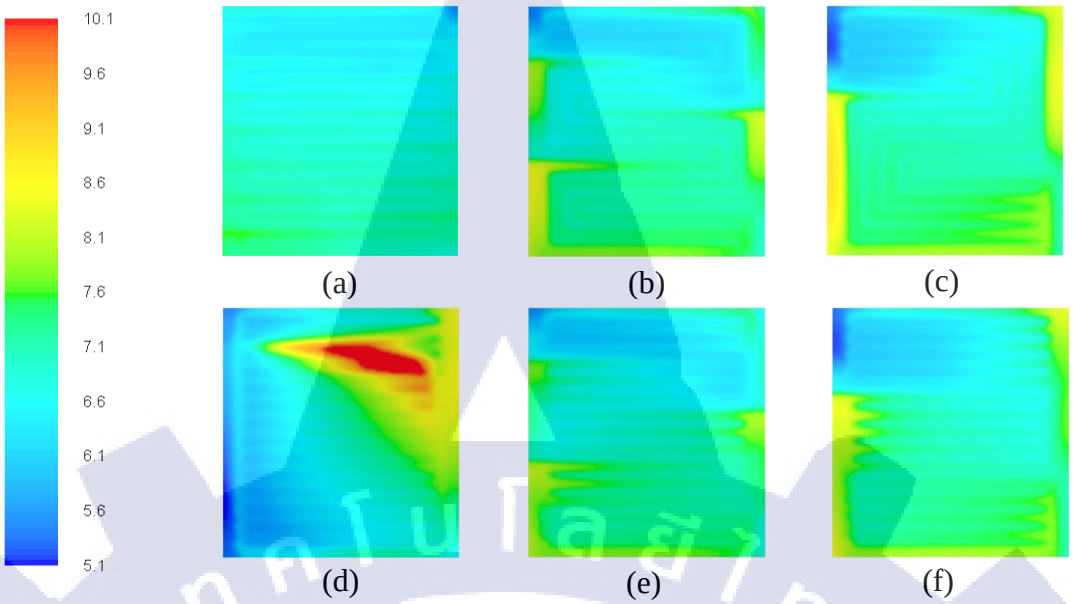


Figure 4.20 Proton conductivity on the anode CL/MEM interface at 0.8 A/cm$^2$ a) 1S b) 3S c) 5S d) parallel e) 3PIS and f) 5PIS flow fields when using air as oxidant

Although there were some differences in other uniformities, the difference in current density uniformity was hardly observed. Since the membrane used in this model is Nafion 112 which is a thin membrane, the membrane is easily hydrated. Therefore, it could be implied that the proton conductivity of the membrane was high enough for the protons to transfer to the cathode. As seen from Fig. 4.20a-f, the protonic conductivity of the membrane on the anode side shared the same trend with the water content. Even though the protonic conductivity distribution looks different in each area but considering the current density that is uniformly distributed, it can be implied that these MEAs used almost maximum capability of theirs utilizable catalyst at the triple-phase boundary.

Fig. 4.21 shows the temperature distribution at the triple-phase boundary. The results revealed that the parallel flow field provided a very bad uniformity as expected since there were some areas where no electrochemical reaction took place and thus no reaction heat. Same as when using oxygen, the 1S contributed the most uniform distribution of the temperature, while the PIS flow fields provided a slightly higher temperature as compared to the multi-channel S flow fields. Besides the amount of the water, the higher temperature in the PIS flow fields was caused by the design of the

flow fields itself. Since the ribs around the corners of the PIS flow fields are not connected, the area to transfer the heat out through the BP is slightly lower than that in the multi-channel S flow fields, resulting in an accumulated heat around that area. As mentioned earlier, although the parallel flow field performed very badly in temperature distribution, the temperature differences were still on the safety limit of 5 K [86] which contributed no significant effect on the MEA durability.

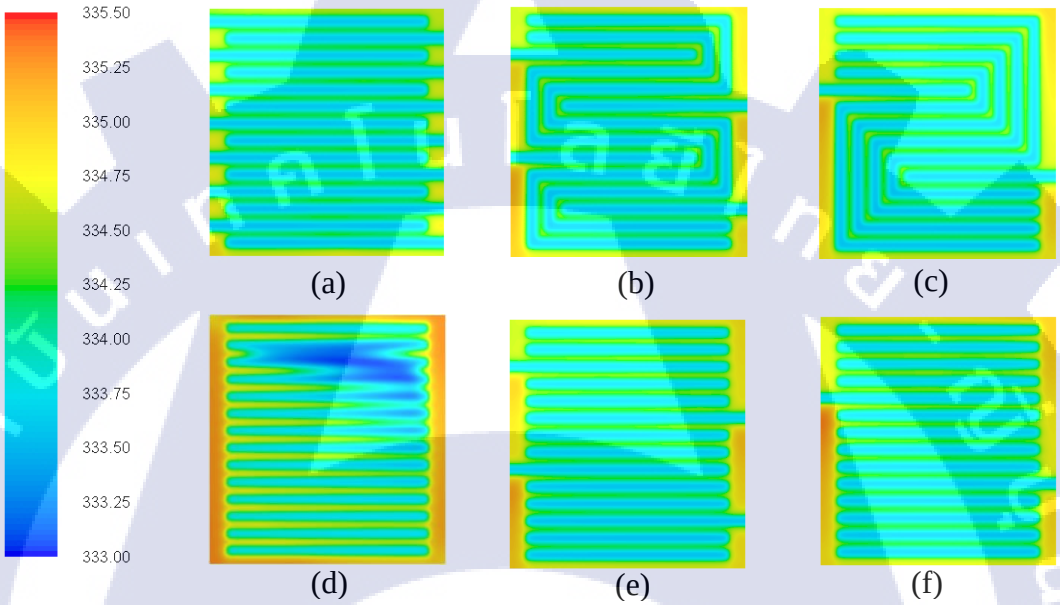


Figure 4.21 Temperature distribution (K) at 0.8 A/cm$^2$ of a) 1S b) 3S c) 5S d) parallel e) 3PIS and f) 5PIS flow fields on the cathode CL/MEM interface when using air as oxidant

As mentioned in the previous section that the pressure drop is one of the most important factors which reduces the overall system performance. Though using air as the oxidant reduces the storage problem, the required blower for forcing air into the stack adds the complexity into the designed system. Thus, designing the system for the applications has to be considered carefully. Same as it was found when oxygen is used as oxidant, the 1S flow field was the best in cell performance and water management. However, the required power for compensating the pressure drop is approximately 10 times higher than that of the 3 channels flow fields and approximately 20 times higher than that of the 5 channels flow fields (see Fig 4.22), although the magnitude is hugely

different. This implied that the pressure drop increased highly with the less number of channels. It was also found that the PIS flow fields slightly produced the higher pressure drop as compared to the multi-channel S flow fields, as expected. In addition, the higher pressure drop may also occur due to a slightly longer channel length of the PIS flow field. Therefore, it can be concluded that the magnitude of the pressure drop is largely depend on the reactant flow rate. Since the pressure drop is proportional to the flow rate square [88], the pressure drop did play an important role on the system efficiency in the large cell area rather than the small cell area. The results also revealed that the type of flow fields showed less effect on the pressure drop as compared to the number of channels. It has to be noted that these pressure drops do not take the effect of the blockage of liquid water in the gas flow channel into account due to the limitation of the model itself.

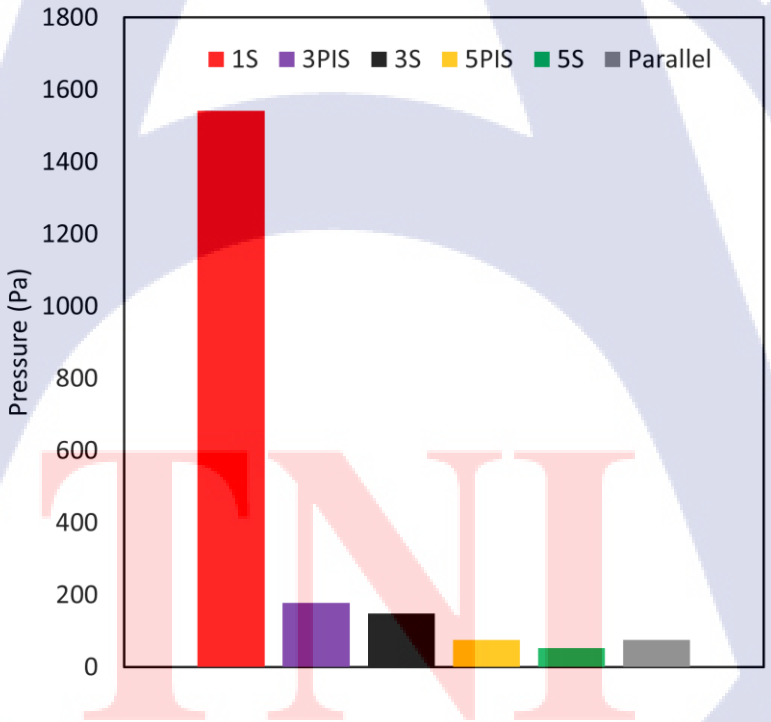


Figure 4.22 Pressure drop at 0.8 A/cm$^2$ when using air as oxidant

Water saturation is another kind of water associated in PEFC affecting greatly the cell performance, durability and stability in which the liquid water clog up the pores preventing the reactants to diffuse through the GDL. As mentioned earlier, the liquid

water in the porous media might form up when the water content is higher than 14. The liquid water in the MEA did exist as confirmed by the water saturation distribution in Fig. 4.23a-f, in which the pore in cathode GDL of the flow fields was full with the volume of liquid water. Since the 1S flow field consisted only one flow path, the reactants were forced down to eliminate the liquid water in GDL out through the channel and to reach the reactive site, and thus the 1S performed best in both cell performance and water management. The other flow fields also forced the liquid water out of the channel but could not eliminate the liquid water as much as the 1S flow field, resulting in the accumulated amount of liquid water at the outlet. The presence of these liquid water caused the flooding in GDL and thus the lower performance. From the results, it can be observed that the liquid water in the parallel and 5S flow field were very high as compared to that of the others. The PIS flow fields provided more uniform distribution than the multi-channel S flow fields with the same number of channel, although there is a very small difference in the 3 channels flow fields. Moreover, the flow fields with lower number of channels tend to handle the flooding situation better than the higher.

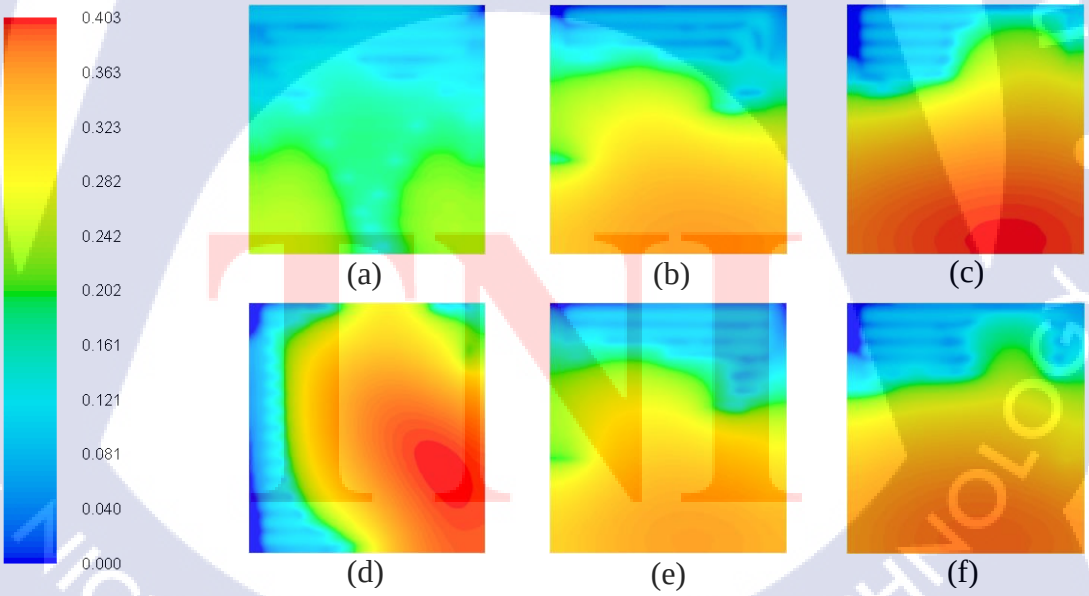


Figure 4.23 Water saturation at 0.8 A/cm$^2$ a) 1S b) 3S c) 5S d) parallel e) 3PIS and f) 5PIS flow fields when using air as oxidant

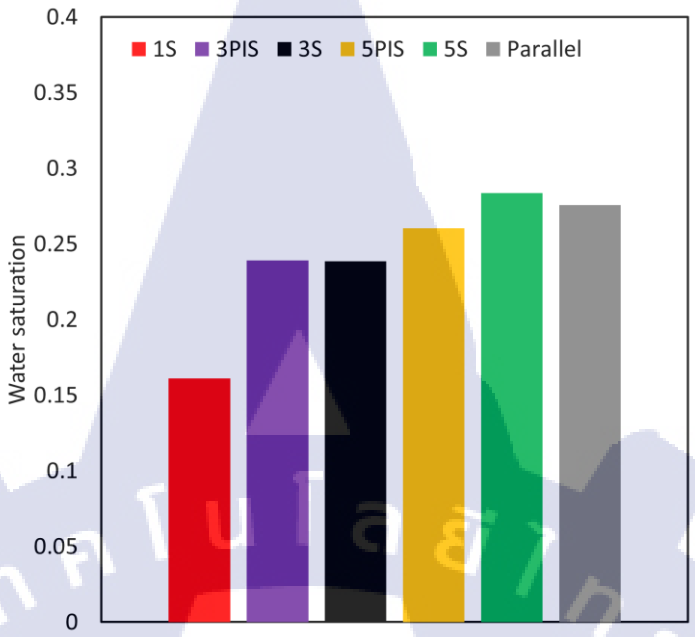


Figure 4.24 Water saturation in cathode gas diffusion layer at 0.8 A/cm$^2$

Wang and Van Nguyen [8] conducted an experiment to observe the stability of PEFC during flooding situation, as mentioned earlier. It was found that, in most cases, when the average water saturation level reached 0.2, the voltage of PEFC would be unstable. Therefore, considering the amount of average water saturation in cathode porous layer (see Fig. 4.24), the cell voltage of all flow fields, except the 1S, would become unstable.

By considering all aspects, it can be concluded that the 1S flow field would be the optimal choice for making a stack with a small size PEFC MEA same as when using oxygen as oxidant since it offered outstanding advantages among other flow fields. Although the pressure drop of the 1S flow field was extremely high as compared to the others, it required a power for forcing the reactant through the channel only around 0.2% of its generated power, which is very low.

Finally, the key findings in this study are summarized in Table 4.1.

Table 4.1 Summary of the key findings in this study

| Key findings | Remark |
|---|---|
| Performance | • When oxygen is used as an oxidant, the 1S flow field provided the highest power followed by 3S, 3PIS, 5S, 5PIS and parallel flow field, respectively.<br>• When using air as an oxidant, in the high potential region, the power contributed by each flow field arranged in order exactly the same with when oxygen is used.<br>• Differently, in the low potential region, the PIS flow fields provided a slightly better performance as compared to the multi-channel S flow fields with the same number of channels. |
| Water management | • The PIS flow fields handled the flooding situation slightly better than the multi-channel S flow fields with the same number of channels.<br>• The flow fields with a less number of channels contributed a better water management than the higher.<br>• Considering the amount of the average water saturation level in the porous media, the cell voltage of all flow fields was still stable when oxygen is used.<br>• However, the cell voltage of all flow fields, except the 1S, would become unstable when air is used. |
| Heat management | • As compared to the multi-channel S flow fields, the PIS flow fields provided a slightly higher temperature in some areas.<br>• Besides the amount of the water that is lower in the PIS, the higher temperature in the PIS flow fields was caused by the design of the flow fields where the ribs around the corners of the PIS flow fields are not connected, resulting in an accumulated heat around that area.<br>• However, the maximum temperature differences of each flow field were in the safety limit which ensured that it would not affect the cell durability. |
| Geometric parameters | • With a serpentine based flow field as studied in this work, the performance and uniformity were affected greatly by the number of channels greatly much more than the design of the flow field.<br>• For a small size MEA, a flow field with a less number of channels contributed a better uniformity and performance. |

# Chapter 5
# Conclusions and Recommendations

## 5.1 Conclusions

The conclusions on the numerical modeling of a polymer electrolyte fuel cell in different flow field geometric configurations using ANSYS FLUENT are summarized here as follows.

The models of a macroscopic level based on finite volume method are successfully developed and validated against the experimental results obtained from our previous work. The results show a good agreement between the experimental data and numerical solutions. However, there is a small discrepancy between the results which was caused by the limitation of the ANSYS FLUENT software itself.

When pure oxygen was used as oxidant, the 1S flow field showed the highest performance followed by 3S, 3PIS, 5S, 5PIS and parallel flow field, respectively, in every current density. However, there are differences when using air as oxidant. In high potential region (above 0.7 V), the 1S flow field also provided the highest power followed by 3S, 3PIS, 5S, 5PIS and parallel flow field, respectively, which concur with when using oxygen as oxidant. In the low potential region (below 0.7 V), with the same number of channel, the PIS flow fields performed better than the multi-channel S flow fields which indicated that the PIS flow fields could handle the water flooding problem in the porous media slightly better than the multi-channel S flow fields.

The 1S flow field provided the best power and uniformity, while the parallel flow field performed worst in both. With the same number of channels, the PIS flow fields provided a slightly lower performance as compared to the multi-channel S flow fields but a better uniformity. Flow fields with a less number of channels tended to have a higher performance and uniformity. For a pressure drop, the required power of the 1S flow field for compensating them is approximately 10 times higher than the 3 channel flow fields and approximately 20 times higher than the 5 channel flow fields which were the same in both cases (using oxygen and air), although the magnitude is extremely different. By considering all aspects, it can be concluded that, with a

serpentine based flow field as studied in this work, number of channels greatly affected the performance and uniformity much more than the design of the flow field.

When using oxygen (high flow rate case), the cell voltage of all flow fields was still stable, although it was found that the liquid water in the parallel flow field was very high as compared to that of the others from considering the amount of the average water saturation level in porous media. Nevertheless, the cell voltage of all flow fields, except the 1S, would become unstable when air is used (low flow rate case). Thus, the 1S is the best flow field for a small-scaled MEA applications due to its outstanding advantages among other flow fields in these given operating conditions.

## 5.2 Recommendations

The recommendations that could be implemented for further research to receive better results of PEFC modelling and more practical results for a commercial-scale application are described as follows.

- Since ANSYS FLUENT is based on the finite volume method which solves the macroscopic equations (i.e. the Navier-Stokes equations), the developed model cannot accurately predict the cell voltage in the high potential region (electrochemical reaction dominated region). The microscopic simulation is required to solve such a problem.
- Although the developed model has already taken the two-phase flow (flow of liquid and water vapor) in the porous media into account, the flow through the gas flow channel is treated as a fine mist (no liquid water clogging in the flow channel). To make the model become more realistic, some modification in the user defined function (UDF) has to be done.
- Due to the non-linearity of the governing equations, the transport behaviors may behave differently when the flow field is changed. Therefore, this model may valid only for the stack which uses a small PEFC MEA. The investigation on the transport behavior of the commercial PEFC has to be done in case by case depend on the design of the system.
- A novel design flow field has to be designed to compete with the 1S flow field since the pressure drop of the flow field is extremely high.

- Recently, Toyota motor corporation launched its fuel cell vehicle called Toyota Mirai and claimed that the flow field (called 3D fine-mesh), which is the multi-inlets flow field, used in this car at the cathode side provided a uniform distribution, improved water removal and air diffusion. Therefore, a further study of the multi-inlets flow field should be carried out.

**References**

# References


[1] A. Iranzo, M. Munoz, F. Rosa, and J. Pino, "Numerical model for the performance prediction of a PEM fuel cell. Model results and experimental validation," *International Journal of Hydrogen Energy*, vol. 35, no. 20, pp. 11533 – 11550, October 2010.

[2] A. Arvay, A. Ahmed, X.-H. Peng, and A.M. Kannan, "Convergence criteria establishment for 3D simulation of proton exchange membrane fuel cell," *International Journal of Hydrogen Energy*, vol. 37, no. 3, pp. 2482 – 2489, February 2012.

[3] S. Kamarajugadda and S. Mazumder, "On the implementation of membrane models in computational fluid dynamics calculations of polymer electrolyte membrane fuel cells," *Computers and Chemical Engineering*, vol. 32, no. 7, pp. 1650 – 1660, July 2008.

[4] S. Shimpalee, S. Greenway, D. Spuckler, and J. W. Van Zee, "Predicting water and current distributions in a commercial-size PEMFC," *Journal of Power Sources*, vol. 135, no. 1 – 2, pp. 79 – 87, September 2007.

[5] G. He, Y. Yamazaki, and A. Abudula, "A three-dimensional analysis of the effect of anisotropic gas diffusion layer(GDL) thermal conductivity on the heat transfer and two-phase behavior in a proton exchange membrane fuel cell(PEMFC)," *Journal of Power Sources*, vol. 195, no. 6, pp. 1551 – 1560, March 2010.

[6] S. Shimpalee, U. Beuscher, and J. W. Van Zee, "Analysis of GDL flooding effects on PEMFC performance," *Electrochemica Acta*, vol. 52, no. 24, pp. 6748 – 6754, August 2007.

[7] K. -S. Choi, B. -G. Kim, K. Park, and H. -M. Kim, "Flow control of under-rib convection enhancing the performance of proton exchange membrane fuel cell," *Computers & Fluids*, vol. 69, pp. 81 – 92, October 2012.

[8] D. H. Jeon, S. Greenway, S. Shimpalee, and J. W. Van Zee, "The effect of serpentine flow-field designs on PEM fuel cell performance," *International Journal of Hydrogen Energy*, vol. 33, no. 3, pp. 1052 – 1066, February 2008.

[9] A. P. Manso, F. F. Marzo, M. Garmendia Mujika, J. Barranco, and A. Lorenzo, "Numerical analysis of the influence of the channel cross-section aspect ratio on the performance of a PEM fuel cell with serpentine flow field design," *International Journal of Hydrogen Energy*, vol. 36, no. 11, pp. 6795 – 6808, June 2001.

[10] A. P. Manso, F. F. Marzo, J. Barranco, X. Garikano, and M. Garmendia Mujika, "Influence of geometric parameters of the flow fields on the performance of a PEM fuel cell. A review," *International Journal of Hydrogen Energy*, vol. 37 no. 20, pp. 15256 – 15287, October 2012.

[11] S. Maharugrayya, S. Jayanti, and A. P. Despande, "Pressure drop and flow distribution in multiple parallel-channel configurations used in proton-exchange membrane fuel cell stacks," *Journal of Power Sources,* vol. 157 no. 1, pp. 385 – 367, June 2006.

[12] X. -D. Wang, Y. -Y. Duan, W. -M. Yan, and X. -F. Peng, "Local transport phenomena and cell performance of PEM fuel cells with various serpentine flow field designs," *Journal of Power Sources,* vol. 175, no. 1, pp. 397 – 407, January 2008.

[13] J. Lobato, P. Canizarez, M. A. Rodrigo, F. J. Pinar, and D. Ubeda, "Study of flow channel geometry using current distribution measurement in a high temperature polymer electrolyte membrane fuel cell," *Journal of Power Sources,* vol. 196, no. 9, pp. 4209 – 4217, May 2011.

[14] ANSYS, *ANSYS FLUENT Fuel Cell Modules Manual*. USA: ANSYS, 2011.

[15] C. Y. Wang, "Fundamental models for fuel cell engineering," *Chemical reviews,* vol. 104, no. 10, pp. 4727 – 4766, October 2004.

[16] A. Z. Weber and J. Newman, "Modeling transport in polymer-electrolyte fuel cells," *Chemical reviews,* vol. 104, no. 10, pp. 4679-4726, October 2004.

[17] C. Siegel, "Review of computational heat and mass transfer modeling in polymer-electrolyte-membrane (PEM) fuel cells," *Energy,* vol. 33, no. 9, pp. 1331 – 1352, September 2008.

[18] J. Y. Nam and M. Karviany, “Effective diffusivity and water-saturation distribution in single- and two layer PEMFC diffusion medium,” *International Journal Heat and Mass Transfer*, vol. 46, no. 24, pp. 4595 – 4611, November 2003.

[19] T. V. Nguyen, “Modeling two-phase flow in the porous electrodes of proton exchange membrane fuel cells using the interdigitated flow fields,” *Tutorials in Electrochemical Engineering Mathematical Modeling*, vol. 99, no. 14, pp. 222–241, 1999.

[20] T. E. Springer, T. A. Zawodzinski, and S. Gottesfeld, “Polymer electrolyte fuel cell model,” *Journal of the Electrochemical Society*, vol. 138, no. 8, pp. 2334–2342, August 1991.

[21] The American Institute of Aeronautics and Astronautics, *Guide for the Verification and Validation of Computational Fluid Dynamics Simulations.* n.p.: AIAA, 1998.

[22] European Research Community on Flow, Turbulence and Combustion, *ERCOFTAC Best Practice Guidelines for Industrial Computational Fluid Dynamics of Single-Phase Flows*. n.p.: ERCOFTAC, 2000.

[23] European Cooperation in Science and Technology, *Best Practice Guideline for the CFD Simulation of Flows in the Urban Environment*. n.p.: Cost Office, 2007.

[24] Y. Zhou, K. Jiao, Q. Du, Y. Yin, and X. Li, “Gas diffusion layer deformation and its effect on the transport characteristics and performance of proton exchange membrane fuel cell,” *International Journal of Hydrogen Energy*, vol. 38, no. 29, pp. 12891 – 12903 September 2013.

[25] G. Hu, J. Fan, S. Chen, Y. Liu, and K. Cen, “Three-dimensional numerical analysis of proton exchange membrane fuel cells (PEMFCs) with conventional and interdigitated flow fields,” *Journal of Power Sources*, vol. 136, no. 1, pp. 931 – 940, September 2004.

[26] E. Birgersson and M. Vynnycky, “A quantitative study of the effect of flow-distributor geometry in the cathode of a PEM fuel cell,” *Journal of Power Sources*, vol. 153, no. 1, pp. 76 – 88, January 2006.

[27] A. Kumar and R. G. Reddy, "Effect of gas flow-field design in the bipolar/end plates on the steady and transient state performance of polymer electrolyte membrane fuel cells," *Journal of Power Sources,* vol. 155, no. 2, pp. 264 – 271, April 2006.

[28] Y. M. Ferng and A. Su, "A three-dimensional full-cell CFD model used to investigate the effects of different flow channel designs on PEMFC performance," *International Journal of Hydrogen Energy*, vol. 32, no. 17, pp. 4466 – 4476, December 2007.

[29] J. H. Jang, W. M. Yan, H. Y. Li, and W. C. Tsai, "Three-dimensional numerical study on cell performance and transport phenomena of PEM fuel cells with conventional flow fields," *International Journal of Hydrogen Energy,* vol. 33, no. 1, pp. 156 – 164, January 2008.

[30] W. Zhang, P. Hu, X. Lai, and L. Peng, "Analysis and optimization of flow distribution in parallel-channel configurations for proton exchange membrane fuel cells", *Journal of Power Sources,* vol. 194, no. 2, pp. 931 – 940, December 2009.

[31] X. D. Wang, X. X. Zhang, W. M. Yan, D. J. Lee, and A. Su, "Determination of the optimal active area for proton exchange membrane fuel cells with parallel, interdigitated or serpentine designs," *International Journal of Hydrogen Energy*, vol. 34, no. 9, pp. 3823 – 3832, May 2009.

[32] R. Boddu, U. K. Marupakula, B. Summers, and P. Majumdar, "Development of bipolar plates with different flow channel configurations for fuel cells," *Journal of Power Sources,* vol. 189, no. 2, pp. 1083 – 1092, April 2009.

[33] S. Lee, T. Kim, and H. Park, "Comparison of multi-inlet and serpentine channel design on water production of PEMFCs," *Chemical Engineering Science,* vol. 66, no. 8, pp. 1748 – 1758, April 2011.

[34] B. Ramos-Alvarado, A. Hernandez-Guerrero, D. Juarez-Robles, and P. Li, "Numerical investigation of the performance of symmetric flow distributors as flow channels for PEM fuel cells," *International Journal of Hydrogen Energy,* vol. 37, no. 1, pp. 436 – 448, January 2012.

[35] S. W. Cha, R. O'Hayre, Y. Saito, and F. B. Prinz, "The scaling behavior of flow patterns: a model investigation," *Journal of Power Sources*, vol. 134, no. 1, pp. 57 – 71, July 2004.

[36] X. D. Wang, J. L. Xu, W. M. Yan, D. J. Lee, and A. Su, "Transient response of PEM fuel cells with parallel and interdigitated flow field designs," *International Journal of Heat and Mass Transfer*, vol. 54, no. 11 – 12, pp. 2375 – 2386, May 2011.

[37] H. Y. Li, W. C. Weng, W. M. Yan, and X. D. Wang, "Transient characteristics of proton exchange membrane fuel cells with different flow field designs," *Journal of Power Sources*, vol. 196, no. 1, pp. 235 – 245, January 2011.

[38] S. -H. Ge and B. -L. Yi, "A mathematical model for PEMFC in different flow modes," *Journal of Power Sources*, vol. 124, no. 1, pp. 1 – 11, October 2003.

[39] S. Shimpalee, S. Greenway, and J. W. Van Zee, "The impact of channel path length on PEMFC flow-field design," *Journal of Power Sources*, vol. 160, no. 1, pp. 398 – 406, September 2006.

[40] A.D., Santamaria, N.J., Cooper, M.K., Becton, and J.W., Park, "Effect of channel length on interdigitated flow-field PEMFC performance: A computational and experimental study," *International Journal of Heat and Mass Transfer*, vol. 38, no. 36, pp. 16253-16263, December 2013.

[41] H. C. Liu, W. M. Yan, C. Y. Soong, and F. Chen, "Effects of baffle-blocked flow channel on reactant transport and cell performance of a proton exchange membrane fuel cell," *Journal of Power Sources*, vol. 142, no. 1 – 2, pp. 125 – 133, March 2005.

[42] C. Y. Soong, W. M. Yan, C. Y. Tseng, H. C. Liu, F. Chen, and H. S. Chu, "Analysis of reactant gas transport in a PEM fuel cell with partially blocked fuel flow channels," *Journal of Power Sources*, vol. 143, no. 1 – 2, pp. 36 – 47, April 2005.

[43] X. D. Wang, Y. Y. Duan, and W. M. Yan, "Novel serpentine-baffle flow field design for proton exchange membrane fuel cells," *Journal of Power Sources*, vol. 173, no. 1, pp. 210 – 221, November 2007.

[44] J. H. Jang, W. M. Yan, H. Y. Li, and Y. C. Chou, "Humidity of reactant fuel on the cell performance of PEM fuel cell with baffle-blocked flow field designs," *Journal of Power Sources*, vol. 159, no. 1, pp. 468 – 477, September 2006.

[45] A. Kumar and R. G. Reddy, "Effect of channel dimensions and shape in the flow-field distributor on the performance of polymer electrolyte membrane fuel cells," *Journal of Power Sources*, vol. 113, no. 1, pp. 11 – 18, January 2003.

[46] D. H. Ahmed and H. J. Sung, "Effects of channel geometrical configuration and shoulder width on PEMFC performance at high current density," *Journal of Power Sources*, vol. 162, no. 1, pp. 327 – 339, November 2006.

[47] S. Shimpalee, V. Lilavivat, J. W. Van Zee, H. McCrabb, and Lozano-Morales, A., "Understanding the effect of channel tolerances on performance of PEMFCs," *International Journal of Hydrogen Energy*, vol. 36, no. 19, pp. 12512 – 12523, September 2011.

[48] W. Sun, B. A. Peppley, and K. Karan, "Modeling the influence of GDL and flow-field plate parameters on the reaction distribution in the PEMFC cathode catalyst layer," *Journal of Power Sources*, vol. 144, no. 1, pp. 42 – 53, June 2005.

[49] W. Ying, T. H. Yang, W. Y. Lee, J. Ke, and C. S. Kim, "Three-dimensional analysis for effect of channel configuration on the performance of a small air-breathing proton exchange membrane fuel cell (PEMFC)," *Journal of Power Sources*, vol. 145, no. 2, pp. 572 – 581, August 2005.

[50] S. Lee, H. Jeong, B. Ahn, T. Lim, and Y. Son, "Parametric study of the channel design at the bipolar plate in PEMFC performances," *International Journal of Hydrogen Energy*, vol. 33, no. 20, pp. 5691 – 5696, October 2008.

[51] S. Shimpalee and J. W. Van Zee. "Numerical studies on rib & channel dimension of flow-field on PEMFC performance," *International Journal of Hydrogen Energy*, vol. 32, no. 20, pp. 842 – 856, May 2007.

[52] J. Scholta, G. Escher, W. Zhang, L. Kuppers, L. Jorissen, and W. Lehnert, "Investigation on the influence of channel geometries on PEMFC performance," *Journal of Power Sources*, vol. 155, no. 1, pp. 66 – 71, April 2006.

[53] X. D. Wang, Y. Y. Duan, and W. M. Yan, "Numerical study of cell performance and local transport phenomena in PEM fuel cells with various flow channel area ratios," *Journal of Power Sources*, vol. 172, no. 1, pp. 265 – 277, October 2007.

[54] W. M. Yan, H. C. Liu, C. Y. Soong, F. Chen, and C. H. Cheng, "Numerical study on cell performance and local transport phenomena of PEM fuel cells with novel flow field designs," *Journal of Power Sources*, vol. 161, no. 2, pp. 907 – 919, October 2006.

[55] H. C. Liu, W. M. Yan, C. Y. Soong, F. Chen, and H. S. Chu, "Reactant gas transport and cell performance of proton exchange membrane fuel cells with tapered flow field design," *Journal of Power Sources*, vol. 158, no. 1, pp. 78 – 87, July 2006.

[56] W. M. Yan, H. Y. Li, P. C. Chui, and X. D. Wang, "Effects of serpentine flow field with outlet channel contraction on cell performance of proton exchange membrane fuel cells," *Journal of Power Sources*, vol. 178, no. 1, pp. 174 – 180, March 2008.

[57] X. D. Wang, Y. X. Huang, C. H. Cheng, J. Y. Jang, D. J. Lee, W. M. Yan, and A. Su, "An inverse geometry design problem for optimization of single serpentine flow field of PEM fuel cell," *International Journal of Hydrogen Energy*, vol. 35, no. 9, pp. 4247 – 4257, May 2010.

[58] É. Fontana, E. Mancusi, A. Da Silva, V. C. Mariana, A. A. Ulson de Souza, and S. Ulson de Souza, "Study of the effects of flow channel with non-uniform cross-sectional area on PEMFC species and heat transfer," *International Journal of Heat and Mass Transfer*, vol. 54, no. 21 – 22, pp. 4462 – 4472, October 2011.

[59] K. S. Choi, H. M. Kim, and S. M. Moon, "Numerical studies on the geometrical characterization of serpentine flow-field for efficient PEMFC," *International Journal of Hydrogen Energy*, vol. 36, no. 2, pp. 1613 – 1627, January 2011.

[60] J. K. Kuo, T. H. Yen, and C. K. Chen, "Three-dimensional numerical analysis of PEM fuel cells with straight and wave-like gas flow fields channels," *Journal of Power Sources*, vol. 177, no. 1, pp. 96 – 103, February 2008.

[61] C. T. Wang, Y. C. Hu, and P. L. Zheng, "Novel biometric flow slab design for improvement of PEMFC performance," *Applied Energy*, vol. 87, no. 4, pp. 1366 – 1375, April 2010.

[62] J. P. Kloess, X. Wang, J. Liu, Z. Shi, and L. Guessous, "Investigation of bio-inspired flow channel designs for bipolar plates in proton exchange membrane fuel cells," *Journal of Power Sources*, vol. 188, no. 1, pp. 132 – 140, March 2009.

[63] R. Roshandel, F. Arbabi, and G. K. Moghaddam "Simulation of an innovative flow-field design based on a bio inspired pattern for PEM fuel cells," *Renewable Energy*, vol. 41, pp. 86 – 95, May 2012.

[64] I. Khazaee and M. Ghazikhani, "Performance improvement of proton exchange membrane fuel cell by using annular shaped geometry," *Journal of Power Sources*, vol. 196, no. 5, pp. 2661 – 2668, March 2011.

[65] I. Khazaee, M. Ghazikhani, and M. N. Esfahani, "Effect of gas diffusion layer and membrane properties in an annular proton exchange membrane fuel cell," *Applied Surface Science*, vol. 258, no. 6, pp. 2141 – 2148, January 2012.

[66] S. Cano-Andrade, A. Hernandez-Guerrero, M. R. von Spakovsky, C. E. Damian-Ascencio, and J. C. Rubio-Arana, "Current density and polarization curves for radial flow field patterns applied to PEMFCs (Proton Exchange Membrane Fuel Cells)," *Energy*, vol. 35, no. 2, pp. 920 – 927, February 2010.

[67] V. H. Rangel-Hernandez, C. E. Damian-Ascencio, D. Juarez-Robles, A. Gallegos-Munoz, A. Zaleta-Aguilar, and H. Plascencia-Mora, "Entropy generation analysis of a proton exchange membrane fuel cell (PEMFC) with a Fermat spiral as a flow distributor," *Energy*, vol. 36, no. 8, pp. 4864 – 4870, August 2011.

[68] D. Juarez-Robles, A. Hernandez-Guerrero, B. Ramos-Alvarado, F. Elizalde-Blancas, and C. E. Damian-Ascencio, "Multiple concentric spirals for the flow field of a proton exchange membrane fuel cell," *Journal of Power Sources,* vol. 196, no. 19, pp. 8019 – 8030, October 2011.

[69] A. M. Lopez, F. Barreras, A. Lozano, J. A. Garcia, L. Valino, and R. Mustata, "Comparison of water management between two bipolar plate flow-field geometries in proton exchange membrane fuel cells at low-density current range," *Journal of Power Sources,* vol. 192, no. 1, pp. 94 – 99, July 2009.

[70] J. M. Sierra, J. Moreira, and P. J. Sebastian, "Numerical analysis of the effect of different gas feeding modes in a proton exchange membrane fuel cell with serpentine flow-field," *Journal of Power Sources,* vol. 196, no. 11, pp. 5070 – 5076, June 2011.

[71] Y. Lu and R. G. Reddy, "Performance of micro-PEM fuel cells with different flow fields," *Journal of Power Sources,* vol. 195, no. 2, pp. 503 – 508, January 2010.

[72] J. Lobato, P. Canizares, M. A. Rodrigo, F. J. Pinar, and D. Ubeda, "Study of flow channel geometry using current distribution measurement in a high temperature polymer electrolyte membrane fuel cell," *Journal of Power Sources,* vol. 196, no. 9, pp. 4209 – 4217, May 2011.

[73] J. Lobato, P. Canizares, M. A. Rodrigo, F. J. Pinar, E. Mena, and D. Ubeda, "Three-dimensional model of a 50 $cm^2$ high temperature PEM fuel cell. Study of the flow channel geometry influence," *International Journal of Hydrogen Energy,* vol. 35, no. 11, pp. 5510 – 5520, June 2010.

[74] A. Iranzo, P. Boillat, and F. Rosa, "Validation of a three dimensional PEM fuel cell CFD model using local liquid water distributions measured with neutron imaging," *International Journal of Hydrogen Energy,* vol. 39, no. 13, pp. 7089 – 7099, April 2014.

[75] N. Limjeerajarus, Y. Nishiyama, H. Ohashi, T. Ito, and T. Yamaguchi, "Modeling for PEFC MEAs based on reaction rate on Pt surface and microstructures of catalyst layers," *Journal of Chemical Engineering of Japan,* vol. 42, no. 8, pp. 616 – 631, January 2009.

[76] H. K. Versteeg and W. Malalasekera, *An Introduction to Computational Fluid Dynamics: The Finite Volume Method*. England: Pearson Education, 2007.

[77] E. C. Kumbur, K. V. Sharp, and M. M. Mench, "Liquid droplet behavior and instability in a polymer electrolyte fuel cell flow channel," *Journal of Power Sources*, vol. 161, no. 1, pp. 333 – 345, October 2006.

[78] M. Khandelwal and M. M. Mench, "Direct measurement of through-plane thermal conductivity and contact resistance in fuel cell materials," *Journal of Power Sources*, vol. 161, no. 2, pp. 1106 – 1115, October 2006.

[79] F. Barbir, *PEM Fuel Cells: Theory and Practice*. Burlington: Academic Press, 2012.

[80] B. Carnes, D. Spernjak, G. Luo, L. Hao, K. S. Chen, C. Y. Wang, R. Mukundan, and R. L. Borup, "Validation of a two-phase multidimensional polymer electrolyte membrane fuel cell computational model using current distribution measurements," *Journal of Power Sources*, vol. 236, pp. 126 – 137, August 2013.

[81] M. M. Mench, C. Y. Wang, and S. Thynell, "An introduction to fuel cells and related transport phenomena," *International Journal of Transport Phenomena*, vol. 3, pp. 151 – 176, 2001.

[82] M. M. Mench, E. C. Kumbur, and T. N. Veziroglu, *Polymer Electrolyte Fuel Cell Degradation*. U.S.A.: Academic Press, 2011.

[83] J. Zhang, H. Zhang, J. Wu, and J. Zhang, *PEM Fuel Cell Testing and Diagnosis*. Great Britain: Elsevier, 2013.

[84] J. -H. Wee, "Applications of proton exchange membrane fuel cell systems," *Renewable and Sustainable Energy Reviews*, vol. 11, no. 8, pp. 1720 – 1738, January 2012.

[85] X. Wang and T. V. Nguyen, "An experimental study of the liquid water saturation level in the cathode gas diffusion layer of a PEM fuel cell," *Journal of Power Sources*, vol. 197, pp. 50 – 56, January 2012.

[86] U. Pasaogullari, "Heat and water transport models for polymer electrolyte fuel cells," *Handbook of Fuel Cells*, 2010.

[87] N. Limjeerajarus, T. Yanagimoto, T. Yamamoto, T. Ito, and T. Yamaguchi, "Quantitative analysis of oxygen-containing species adsorbed on the Pt surface of a polymer electrolyte fuel cell membrane electrode assembly electrode using stripping voltammetry," *Journal of Power Sources*, vol. 185, no. 1, pp. 217 – 221, October 2008.

[88] M. M. Mench, *Fuel Cell Engines.* U.S.A: John Wiley and Sons, 2008.